AD-A055 942 HUGHES AIRCRAFT CO FULLERTON CALIF GROUND SYSTEMS GROUP F/G 17/4
UHF ADAPTIVE ARRAY DEVELOPMENT PROGRAM.(U)
JUL 77 D D EFFINGER, W R JONES, W R MASENTEN N00173-76-C-0353
UNCLASSIFIED FR77-14-763 NL

1 OF 2
ADA
055942

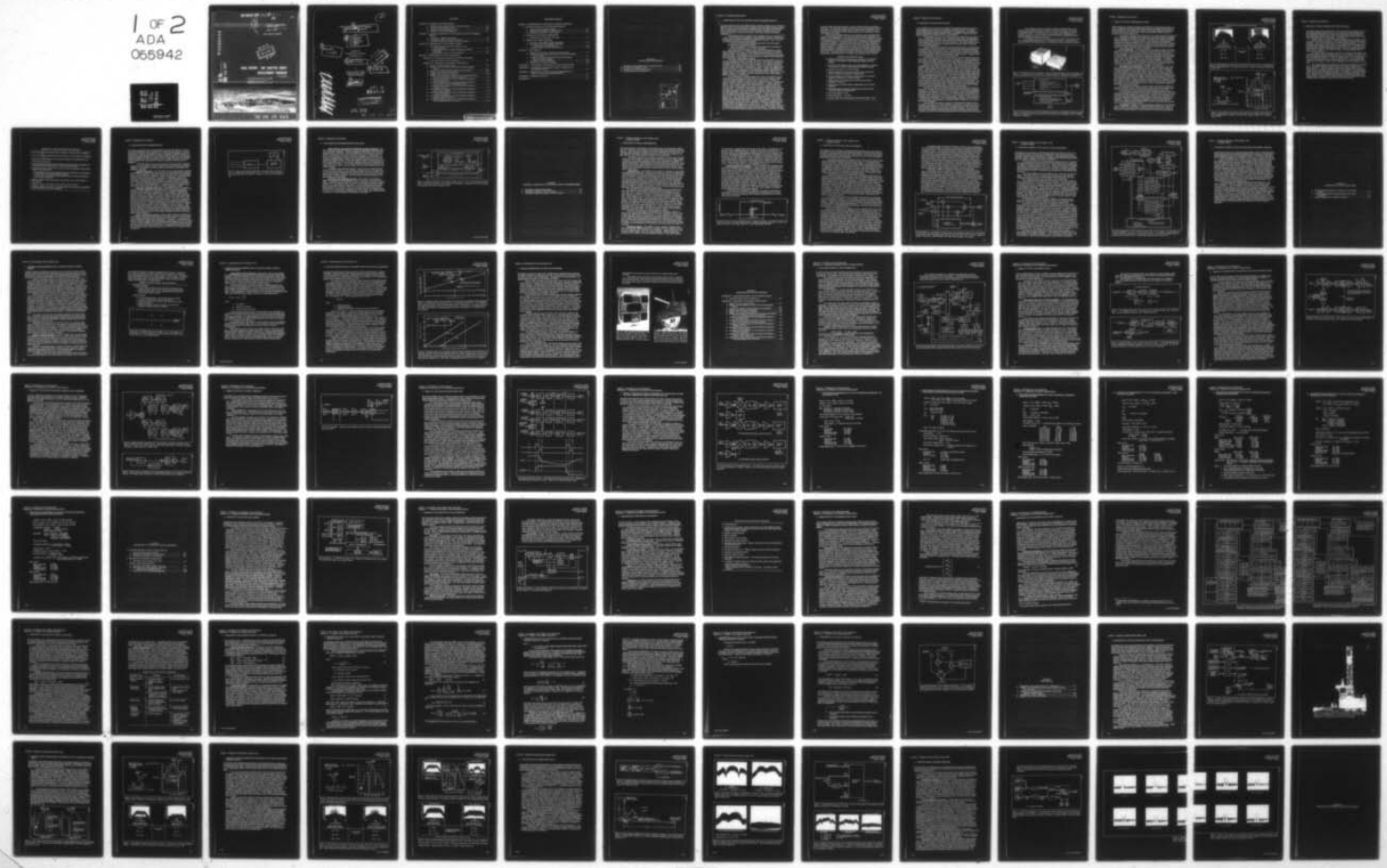

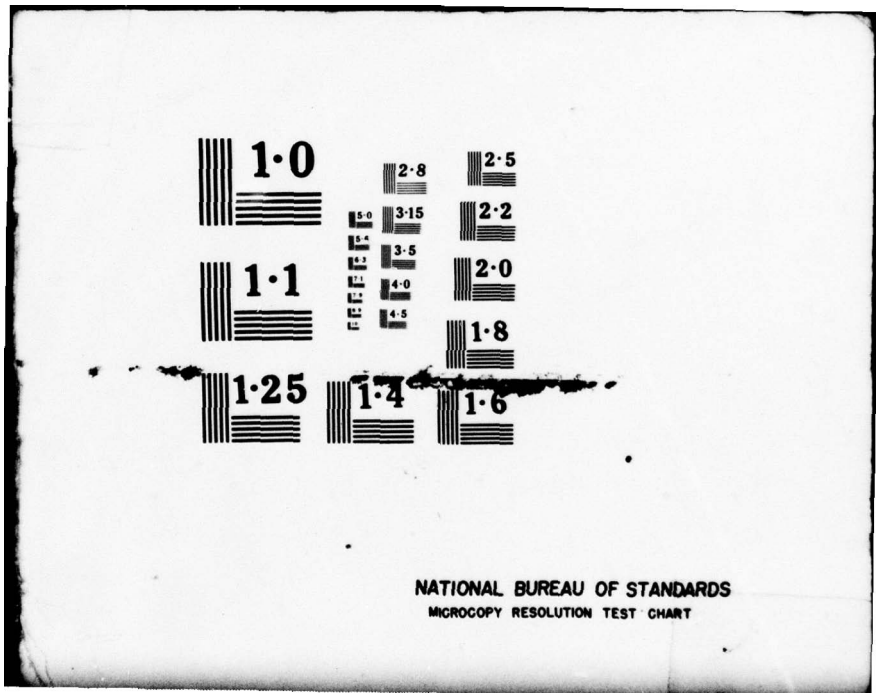
1·0
1·1
1·25
1·4
1·6
1·8
2·0
2·2
2·5
2·8
3·15
3·5
4·0
4·5
5·0
NATIONAL BUREAU OF STANDARDS
MICROCOPY RESOLUTION TEST CHART

FINAL REPORT - UHF ADAPTIVE ARRAY DEVELOPMENT PROGRAM

N00173-76-C-0353
1 JULY 1977

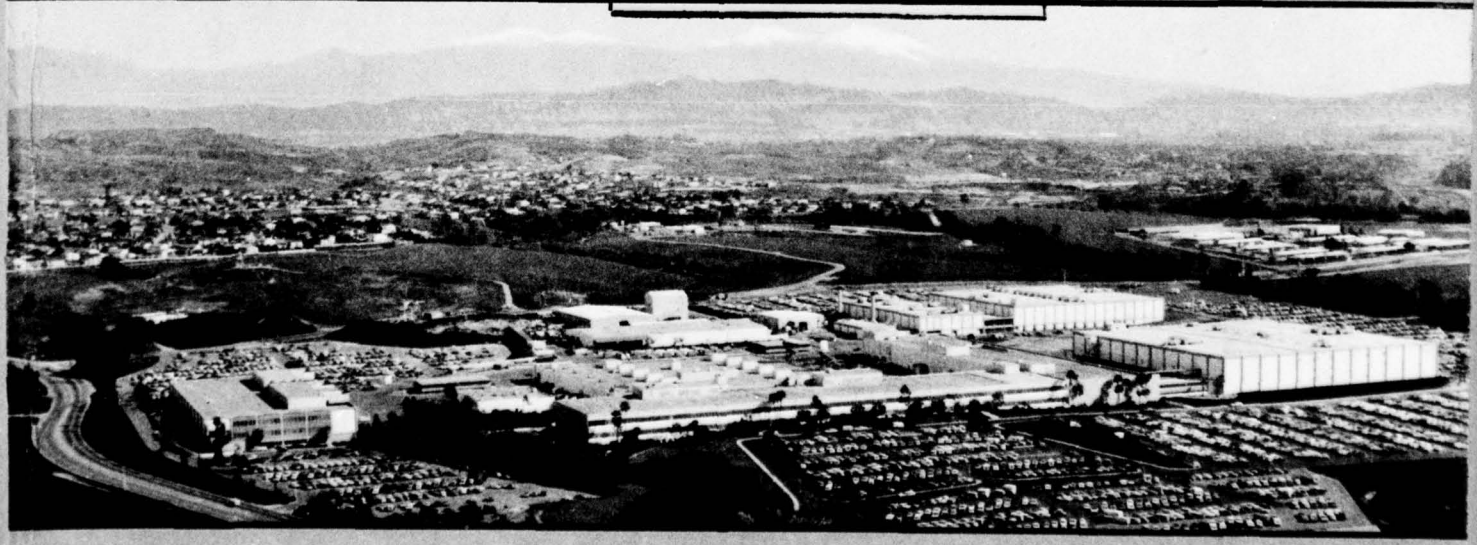

(2)

(6) FINAL REPORT - UHF ADAPTIVE ARRAY DEVELOPMENT PROGRAM,

by

(10) D. D. Effinger,
W. R. Jones,
W. R. Masenten,
T. W. Miller
W. G. Tees

(9) Final rept.,

Submitted to

Naval Research Laboratory
Washington, D. C.

(15) Under Contract
N00173-76-C-0353

(12) 126 pp

by

Hughes Aircraft Company
Ground Systems Group
Fullerton, California

(11) 1 July 1977
(14) FR 77-14-763

CONTENTS

CONTENTS (Continued)

SECTION S
INTRODUCTION AND SUMMARY

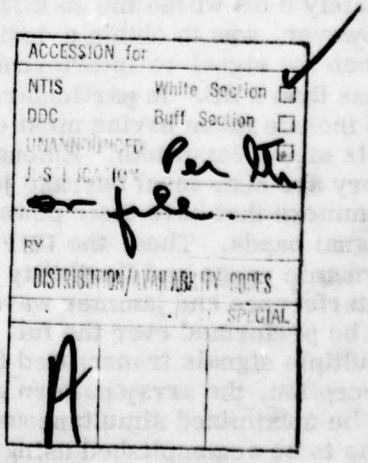

1. OBJECTIVES OF THE UHF ADAPTIVE ARRAY PROCESSOR PROJECT

The prime objective of the UHF adaptive array processor program was to develop an adaptive array to provide rejection of interference in Naval communications systems. The major goals were: maximizing the signal-to-noise and signal-to-interference ratios, suppressing jammers over a 10 MHz bandwidth, operating with any four-element antenna array, and accommodating a wide range of jammer and signal waveforms.

The requirement for an adaptive array capability has been recognized as a result of the observed susceptability of communications systems to both friendly (inadvertent) and unfriendly (deliberate) interference sources. One or more of the following contribute to this susceptability:

- Low level communications signals, particularly SATCOM signals
- Proximity to interference sources
- Lack of conventional AJ techniques such as waveform processing because of bandwidth, cost, or other restrictions.

The purpose of the UHF adaptive array processor development project was to design and build a four-element adaptive array processor to be used for research leading to the design of a fleet-deployable adaptive antenna for Naval communications. The processor's major function is to provide increased antijam (AJ) protection for Naval shipboard and airborne line-of-sight (LOS) communications and satellite communications systems.

This project addressed the problem of reducing susceptability of communications channels in the 225 to 400 MHz UHF band. The signals of interest have information bandwidths less than 25 kHz and use any of the common modulation techniques, such as AM, FM, FSK, PSK, or QPSK. The received signal level can vary widely depending on the application, since the signal may originate from a distant satellite or a near-in airborne transmitter. A given communications channel can contain a multiplicity of these narrowband signals separated in frequency within a 10 MHz bandwidth and all transmitted from the same source. The gapfiller satellite, for example, transmits multiple down-link communications signals in the 248 to 256 MHz band.

The interference (or jammer) signals of interest were defined as having a spectral power bandwidth of at least 100 kHz with a power component within the 25 kHz signal bandwidth not greater than the signal power. This latter condition ensures a signal-to-interference-plus-noise ratio greater than approximately 0 dB within the 25 kHz desired signal bandwidth. A further objective, however, was to obtain a design which would effectively suppress interference when the signal-to-interference ratio within the desired signal band was much less than 0 dB. In particular, the interference signals of interest were expanded to include those having most of their energy concentrated outside the desired 25 kHz signal bandwidth. Among the jammers or interferers that fall into this category are high-level barrage jammers (or wideband, > 10 MHz) and narrowband jammers that have their power concentrated within one of the multiple desired signal bands. Thus, the UHF adaptive array implementation is to provide the dynamic range and flexibility necessary to effectively suppress a wide range of interference and jammer waveforms. Jammer or interference suppression was to be performed over the full 10 MHz bandwidth to provide AJ protection for the multiple signals transmitted from a single source. To further enhance signal reception, the array pattern gain in the direction of the desired signal source was to be maximized simultaneously with jammer suppression. This latter objective was to be accomplished using knowledge of the desired signal spectrum but without

prior knowledge of the desired signal or jammer signal locations or waveform structures. In addition the adaptive array processor was to be designed to interface with any four-element antenna array to the extent that a particular array geometry or set of antenna element characteristics are not necessary to implement adaptive processing.

These general requirements led to the definition of more specific design objectives and requirements. One objective was to maintain a high-degree of adaptive control flexibility to permit implementation of a broad variety of adaptive control algorithms that best accommodate different jammer and signal situations and jammer strategies. A second objective was to demonstrate a capability for improving the signal-to-interference-plus-noise ratio by at least 20 dB under wideband interference conditions and by at least 30 dB under narrowband interference conditions. An added goal was to adapt from a random to a steady-state maximum signal-to-interference-plus-noise ratio within 10 milliseconds without causing significant modulation of the desired signal as a result of adaptive feedback control. Example hardware requirements included an array noise figure of less than 6 dB, a sensitivity of -117 dBm, and a dynamic range of 87 dB.

SUMMARY OF PROGRAM GOALS

- Design and build a four-element array processor to be used for research in the design of a fleet-deployable adaptive antenna system
- Demonstrate the adaptive array's increased capability to provide AJ protection for naval communication and satellite systems
- Maximize the array's S/N and S/I ratios
- Design algorithms into the control software that provide flexibility in modifying the adaptive antenna pattern
- Provide capability for the array to adapt within 10 ms without significant modulation of the desired signal
- Adaptive array to be applicable to systems using common modulation techniques
- Adaptive array to provide jammer suppression over a 10 MHz bandwidth
- Implement adaptive processor independent of array geometry or antenna element characteristics
- Array noise figure: < 6 dB
- System sensitivity: -117 dBm
- Dynamic range of the antenna pattern forming network: 87 dB

2. OVERVIEW OF DEVELOPMENT EFFORT

A UHF adaptive array processor for adaptively controlling the pattern of any four-element antenna array has been developed and extensively tested. The hybrid analog/digital design combines the advantages of IF weighting with the flexibility of software implemented adaptive feedback control algorithms to suppress jammers while providing the maximum gain from desired signals.

The adaptive array processor development was divided into three tasks. Task I, Design and Fabrication, was concerned with the design and fabrication of the analog and digital hardware and the integration of this hardware with the antenna elements and the PDP-11/05 control computer. This task included an analysis to determine such hardware requirements as dynamic range, component tolerances, and bandwidth.

Task II, Software Development, included the development of selected adaptive algorithms to control the array antenna pattern and background subroutines required to control the transfer of data. The algorithms currently implemented are confined to those required to demonstrate the hardware and thus do not reflect the full flexibilities available through computer software control. Further development of algorithms is an area for subsequent study.

The final task, Systems Test and Evaluation, included both laboratory and field testing of the adaptive array processor (see Figure A). The field testing was performed on the Hughes antenna test range, with additional performance evaluation obtained from tests conducted aboard the Naval destroyer USS Richard E. Byrd.

Briefly, the adaptive array processor shapes the antenna array pattern by controlling the array antenna element weights. The general objective is to automatically steer pattern nulls on jammers and a pattern maximum on the desired signal. Adaptive control is based on estimates of the cross-covariance of the output from the weighted array and the individual antenna element outputs. Measured values of the cross-covariance of each (hard-limited) antenna element signal with the array output provide a vector input to the processor weight control subsystem to effect the adaptive feedback control. The cross-covariance measurements convey sufficient information to obtain a set of weighting coefficients which optimize or nearly optimize (within 3 dB) the output signal-to-interference plus thermal-noise ratio without prior knowledge of jammer locations or characteristics. The implementation accommodates several different techniques for maximizing gain on the desired communications signal, including the use of known desired signal location or spectral information (per the contract requirements).

The use of computer-controlled weighting functions allows for a general-purpose UHF adaptive processor which can implement a broad class of adaptation algorithms. For example, the processor can be used in open-loop beamforming, constrained main beam null-steering, or fully adaptive (main beamforming/null-steering) modes of operation (see Section 4). The processor can also be used to implement other algorithms as they are developed. Computer control also allows the parameters of adaptation, or the adaptive algorithm itself, to be selected on a real-time basis to accommodate a particular signal environment or to counter new jammer strategies.

The processor consists of an analog RF subsystem and a digital control subsystem (see Figure B). These subsystems interface at the output of the cross-covariance measurement circuits and at the antenna element weights and represent an optimum utilization of the analog and digital hardware. The PDP-11/05 computer in the digital control subsystem was chosen because of its powerful instruction set and the ease with which peripherals can be integrated into the system.

The weighting and cross-covariance circuits are implemented at an IF frequency (IF) to allow tuning over the 225 to 400 MHz UHF band. The 10 MHz processing bandwidth is established at the IF, prior to the weighting and cross-covariance circuits. Cross-covariance measurements are averaged prior to analog-to-digital conversion to reduce real-time processing requirements while allowing continuous monitoring of the data.

The adaptive array has been tested with a four-element OE-82 Navy satellite communications antenna and a four-element linear array. Typical test results are given in the following topic, with additional results appearing in Section 5.

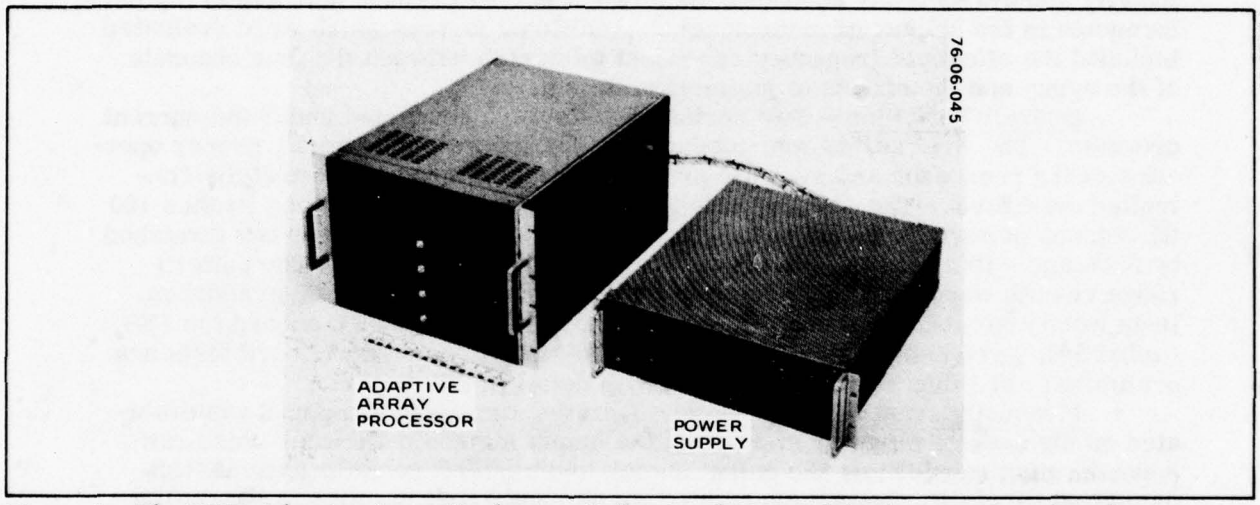

Figure A. The UHF Adaptive Array Hardware. Following design and implementation, the adaptive array processor was laboratory and field tested, with additional evaluations resulting from shipboard tests.

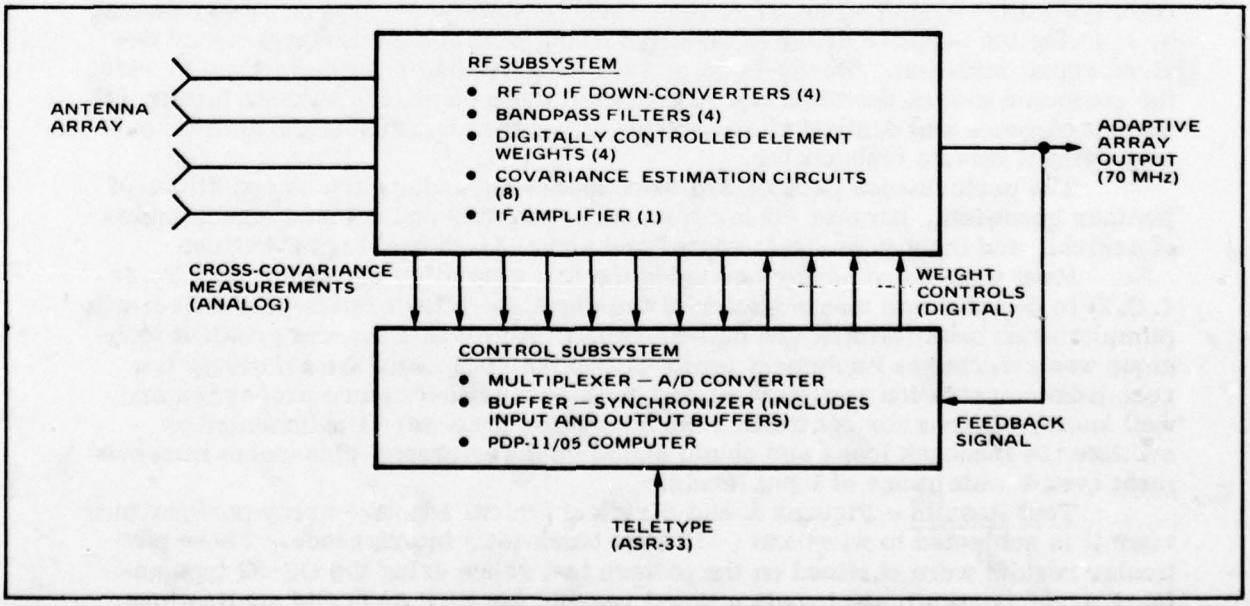

Figure B. Functional Overview of the UHF Adaptive Array Processor. This adaptive computer-controlled processor can implement all covariance estimation based adaptive control algorithms with its programmable control subsystems.

3. RESULTS OF ARRAY PERFORMANCE TESTS

System tests were conducted to evaluate the adaptive array performance under laboratory conditions and under conditions similar to those encountered aboard ship. In pattern range tests, the adaptive array improved the output signal-to-interference-plus-noise ratio by up to 28 dB under wideband interference conditions and up to 36 dB for narrowband interference.

The primary objective of the system tests was to demonstrate the adaptive array's capability for significantly reducing the vulnerability of Navy communications to interference and jammer sources. The tests were conducted to evaluate measured performance compared with the overall objectives and to attempt to identify and evaluate any additional factors which could reduce adaptive array performance in the shipboard environment. Additional factors which were evaluated included the effects of frequency dependent mismatch between the four channels of the array and the effects of jammer multipath.

Overall Test Plan – Two series of tests were conducted under the current program. The first series was conducted in the laboratory to verify proper operation of the processor and evaluate processor parameters under carefully controlled conditions. The second series of tests were conducted on the Hughes 100 ft. antenna pattern range using the four-element OE-82B antenna array furnished by NRL and a four-element linear array constructed by Hughes. The pattern range results were used to evaluate overall system performance. In addition, tests were also conducted under a subsequent contract with NRL aboard the USS Richard E. Byrd using the OE-82B array. Results from the shipboard tests are preliminary and thus are not presented with detail in this report.

Measuring Array Performance – Adaptive array performance was evaluated on the pattern range by measuring the output signal-to-thermal-noise ratio (beamforming capability), the output signal-to-interference ratio (cancellation or nulling capability), and the steady-state antenna array patterns. Adaptation time was measured by observing the system signal output as a function of computer measurable adaptation time after the computer releases the weighting loops from the initial omnidirectional setting. Steady-state performance was measured by allowing the adaptive array to stabilize to the particular interference and desired signal situation. Steady-state pattern measurements were obtained by using the computer to lock the weighting networks at their stabilized values, turning off the interference and desired signal sources, and then measuring the antenna pattern using a remote transmitter.

The performance parameters were measured under various conditions of jammer bandwidth, jammer center frequency, jammer and desired signal angles of arrival, and input jammer-to-signal and signal-to-thermal noise ratios.

Most tests were performed using the full adaptation algorithm (see Topic 4.C.2) to demonstrate maximization of the signal-to-interference-plus-noise ratio (simultaneous beamforming and null-steering). A steepest descent gradient technique was selected to implement feedback control because of the relatively low real-time computation requirement and because its convergence properties are well known. Means for controlling the adaptation time were implemented to stablize the feedback loops and obtain signal-to-interference-plus-noise improvement over a wide range of input levels.

Test Results – Figures A and B reflect typical adaptive array performance when it is subjected to wideband (~12 MHz bandwidth) interference. These particular results were obtained on the pattern test range using the OE-82 type antenna array currently deployed on Naval vessels for UHF SATCOM applications.

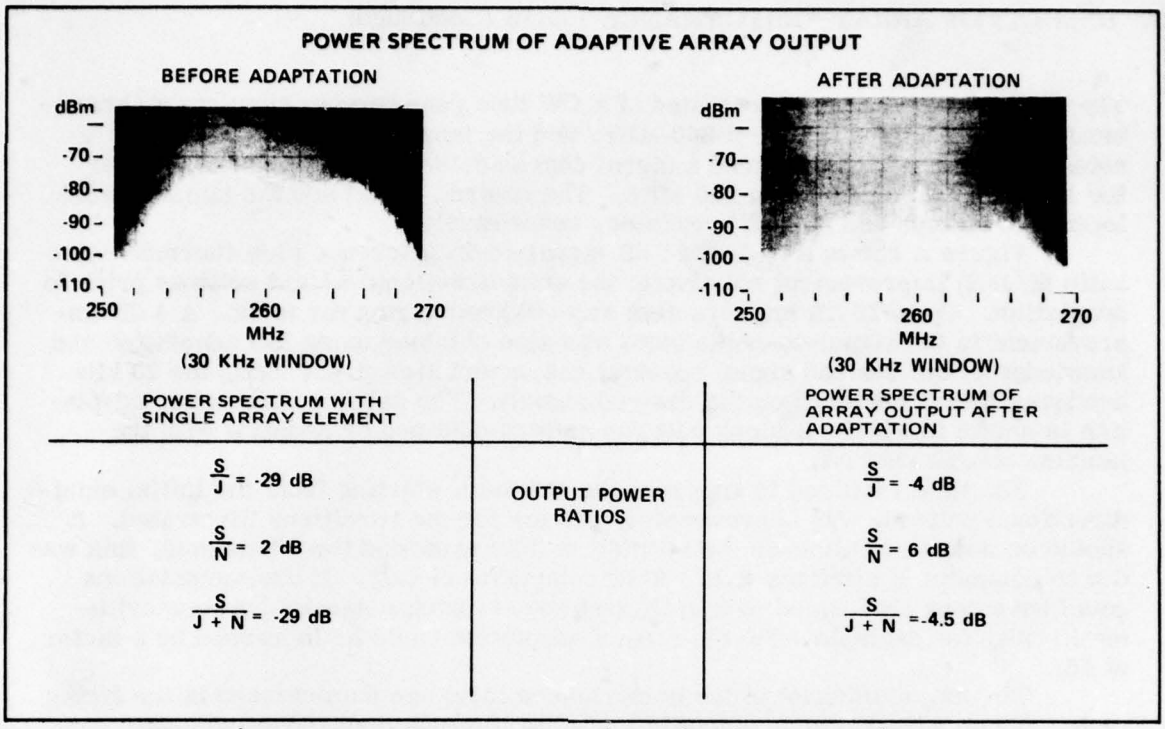

Figure A. UHF Adaptive Array Processor Typical Results Showing 24 dB J + N Improvement; CW Signal, Wideband Jammer. The adaptive processor also improves the signal-to-thermal noise ratio by 4 dB.

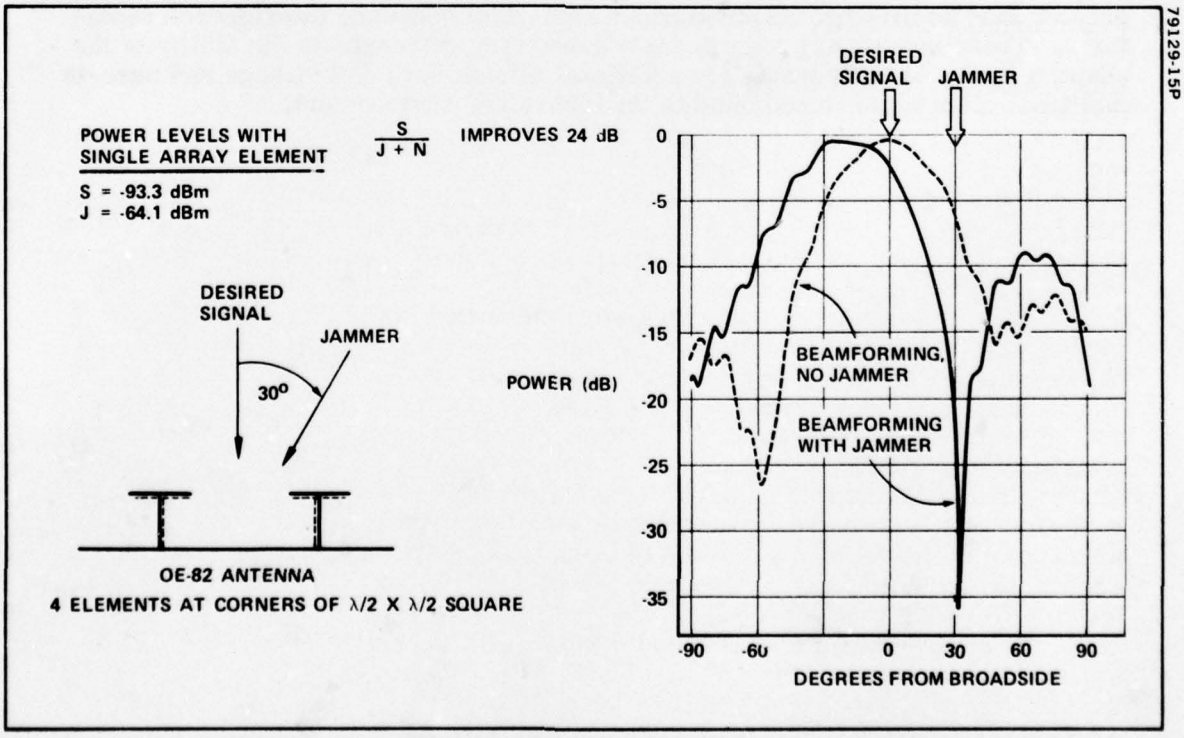

Figure B. UHF Adaptive Array Patterns After Adaptation, CW Signal, Wideband Jammer. For a wideband jammer (12 MHz), the improvement in signal-to-jammer ratio is approximately 24 dB.

3. RESULTS OF ARRAY PERFORMANCE TESTS (Continued)

The desired signal source consisted of a CW tone generator to simulate a narrowband communications signal at 260 MHz, and the jammer source consisted of a noise generator which produced a signal characterized by a flat spectrum over the 12 MHz band centered on 260 MHz. The desired signal and the jammer were located broadside and 30° off broadside, respectively.

Figure A shows a typical 24 dB signal-to-interference plus-thermal-noise ratio (S/J+N) improvement relative to the omnidirectional weight settings prior to adaptation. Up to 28 dB improvement was obtained during the tests. A 4 dB improvement in the signal-to-noise ratio was also obtained using full adaptation and knowledge of the desired signal spectral characteristics (i.e., using the 25 kHz bandpass filters centered on the desired signal). The array pattern after adaptation is shown in Figure B along with the pattern obtained by adapting with the jammer source shut off.

The time required to suppress the jammer, starting from the initial omnidirectional pattern, was approximately 200 ms for the conditions illustrated. It should be noted that although the adaptation time exceeded the 10 ms goal, this was due to computer limitations (i.e., slow computation) only. If the computations could have been performed with sufficient speed (using a special purpose arithmetic unit, for example), the the rate of adaptation could be increased by a factor of 40.

The major findings of the performance tests are summarized in the facing table. The configuration and detailed results of the pattern range tests are given in Section 5. Although detailed results of the shipboard tests are not presented herein, preliminary findings indicate that the adaptive array performed nearly as well in the shipborne environment. For example, S/J+N improvements greater than 20 dB were obtained under high-level wideband interference conditions. These results are significant because they demonstrate the ability of the adaptive array to compensate for additional effects such as blockage and near-in multipath often encountered outside the laboratory environment.

SUMMARY OF ADAPTIVE ARRAY TEST RESULTS

- Up to 28 dB $\frac{S}{J+N}$ improvement under wideband (>10 MHz) jammer conditions.
- Up to 36 dB $\frac{S}{J+N}$ improvement under narrowband (<<1 MHz) jammer conditions.
- $\frac{S}{J+N}$ improvement generally several dB less using OE-82 antenna due to antenna element mismatch.
- Less improvement obtained under wideband interference due to frequency dependent mismatch between the four array processor channels.
- Antenna gain was increased in the direction of the desired signal while nulling high-level jammers using
  - desired signal spectral characteristics when the interference was wideband or outside the 25 kHz desired signal bandwidth
  - a known code to spread the desired signal spectrum when the interference has an arbitrary spectrum
- Signal-to-jammer ratio improvement was obtained over an 87 dB range of input signals.
- Adaptation times on the order of 200 ms due to slow computer.
- Wideband weights are required to prevent significant performance degradation due to the presence of jammer multipath.

4. CONCLUSIONS AND RECOMMENDATIONS

The results of extensive tests have demonstrated that the UHF adaptive array can be used to significantly reduce interference in communications systems. Possible growth items to improve and expand the basic performance capability include: the development of adaptive algorithms in software to effectively counter sophisticated jammer strategies, adding a 9-bit high-speed arithmetic/buffer unit for processing complicated algorithms without through-put delay, adding delay loops for multipath delay cancellation and compensation of frequency dependent mismatch between channels.

The UHF adaptive array project allowed for the opportunity to identify areas for potential growth in order to improve and expand the basic performance capability. The details of several possible growth items are described in the following paragraphs.

Adaptive Algorithms – The UHF adaptive array implementation provides the flexibility to evaluate various algorithms by software programming modifications. This program did not attempt to develop new algorithms or to analytically evaluate those currently in existence. Rather, the goal was to evaluate the flexibility of computer programming to incorporate a meaningful number of the repertoire of existing mean square algorithms. A further algorithm development effort is recommended to accommodate sophisticated jammer strategies (e.g., cooperative blinking jammers) and to improve convergence properties of the current adaptive array algorithms. A detailed discussion of adaptive algorithms is given in Subsections 4.B and 4.C and in Appendices B and C.

High Speed Arithmetic/Buffer Unit – The adaptation time of the adaptive array is currently limited by the through-put delay in the selected computer. For example, the time required to compute a new set of weighting coefficients increased the interval between weight updates to approximately 8 milliseconds, which is a factor of 40 longer than the time required to measure the covariance data from which these weights are computed. Unfortunately, high-speed computation is not available in off-the-shelf minicomputers. The PDP-11/05 was selected in the current program to perform the required control and computations because of the ease with which the peripherals can be integrated and because of its asynchronous bus. In future implementations, the PDP-11/05 can be utilized as the control and programmer for the configuration shown in Figure A. This growth configuration utilizes a high speed arithmetic unit with a limited instruction set selected for the specific functions required by the adaptation algorithms. This growth option also incorporates a faster sampling rate (less than 200 μs between measurement samples) to allow greater flexibility and faster convergence under certain conditions.

Surface Acoustic Wave Filters – Unique, highly selective IF bandpass filters that have a linear phase characteristic and identical tracking characteristics can be implemented using surface acoustic wave (SAW) filters. Of special interest is the ability to produce units with identical – "matched" – transfer functions. Failure of the four adaptive array IF channel transfer functions to track each other over the 10 MHz bandwidth was a limiting factor in the wideband jammer cancellation performance of the UHF adaptive array. A detailed discussion of the limitations caused by phase/amplitude tracking errors in the RF or IF channel is given in Topic 2.2.

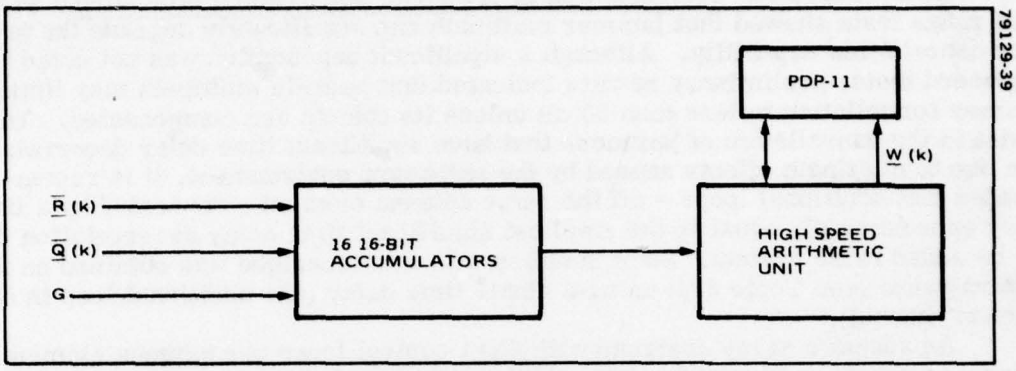

Figure A. High Speed Arithmetic/Buffer Unit. The PDP-11/05 was selected in the current project with the objective of utilizing it as the control and programmer.

4. CONCLUSIONS AND RECOMMENDATIONS (Continued)

Delay Loops for Compensation of Multipath and Channel Mismatch – Pattern range tests showed that jammer multipath can significantly degrade the jammer cancellation capability. Although a significant degradation was not noted in shipboard tests, preliminary results indicated that near-in multipath may limit jammer cancellation to less than 30 dB unless its effects are compensated. To assist in the cancellation of jammers that have significant time delay decorrelation due to multipath effects caused by the shipboard environment, it is recommended that additional loops – off the same antenna element – separated by a time delay approximately equal to the smallest significant time delay decorrelation delay be added to the system. Some success with this technique was obtained on the pattern range (see Topic 5.4) using a single time delay (one additional loop in one antenna channel).

An adaptive array designed with 2N+1 control loops per antenna element channel is shown in Figure B. The addition of multiple loops in each single channel not only provides compensation for multipath effects, but also partially compensates for frequency-dependent mismatch channel transfer functions caused by non-tracking of antenna element or of RF/IF hardware transfer functions, or by finite antenna array bandwidth.

Resolution of the Weighting Elements – Each in-phase (or quadrature) weight was implemented using digitally controlled attenuators with 0.25 dB resolution. This finite resolution limited the jammer cancellation capability to approximately 36 dB. Techniques which can improve cancellation performance include the use of (1) higher resolution attenuators, (2) analog weight multipliers with a high resolution A/D converter, and (3) a low-gain analog control loop added to each channel for the purpose of "tweeking" the weight values. The latter technique can take on more sophisticated configurations such as tapped delay weighting in the low gain loop to obtain multipath and mismatch compensation.

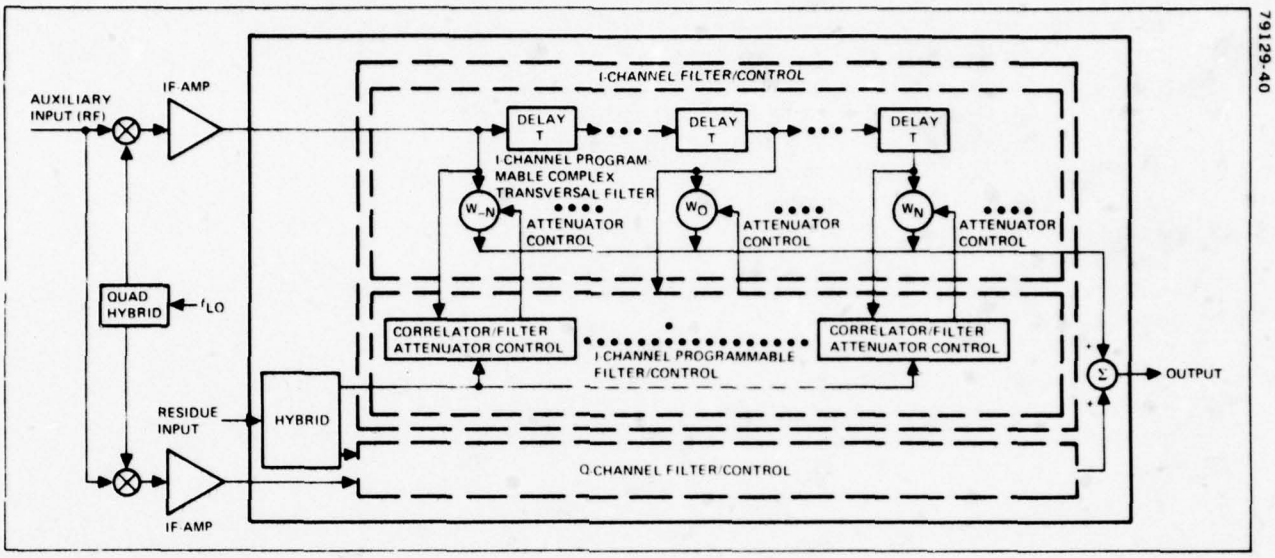

Figure B. Multiple Loop Design of the Adaptive Weight Function. The use of multiple tapped delay loops in each antenna channel can improve jammer cancellation by compensating for jammer multipath, array bandwidth, and antenna dispersion effects.

SECTION 1
TECHNICAL APPROACH TO UHF ADAPTIVE ARRAY PROCESSOR DESIGN

Section 1 – Technical Approach to UHF Adaptive Array Processor Design

1. DESCRIPTION OF SIGNAL REQUIREMENTS

The characteristics of both desired communication signals and interference signals which are envisioned in UHF adaptive array LOS and SATCOM applications have been analyzed. While the desired signals are 25 kHz in bandwidth and use any of the common modulation techniques, the interference signals can have any modulation, but they differ from the desired signal in spectrum or code structure.

Although the adaptive array concept is applicable to a wide range of signal situations, overall adaptive array performance improves when the implementation is tailored to the specific application using as much information as possible regarding desired signal characteristics and expected interference situations. These signal and interference characteristics were of particular importance in the UHF adaptive array implementation since they directly influenced the dynamic range requirements, the adaptive algorithms, and the methods used to perform desired signal maximization.

Desired Signals – The adaptive array processor is designed to demonstrate increased antijam protection for shipboard and airborne Naval line-of-sight (LOS) communications and satellite communications (SATCOM) systems. SATCOM channels are vulnerable to in-band jamming because the down-link signals have relatively low levels. Although airborne and shipborne LOS systems generally operate with much higher signal levels, they remain vulnerable in deep penetration missions because of the relative proximity to the jammer sources. Operation with both SATCOM and LOS signals led to the requirements for operation with desired and interference signal levels referred to the antenna element inputs of -117 dBm to -30 dBm at 1 dB gain compression, and for an overall system noise figure less than 7 dB referenced to the antenna array input.

The desired (communications) signals of interest are within the 225-400 MHz UHF band and use any of the common modulation techniques such as AM, FM, FSK, PSK, or QPSK with data bandwidths up to and including 19.2 kbps. These signals are specified to occupy a 1 dB bandwidth that does not exceed 25 kHz. Typical signals to be used with the Navy FLTSAT channels, for example, use 75 bps or 2400 bps data. A given communication channel can contain a multiplicity of such signals with center frequencies allocated over a 10 MHz band. For example, the Gapfiller satellite transmits in three bands which together occupy the 248 to 256 MHz band. The desired signal set also includes P-N code modulations used to spread the signal bandwidth up to 10 MHz, although the P-N code is presumed known so the signal bandwidth can be compressed to an informative bandwidth of less than 25 kHz. The spread-spectrum requirement was added to permit operation with the NRL PTT spread-spectrum modem.

The above specified signal characteristics are sufficient to define a 10 MHz jammer suppression bandwidth and 25 kHz filter bandwidth for spectral separation of the desired signal from jammers. Jammer suppression over the full 10 MHz bandwidth affords AJ protection for the spread-spectrum desired signal or for multiple narrowband signals transmitted from a single source. The 25 kHz filters can be used to maximize gain in the direction of the desired signal using knowledge of the desired signal center frequency (and code modulation if required) but without prior knowledge of the interference and desired signal waveforms and locations.

Interference Signals – The adaptive array is designed to suppress interference and jammer signals coming from an unknown direction within the field of view of the antenna array ($\pm 90^{o}$ from array broadside). Typical interferers would be other FLTSAT signals, UHF voice communications, wideband signals like TATS (from the FLTSAT Air Force wideband channels) or UHF TDMA signals.

CW interference, wideband pulse signals (from UHF radars), and deliberate jammers are also candidate interferers. Deliberate jammers would include CW, barrage, pulsed, and blinking signals designed to disrupt the communication link, and more sophisticated strategies that would attempt to disrupt the adaptive array. Because of its flexible design that allows modification of the adaptive algorithms in software, the UHF adaptive array can be configured to handle this broad class of interfering signals. However, no attempt was made to implement modified algorithms in the current project since test conditions were confined to those necessary to demonstrate the hardware. These modifications are discussed in Sections 4 and 5. Areas of future study are also identified in Topic S.4.

Signal Assumptions for Testing – For the purposes of demonstrating adaptive array performance, the interference (or jammer) signals were defined as stationary (e.g., CW) narrowband (<<1 MHz) or wideband signals. The types of interference signals were further defined by the technique used to separate the desired signal from interference (to allow maximization of the signal-to-interference-plus-thermal noise ratio). For example, in cases where P-N coding gain was used to separate a spread-spectrum desired signal from interference, interference was defined as any signal which did not contain the same code modulation. In cases where separation was obtained on the basis of spectral differences, the interference was defined as any signal which had most of its energy outside of the 25 kHz desired signal bandwidth. The latter category includes wideband interference with spectra as shown in the figure. Also included is interference with spectrum confined to frequencies outside the 25 kHz band of one desired signal but within the band of another (i.e., one of the desired signals transmitted from a multichannel source is being interfered).

To demonstrate a significant AJ capability, the signal-to-interference-plus-thermal noise ratio was to be maximized for input interference to desired signal ratios up to and exceeding 20 dB for wideband interference and 30 dB for narrowband interference.

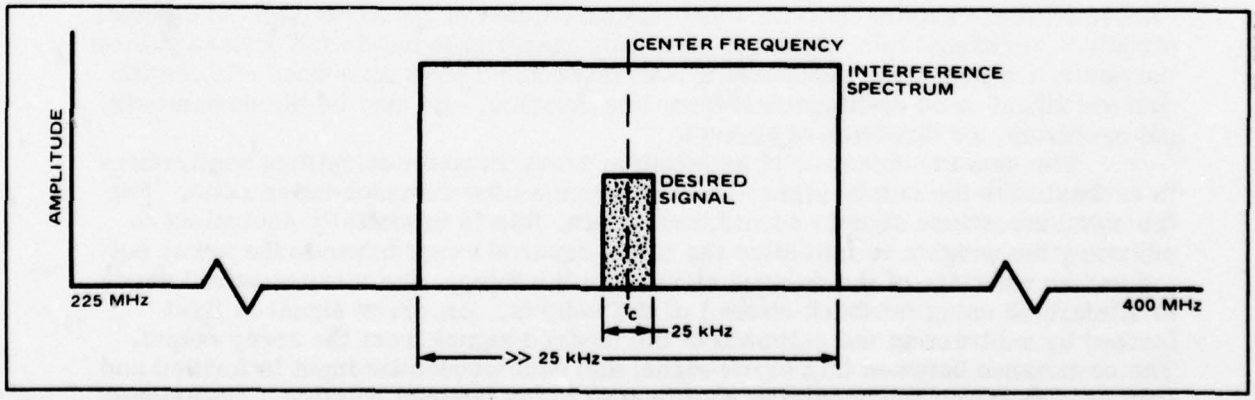

Possible Interference and Desired Signal Spectrum. Wideband interference was defined to include any signal that has most of its energy outside the 25 kHz desired signal bandwidth.

2. PRINCIPLES OF ADAPTIVE ARRAY PROCESSING

The adaptive array is capable of placing deep antenna pattern nulls in the direction of interference sources without prior knowledge of their locations and thus offers a means for reducing system vulnerability to interference. The array is also capable of enhancing the signal-to-thermal-noise power ratio if some a priori information regarding the desired signal is available.

The essential elements of an adaptive array system are the antenna array and the weighting coefficients (illustrated in the figure). The adaptive array basically functions to reshape the array antenna pattern to place pattern nulls in the directions of undesired (interference) signals while maintaining a high gain in the directions of desired (communications) signals. The array pattern is formed by weighting the antenna element outputs (via phase shift and attenuation) and algebraically summing them as shown to form the array output. Phase and amplitude control can be accomplished by adjusting the sign and amplitude of both in-phase and quadrature components of the input signals.

The adaptive antenna array differs from conventional arrays in that the antenna pattern is determined by the interference and desired signal environment. Examples of adapted antenna patterns under various signal and interference conditions are given in the test results of Section 5. It should be noted that the ability of the adaptive array to suppress interference at arbitrary locations while providing gain for desired signals is limited by the antenna array itself. When the interference signal and the desired signal have the same angle of arrival relative to the array, for example, maximization of S/I does not yield any improvement. More generally, the maximum S/N and S/I which can be obtained with an adaptive array depends on antenna array (angular) resolution, the individual antenna element patterns, the angular separation between the desired signal and interference sources, and (usually to a lesser extent) the input-signal-to-interference and signal-to-noise power ratios.

In communications systems, the locations and waveforms of interfering sources are generally unknown. The information required to suppress interference must therefore be obtained from measurements of the array input and output signals. Additional information is generally required to maximize pattern gain on the desired signal while suppressing interference. This information enables the desired signal to be distinguished from interference, and may be the desired signal spectrum, or direction of arrival.

The general objective of an adaptive array in communications applications is to maximize the output-signal-to-interference-plus-thermal-noise ratio. For the communications signals considered herein, this is essentially equivalent to adjusting the weights to minimize the mean-squared error between the array output and an estimate of the desired signal. In the figure, the mean-squared error is minimized using feedback control of the weights. An error signal is first formed by subtracting the estimate of the desired signal from the array output. The covariance between this error signal and each processor input is formed and then used to direct the weighting coefficients to the desired solution. Covariance estimation is performed by averaging the product of the array output signal and each input signal; 2M correlators are required to control the in-phase and quadrature weights in an M-element adaptive array. Ideally, implementing this configuration leads to an optimum adaptive array processor in which the weights converge toward maximization of the output signal-to-interference-plus-thermal-noise ratio in a stationary signal environment.

Assumptions made in the above discussion, however, are too restrictive to apply in most applications of interest, particularly the envisioned UHF adaptive array applications. First, the desired signal conveys information and therefore is unknown a priori. One possible solution is to impose constraints which force the array pattern to have maximum gain in the desired signal direction. This approach can be implemented with the UHF adaptive array but requires knowledge of the desired signal location and presumes full knowledge of antenna element characteristics and location. However, the UHF adaptive array is also required to operate without knowledge of antenna characteristics or desired signal location. In these cases, maximization on the desired signal simultaneous with interference cancellation is achieved by estimating the desired signal based on known spectral or code modulation characteristics. This estimate is then used in estimating the beam-steering (covariance) vector $\underline{Q}$, which can then be used to maximize the signal-to-interference-plus-thermal-noise ratio.

Additionally, accuracy of hardware components and cancellation bandwidth (the bandwidth over which interference correlation is required) affect the adaptive array performance. Failure of the individual antenna elements and weighting circuits (and associated hardware not shown) to track each other across the cancellation bandwidth impairs the degree of achievable cancellation and thus reduces performance. Interference cancellation is also reduced for off-broadside jammers due to propagation delay across the antenna aperture. These and other factors which limit adaptive array performance are discussed in detail in the following sections. It should be noted that the methods described to control the weights and to estimate $\underline{Q}$ for beam-steering incorporate closed-loop techniques which tend to compensate for many hardware imperfections commonly encountered in practice (e.g., anomalies in the antenna patterns caused by mutual coupling and other effects). This was a primary consideration in the selection of closed-loop control over the open-loop control methods (see Section 4).

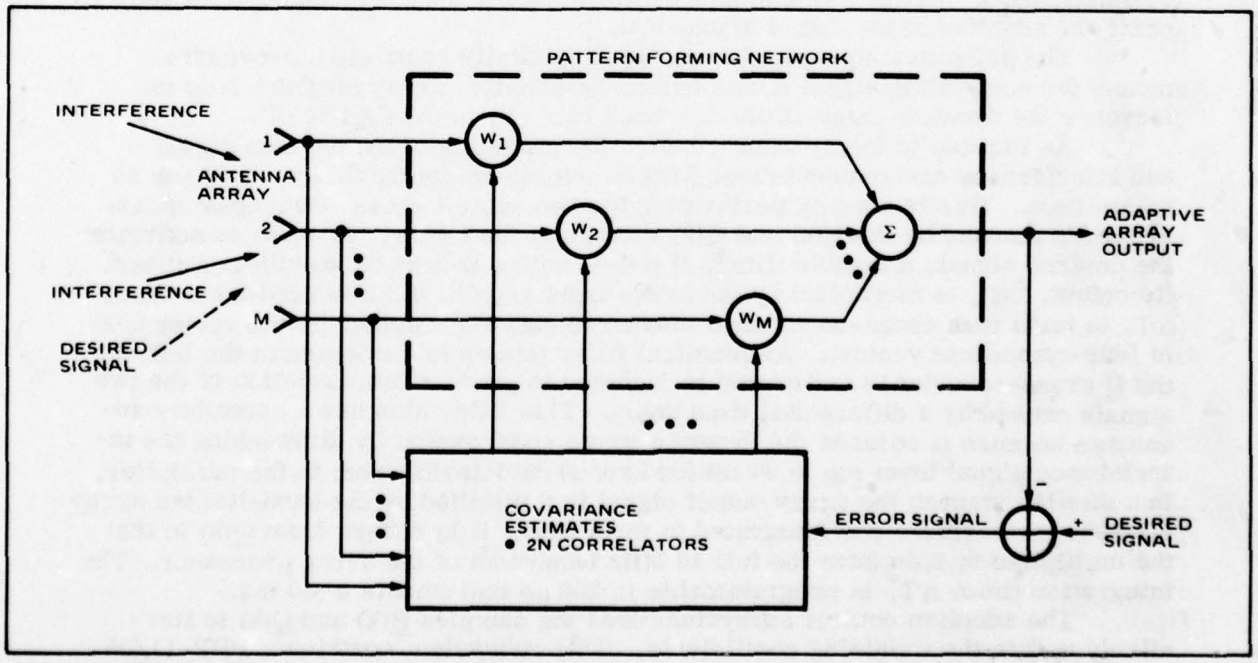

Functional Diagram of an M-Element Adaptive Array. This simplified model illustrates basic adaptive array principles. The UHF adaptive array primarily differs from this model in that the weights are computer controlled for added flexibility and a known desired signal is not required.

3. FUNCTIONAL DESIGN OF THE ADAPTIVE ARRAY PROCESSOR

The adaptive array processor is functionally designed to maximize S/I and S/N by placing pattern nulls in the direction of interference, while increasing the main beam gain in the direction of the signals of interest. In performing these functions computer control is exploited because the programmability feature provides the degree of versatility essential to the control algorithms.

The general functional requirement of the adaptive array is to maximize the signal-to-thermal noise power ratio (S/N) while simultaneously maximizing the signal-to-interference power ratio (S/I). Based on the concept of measuring only the time average estimates of the cross-covariance vectors $\underline{R}(k)$ and $\underline{Q}(k)$, this design has the flexibility to implement a wide range of adaptive algorithms while avoiding the problems (through-put and sampling rate) of processing wide-band data.

A functional diagram of the UHF adaptive array is shown in the opposite figure. The array processor is designed for operation with a four-element antenna array and consists of an antenna pattern forming network, the cross-covariance estimation circuits, and an adaptive control subsystem.

The antenna pattern forming network contains an RF/IF down-converter and a weight control for each of the four antenna signals. The input signals are first down-converted to a 70 MHz IF frequency, passed through 10 MHz IF filters to establish the processor bandwidth (cancellation bandwidth), and then applied to the weighting coefficients. Each weight consists of an in-phase and quadrature attenuator pair to effect full amplitude and phase control. Weighting is performed at IF to allow tuning over the 225-400 MHz UHF band and to ease bandwidth requirements on hardware used to implement the weights and the cross-covariance function. The weight attenuators are digitally controlled using 8 bits plus sign. The weighted IF signals are summed algebraically in a hybrid combiner to generate the adaptive array output signal V(t).

The programmable gain IF amplifier (digitally controlled) provides a means for controlling signal levels within the adaptive array feedback loop to increase the dynamic range of the feedback loops by more than 20 dB.

As implied in the preceding topic, the statistics of the desired signal and interference environment must first be estimated before S/N and S/J can be maximized. This is done by performing the two sets of cross-covariance measurements denoted by the $\underline{R}(k)$ and $\underline{Q}(k)$ vectors in the figure. In order to estimate the desired signal, a tunable filter, $H(f-f_2)$, with a 25 kHz bandwidth is utilized. Its output, $\hat{z}(t)$, is multiplied by the array input signals and averaged for a time, ΔT, to form four cross-covariance measurements represented by the vector $\underline{Q}(k)$ (a four-component vector). An identical filter (shown in the figure to the left of the $\underline{Q}$ cross-covariance estimator) is included to prevent decorrelation of the two signals caused by a differential time delay. This filter also has a secondary advantage because it reduces the dynamic range requirement by diminishing the interference signal level (up to 26 dB for broadband interference) to the multiplier. In a similar manner the array output signal is multiplied by the hard-limited array element input signals and integrated to form $\underline{R}(k)$. $\underline{R}(k)$ differs from $\underline{Q}(k)$ in that the multiplied signals have the full 10 MHz bandwidth of the array processor. The integration time, ΔT, is programmable in 200 μs increments to 50 ms.

The adaptive control subsystem uses the samples $\underline{R}(k)$ and $\underline{Q}(k)$ to iteratively update the weighting coefficients. This subsystem contains a PDP-11/05 minicomputer and associated hardware, such as I/O buffers, sample/holds, and A/D converters, required for interfacing the computer with the covariance

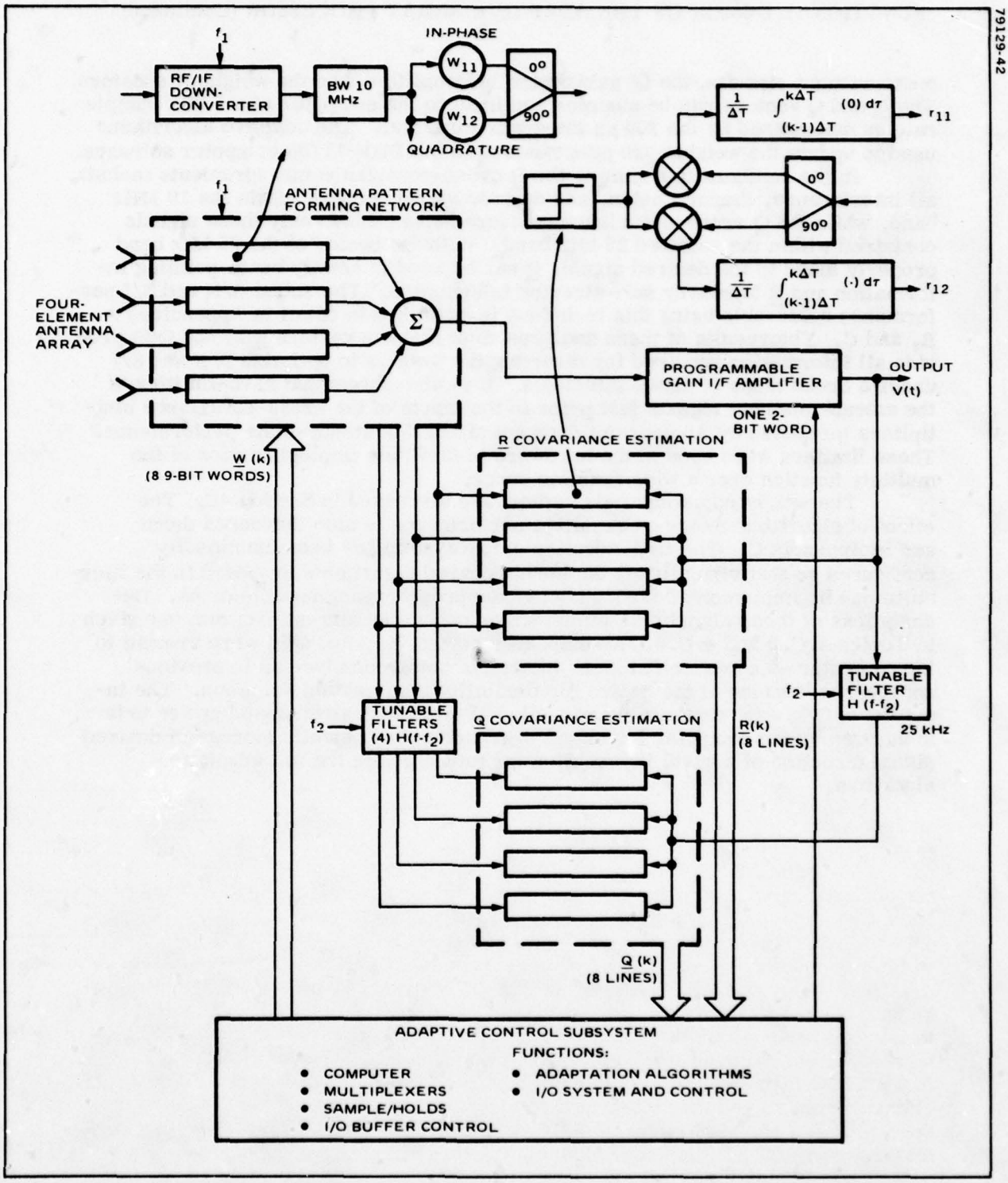

Functional Implementation of UHF Adaptive Antenna Array. The versatility of the algorithms in the controller (computer), operating on the covariance estimates for vectors $\underline{R}(k)$ and $\underline{Q}(k)$, enable the antenna pattern forming network to simultaneously maximize the S/N and the S/I.

3. FUNCTIONAL DESIGN OF THE ADAPTIVE ARRAY PROCESSOR (Continued)

measurement circuits, the IF gain controlled amplifier, and the weight attenuators. The $\underline{R}$ and $\underline{Q}$ vectors can be sampled and input to the computer at a 5 kHz sample rate as determined by the 200 μs integration interval. The adaptive algorithms used to update the weights are programmed in the PDP-11/05 computer software.

In the configuration shown, the $\underline{R}$ cross-covariance measurements include all interference, thermal noise, and desired signal sources within the 10 MHz band, while the $\underline{Q}$ cross-covariance measurements include only those signals contained within the selected 25 kHz band. With the center of the 25 kHz band properly tuned to the desired signal, $\underline{Q}$ can be used to convey beam-pointing information and $\underline{R}$ to convey null-steering information. The actual S/N and S/I performance achievable using this technique is examined in detail in Appendices A, B, and C. The results of these analyses show that the vectors $\underline{R}(k)$ and $\underline{Q}(k)$ provide all information required for directing the weights to optimize S/N and S/I under a broad class of signal situations. It is also shown that hard-limiting of the antenna element signals just prior to the inputs of the cross-covariance multipliers (proposed by Applebaum) does not affect this steady-state performance. These limiters were used in the hardware to facilitate implementation of the multiply function over a wide dynamic range.

The weight adjustment algorithms are discussed in Section 4C. The effect of algorithm choice on resultant performance is also discussed there and in Appendix C. The UHF adaptive array system has been functionally configured so that virtually all the mean squared algorithms proposed in the literature can be implemented through computer programming modifications. Descriptions of those algorithms implemented under the current program are given in Topics 4.C.2 and 4.C.3. As discussed above, $\underline{R}(k)$ and $\underline{Q}(k)$ were brought to the computer as separate functions instead of being combined as in previous approaches because of the desire for flexibility in algorithm selection. The inputting of $\underline{Q}(k)$ as a separate function also allows the desired signal power to be monitored by the computer for signal degradation and permits storage of desired signal direction of arrival information for future use in the full adaptation algorithm.

SECTION 2
DESCRIPTION OF THE ANTENNA ARRAY

Section 2 – Characteristics of the Antenna Array

1. DESIRABLE CHARACTERISTICS FOR AN ADAPTIVE ARRAY ANTENNA DESIGN

Although significant interference cancellation has been achieved with the OE-82B antenna, increased performance would result with an array optimized for use with the processor. Such an array would provide matching between individual elements and possess element spacing designed to eliminate interferometer effects.

System performance during this contract has been constrained to that achievable with the OE-82B antenna array furnished by NRL and with an existing Hughes four-element array. However, increased performance would result if an antenna design were optimized for the adaptive array application. Such an antenna would have the characteristics described in this topic. It should be noted that although the OE-82B array as described in a following topic deviates somewhat from the desired characteristics, significant interference cancellation was nevertheless obtained because the UHF adaptive array processor incorporates output feedback to partially compensate for nonideal antenna characteristics.

The UHF adaptive array processor is designed to maximize the signal-to-jammer-plus-thermal-noise ratio at the summed IF output over a narrow bandwidth. The narrowband signal assumption is equivalent to the condition that the propagation delay across the array is much smaller than B^{-1}, where B is the processing bandwidth. The degree of (wideband) jammer cancellation which can be achieved with the current design is a function of how well this condition is satisfied. For example, cancellation of a wideband (10 MHz bandwidth) jammer is limited to approximately 30 dB when the jammer arrives endfire (worst-case condition) with respect to a two-element $\lambda_o/2$-spaced antenna array (f_o=300 MHz). Frequency dependent mismatch between individual elements of the antenna array also degrades jammer cancellation performance, as discussed in the following topic.

The antenna array aperture and frequency dependent mismatch should thus be minimized, subject to other system requirements (e.g., array resolution), in order to achieve adequate signal-to-jammer-plus-thermal-noise ratio performance under high-level interference conditions without the use of transversal equalizers (see Topic S-4).

Neglecting array bandwidth and mismatch effects, the optimum output signal-to-jammer-plus-thermal-noise ratio depends on the signal and jammer locations and power levels, the number and location of antenna elements, and the shape of the individual element patterns. The facing table lists the general characteristics of an antenna array designed to maximize the optimum signal-to-jammer-plus-thermal-noise ratio. The discussion of these desired characteristics applies to any signal or jammer location.

Number of Antenna Elements – Up to M-1 pattern nulls can be positioned independently by an M-element adaptive array. In effect, this limits the number of separately located jammers which can be nulled to a maximum of M-1. Although the output jammer power continues to be minimized in a mean-squared error sense when this number is exceeded, the signal-to-jammer ratio improvement can be much smaller unless some of the jammers are clustered about one angular location.

Since the desired signal angle of arrival may be near a natural null of the adapted pattern, an additional degree of freedom is often required to obtain an acceptable output signal-to-noise ratio. This additional degree of freedom is generally available if fewer than M-1 jammers are present.

An exception to this rule occurs if all jammers are located in one plane – the azimuth plane defined by the ocean surface, for example – and if at least one

pair of antenna elements is aligned perpendicular to that plane. In this case, the number of jammers (N_J) must be less than $M-N_P$ (where N_P = number of pairs aligned perpendicular to the jammer plane) in order to obtain an additional degree of freedom to beam up on a desired signal in the same plane. For the array in the figure below, N_J must be less than or equal to one for jammers located in the horizontal (or vertical) plane.

DESIRED ANTENNA ARRAY CHARACTERISTICS

Individual Elements

- Nearly identical antenna patterns with gain and phase characteristics that track over the 10 MHz processing bandwidth.
- Antenna patterns that provide sufficient gain toward all possible desired signal locations.

Array Geometry

- $\leq \lambda_0/2$ element spacing or non-uniform element spacing to reduce interferometer (grating null) effects.
- Sufficient resolution for minimum specified desired signal/jammer separation.
- Sufficient number of elements (degrees of freedom) for maximum specified number of jammers.

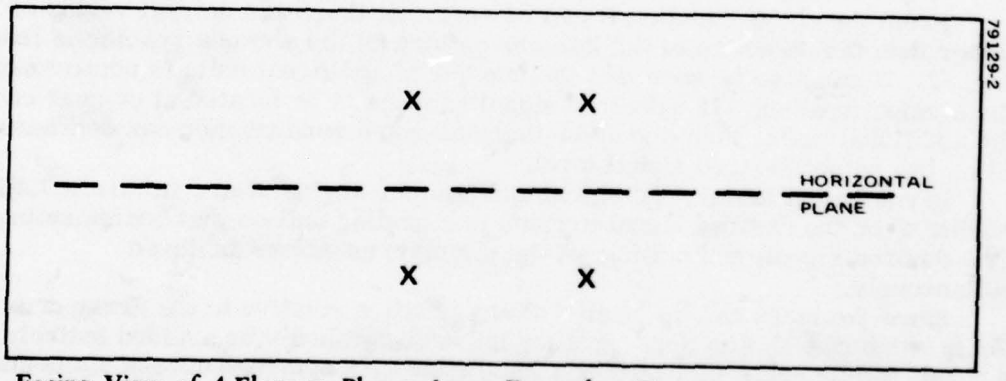

Facing View of 4-Element Planar Array Example. Two or more jammers can be cancelled in the horizontal plane but no beamforming in that plane can be achieved with two or more jammers present.

1. DESIRABLE CHARACTERISTICS FOR AN ADAPTIVE ARRAY ANTENNA DESIGN (Continued)

Positioning The Antenna Elements – The position of the elements within the array determines array resolution and interferometer (grating null) effects. In general, resolution increases as the array diameter increases. Higher array resolution improves the maximum output-signal-to-jammer-plus-thermal-noise ratio when the angular separation between the desired signal and the jammer is small. However, higher resolution implies sharper nulls, thus reducing the ability to place a "broad" null on clustered jammer sources.

Interferometer effects occur when the element spacing exceeds $\lambda_o/2$, where λ_o is the wavelength of the carrier frequency, and are generally undesirable in adaptive array applications. To show how grating nulls can occur, consider a linear equi-spaced array designed to produce an array pattern null at an angle θ_o (corresponding to a jammer location). In the process of forming this null, null, other nulls will occur at angles θ_N given by the following equation.

$$\sin \theta_N = \sin \theta_o - \frac{N\lambda_o}{d}$$

where

N = any integer

λ_o = carrier wavelength

d = spacing between elements

From the above equation it can be seen that there are no real values of θ_N other than the direction of the jammer so long as the element spacing is less than $\lambda_o/2$. It can also be seen that the number of additional nulls is proportional to the element spacing. If a desired signal happens to be located at or near one of the additional nulls, then signal-to-thermal-noise performance can decrease due to a low output desired signal level.

In equivalent terms, the signal and jammer angles of arrival are indistinguishable when the desired signal arrives in a grating null so that beamforming (on the desired signal) and nulling (of the jammer) cannot be achieved simultaneously.

Since jammers can be located at any position relative to the array orientation in shipborne applications, grating null effects should be avoided entirely; this result can be achieved by using a maximum $\lambda_o/2$ spacing between elements ("filled" array). However, if higher array resolution is desired without increasing the number of elements, then the spacing must often exceed $\lambda_o/2$ ("thinned" array). In this case, the elements can be nonuniformly spaced to disrupt the periodic structure of the array and thus reduce the effects of grating nulls.

2. NULLING LIMITATIONS DUE TO ELEMENT SPACING AND 10 MHz BANDWIDTH

Cancellation effectiveness depends principally on three characteristics: jammer bandwidth, element spacing, and frequency dependent mismatch between elements across the cancellation bandwidth. Calculations of the effects of element spacing on cancellation over a 10 MHz bandwidth show that this effect was not a determining factor in the cancellation performance obtained.

The effects of jammer bandwidth, element spacing and frequency dependent element mismatch on processor effectiveness are most easily illustrated by considering the degree of jammer cancellation which can be achieved using two of the antenna elements as shown in Figure A on the facing page. By proper choice of amplitude and phase shift values between elements, a null can be placed at one frequency (the output jammer power is zero in this case). However, if the jammer has a nonzero bandwidth, the other frequencies will not be completely attenuated. Figure A shows the residue jammer power in dB as a function of $B\tau$, where B is the bandwidth and τ is the propagation delay between antenna No. 1 and antenna No. 2. The propagation delay is given by

$$\tau = \frac{d\pi}{c} \sin\theta$$

where

d = element spacing
c = propagation velocity
θ = angular location of the jammer from array broadside

As shown in Figure A, jammer cancellation decreases as the jammer bandwidth (or τ) increases. In particular, the cancellation ratio is inversely proportional to the element spacing, the bandwidth and the jammer location. Using two elements of the OE-82B antenna as an example ($d = \lambda_o/2$, f_o = 300 MHz, B = 10 MHz), the cancellation ratio is limited to 30.5 dB for a worst case angle $\theta = 90^o$ (endfire jammer), and 36.5 dB for $\theta = 30^o$. This cancellation performance is at least 8 dB better than performances obtained in the tests using four elements. This indicates that other factors, such as frequency dependent mismatch between antenna elements and between weighting circuits, were the limiting factors in cancellation performance.

Figure A can also be used to estimate the degree of group delay matching between antenna elements required to obtain a given level of cancellation performance. A constant differential group delay between elements of 1 ns, for example, would limit the cancellation of 10 MHz bandwidth interference signal to -35 dB. Phase and amplitude mismatch between antenna elements across the 10 MHz bandwidth are additional causes of decreased cancellation performance.

Figure B opposite shows the effects of a constant amplitude error across the band with zero phase error and the effects of constant phase error with zero amplitude error for a simple two-element array. The canceller is adjusted for infinite cancellation when the phase and amplitude errors are both zero. The results indicate that the antennas must be matched to within approximately 0.5 dB in amplitude and approximately 1.8^o in phase to obtain 30 dB of cancellation. Unfortunately, available antenna measurement data lacked sufficient accuracy to evaluate these effects on the UHF adaptive array cancellation performance.

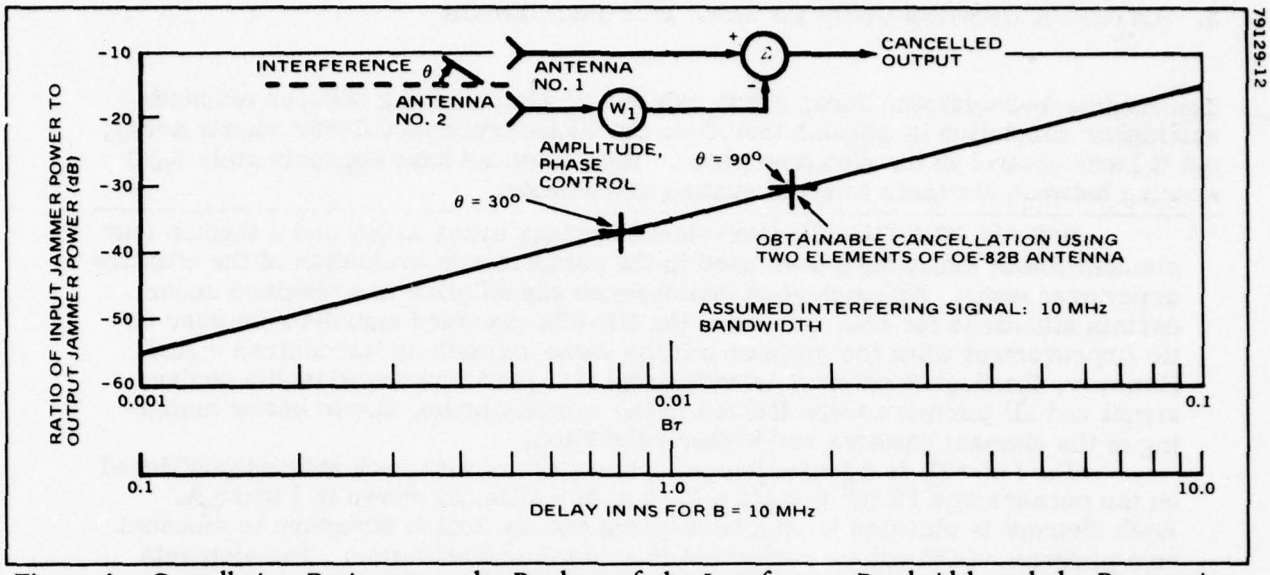

Figure A. Cancellation Ratio versus the Product of the Interference Bandwidth and the Propagation Delay Across the Antenna. The cancellation ratio is inversely proportional to Bτ. The cancellation ratio achievable using two elements of the OE-82B antenna is 30.5 dB for an interfering signal arriving endfire, and 37 dB for an interfering signal arriving 30° off broadside (B = 10 MHz for these two examples).

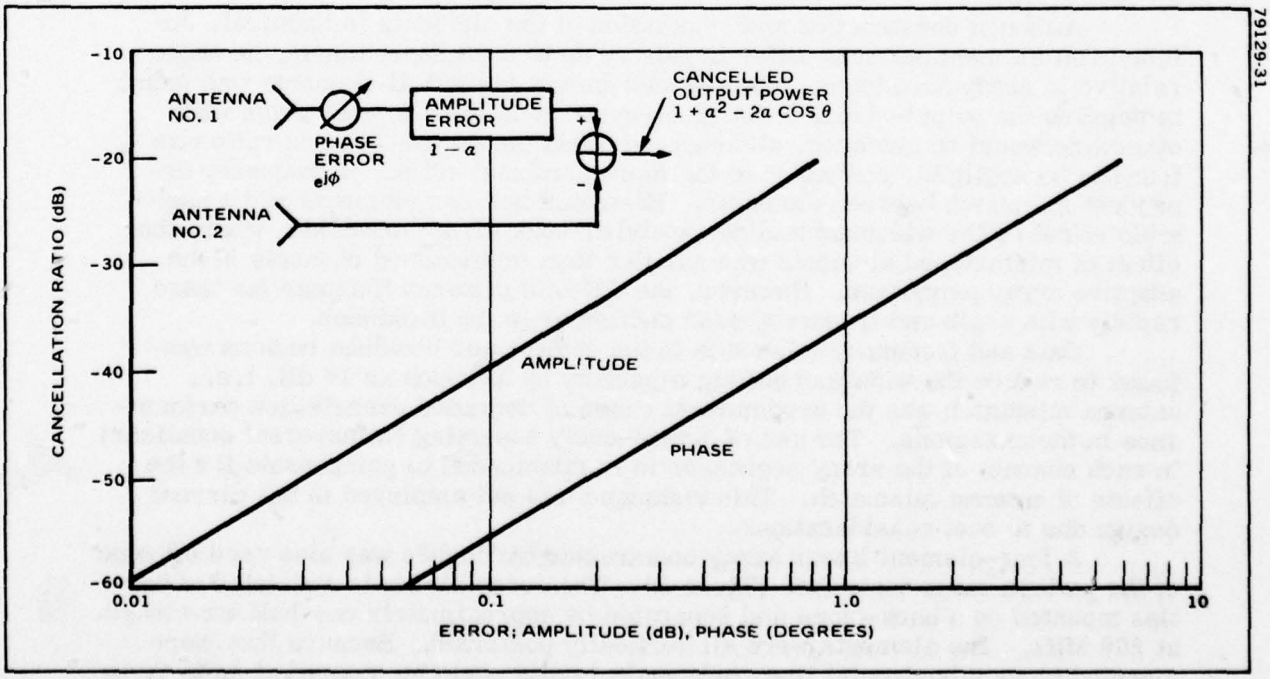

Figure B. Cancellation Ratio versus Amplitude and Phase Mismatch Between Antenna Elements for a Two-Element Array. The top curve shows the effects of a constant amplitude error across the band with zero phase error, and the second curve shows the effects of a constant phase error across the band with zero amplitude error. The effects of propagation delay across the array are neglected.

3. ANTENNA DESIGNS USED TO TEST THE PROCESSOR

The Hughes four-element linear array exhibits closer matching between elements and higher resolution in azimuth than does the NRL-furnished OE-82B planar array, but it lacks control in the elevation plane. Both antennas have approximately $\lambda_o/2$ spacing between elements to avoid grating null effects.

Both the NRL OE-82B four-element planar array array and a Hughes four element linear array have been used in the performance evaluation of the adaptive array processor. Although good interference cancellation was obtained under certain situations for both antennas, the OE-82B provided signal-to-jammer ratio improvement when the jammer had the same azimuth as the desired signal. However, the Hughes antenna provided superior performance when the desired signal and all jammers were located in the azimuth plane, due to better matching of the element patterns and higher resolution.

The OE-82B is a four-element antenna array with each antenna positioned on the corners of a 23 in^2 ($\sim \lambda_o/2 \times \lambda_o/2$ at 260 MHz) as shown in Figure A. Each element is elevated from a back-plane and the entire structure is mounted on a platform which can be controlled in azimuth and elevation. The elements are crossed-dipoles configured for right-hand circular polarization on both transmit and receive. In the pattern range and shipboard tests, cables from each of the four elements were brought out separately and applied to the RF front ends of the antenna interface unit (discussed in more detail in Section 3). The resulting problem of cables wrapping around the pedestal with changes in azimuth can be corrected by retro-fitting the OE-82B with a special rotary joint to handle all four signals.

Although construction and orientation of the elements is identical, the individual element patterns differ in gain by up to 4 dB depending on the angle relative to array broadside. The reduced gain of individual elements was found to degrade the output-signal-to-thermal-noise ratio (by a few dB) from what otherwise would be achieved, although the effect on the cancellation ratio was found to be negligible compared to the more dominant effects of frequency dependent mismatch between elements. Mismatch between elements had a negligible effect on the wideband nulling capability near array broadside, where the effect of mismatched elements was smaller than mismatched channels in the adaptive array processor. However, the OE-82B patterns fluctuate far more rapidly with angle and frequency near endfire or in the backlobes.

Gain and frequency mismatch in the endfire and backlobe regions was found to reduce the wideband nulling capability by as much as 10 dB, i.e., antenna mismatch was the predominant cause of degraded cancellation performance in these regions. The use of tapped-delay weighting (transversal equalizer) in each channel of the array processor is recommended to compensate for the effects of antenna mismatch. This technique was not employed in the current design due to cost considerations.

A four-element linear array constructed by Hughes was also used in some of the pattern range tests (see Figure B). The array elements consisted of bow-ties mounted on a back-plane and separated by approximately one-half wavelength at 260 MHz. The elements were all vertically polarized. Because they were mounted along a horizontal line, independent nulls could be steered at up to three different azimuth angles. Unlike the OE-82B, however, a desired signal can not be independently maximized and a jammer minimized if both sources have the same azimuth (even though their elevations differ). This characteristic may be undesirable for shipboard SATCOM applications because communication could

be disrupted by two jammers located along the same azimuth angle as the satellite.

The adaptive array processor was evaluated with this array to illustrate the performance improvement achieved when the individual element patterns are more closely matched. The evaluation confirmed that higher resolution improves performance when angular separations between a jammer and the desired signal are small.

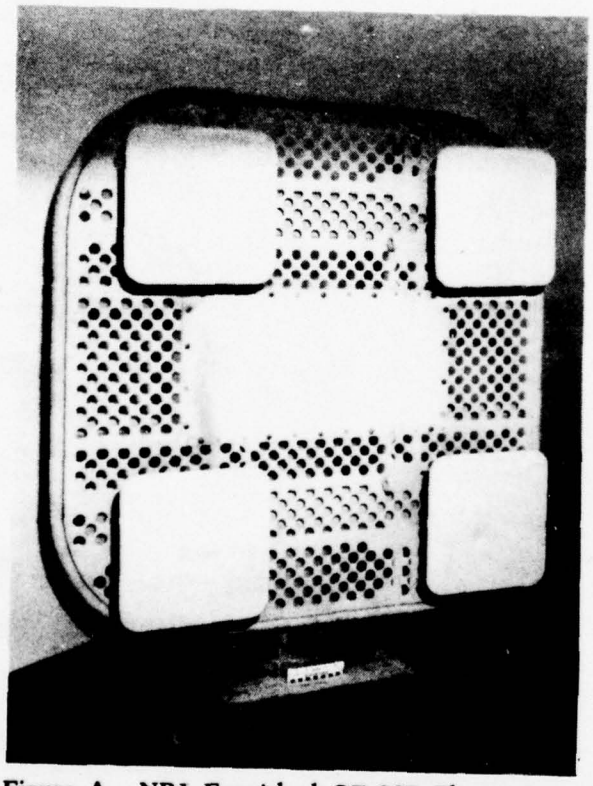

76-12-087

Figure A. NRL-Furnished OE-82B Planar Array. This antenna provides an improved signal-to-jammer ratio when the jammer has the same azimuth as the desired signal, but suffers from degraded performance due to element mismatch.

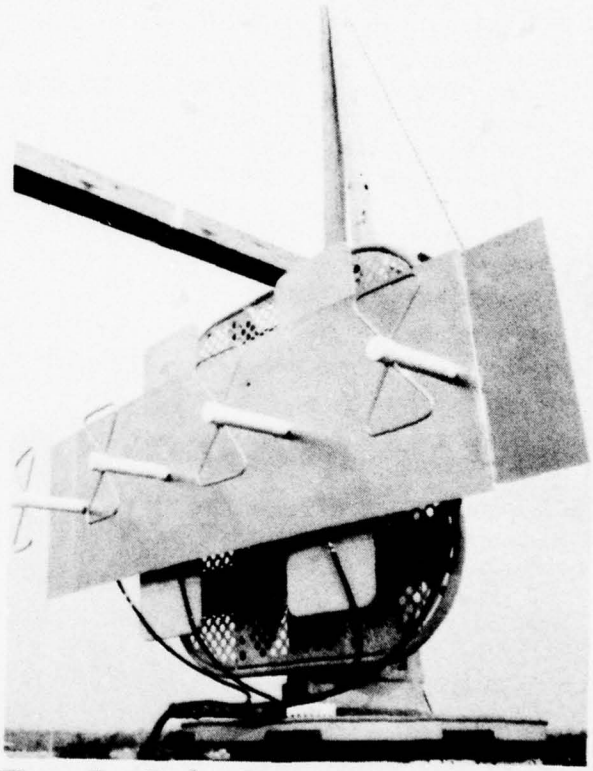

77-02-096

Figure B. Hughes Linear Array. This antenna provides superior performance where the desired signal and all jammers are located in the azimuth plane, but lacks control in elevation. (The linear array was mounted in front of the OE-82B antenna array so that another pedestal was not required.)

SECTION 3
DESCRIPTION OF THE RF SUBSYSTEM

Subsection A – Functional Description of the Processing Elements

Subsection B – Description of the Hardware Implementation

Section 3 – Description of the RF Subsystem
Subsection A – Functional Description of the Processing Elements

1. FUNCTIONAL DESIGN OF THE RF SUBSYSTEM

The RF subsystem provides wideband $\underline{R}$ and narrowband $\underline{Q}$ cross-covariance estimates to the control system, thus allowing adaptive pattern modification through IF weighting. The digitally controlled attenuators implement the IF weights.

The adaptive array processor consists of three major subsystems: the antenna array, the RF subsystem, and the control subsystem. The functions of the RF subsystem include down-conversion of the antenna signals from UHF to IF, IF weighting to form the antenna pattern, and correlation between the processor's inputs and output to obtain the $\underline{R}$ and $\underline{Q}$ cross-covariance measurements. This subsystem also determines the bandwidths over which the $\underline{R}$ and $\underline{Q}$ measurements are performed.

The RF subsystem, as shown opposite, includes the RF amplifier and down-converter chains, controllable IF weights (I and Q attenuators), correlator/integrator circuits, bandpass filters and an IF amplifier with programmable gain. The system uses an externally applied local oscillator (LO) signal at a frequency f_1 to convert the RF frequency (225 - 400 MHz) to a 70 MHz IF frequency with a 10 MHz bandwidth. A second LO signal, at a frequency f_2, is used to select a 25 kHz band within the 10 MHz band by down-converting to an IF of 3 MHz.

The double down-conversion allows the system to be tailored to many applications. For example, the first LO is used to tune to the 10 MHz Gapfiller satellite band, and the second LO is used to tune to one of the desired signals in that band. The $\underline{Q}$ measurement can then be used to beam the pattern on the satellite, while $\underline{R}$ can be used to null jammers which are wideband relative to 25 kHz. Note that either the first LO or second LO (usually the second LO) can be modulated by a known desired signal code to obtain additional processing gain from the 25 kHz filters to process spectrum-spread desired signals.

Most processing is performed at IF rather than at UHF to allow tuning of the RF band and to simplify hardware design. Specifically, limiters and correlators with nearly ideal characteristics can be implemented without resorting to circuits with extremely wide bandwidths. This is particularly critical in limiter design because very wideband components are already required to reduce the insertion phase shift versus input level.

Digitally-controlled attenuators are used to implement the IF weights. The attenuators consist of eight one-bit digital attenuators connected in series as follows:

32 dB, 16 dB, ... 1/2 dB, 1/4 dB.

The minimum 1/4 dB resolution, selected because of cost considerations, limited the jammer cancellation to about 36 dB.

The i^{th} channel ($i = 1, 2, 3, 4$) contains four correlator/integrator modules (two in-phase and two quadrature) to obtain the i^{th} components of the wideband $\underline{R}$ and narrowband $\underline{Q}$ cross-correlation estimates. These are shown in the figure as r_{i1}, r_{i2}, q_{i1}, q_{i2}, respectively. The correlators incorporate the Applebaum technique of using a hard limiter (zero-crossing detector) at the reference input to the module. The cross-covariance measurements are averaged for 204 μs, output to a multiplexer, and then converted sequentially to digital data in the control subsystem (see Section 4). This data is used by the computer to derive feedback control words to set the digital weight function for adaptive pattern modification. Note that although A/D conversion of the integrator outputs is performed sequentially, the actual integration actions are simultaneous.

The 70 MHz IF amplifier has a digitally-controlled gain in order to incorporate gain control via the the computer. This additional feature allows close control of signal levels at various points within the processor and extends the dynamic range of the cross-covariance measurements.

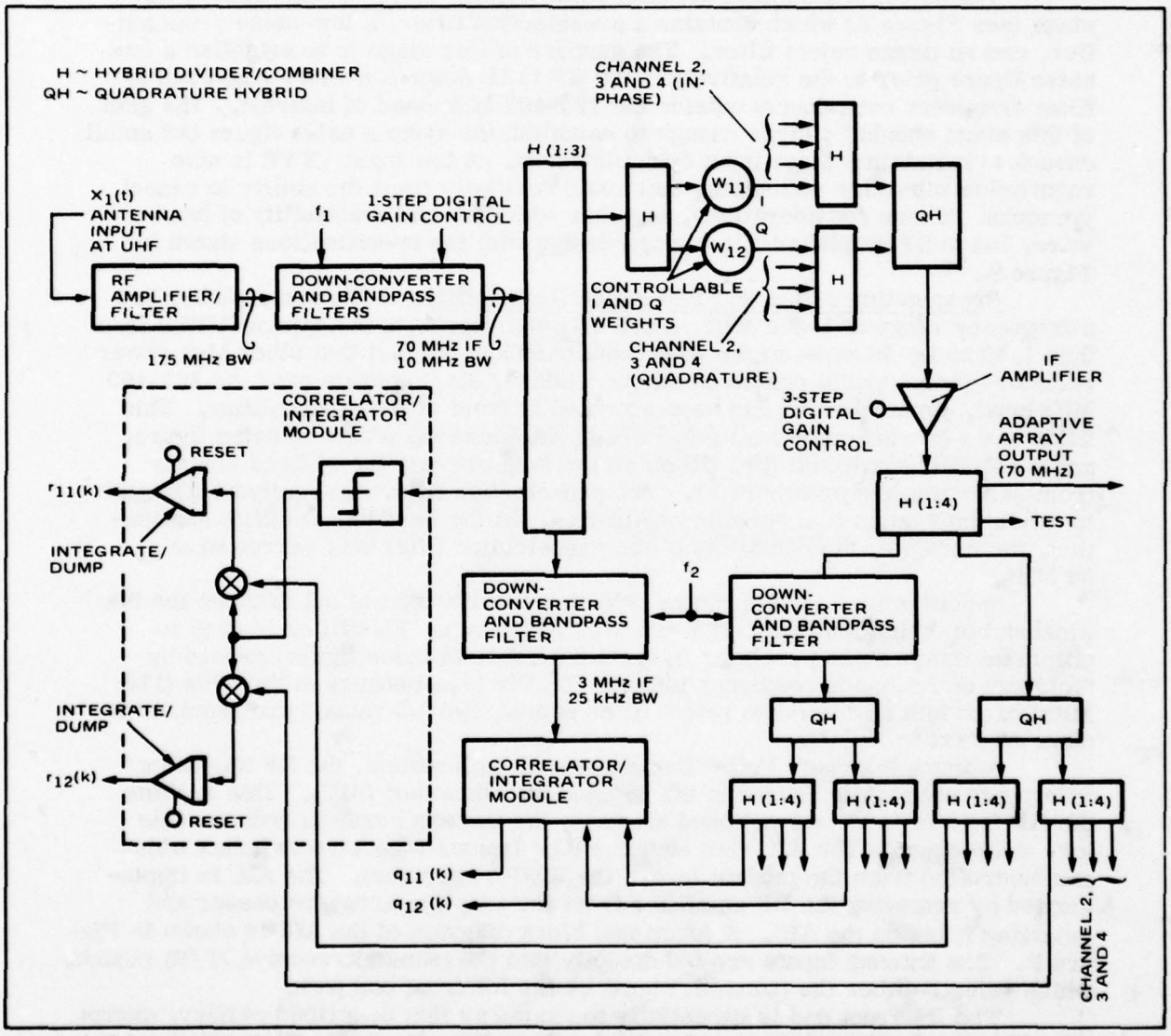

RF Subsystem Block Diagram. This subsystem provides the covariance estimates for the control subsystem and combines the weighted IF antenna element signals to form the system output.

1. DESIGN OF THE RF AMPLIFIER/FILTER

The RF amplifier/filter is used to establish a low noise figure prior to the RF to IF down-converter chain and to filter out those frequency components outside of the 225 to 400 MHz band of interest. The preselection filter can be changed to tailor the system to a specific application.

The output of each antenna element is applied to an RF amplifier/filter stage (see Figure A) which contains a preselection filter, a low-noise preamplifier, and an image reject filter. The purpose of this stage is to establish a low noise figure prior to the relatively noisy RF to IF down-converter chain and to filter frequency components outside the 225-400 MHz band of interest. The gain of this stage should be large enough to establish the system noise figure but small enough to maintain a large input dynamic range. A low input VSWR is also required to minimize reflections that could seriously limit the ability to cancel jammers. These considerations, together with cost and availability of hardware, led to RF amplifier/filter stage design with the specifications shown in Figure A.

Preselection Filter and Low Noise Preamplifier – The preamplifier has a frequency range of 1-500 MHz, a 2.5 dB noise figure, and a typical VSWR less than 1.40 to 1. Because of the wide input band and the fact that other high power radiators (commercial communications, radars, etc.) operate near the 225-400 MHz band, some filtering has been provided in front of the preamplifier. This filter has a low insertion loss (<0.5 dB) to minimize the effect on noise figure, and a 175 MHz bandwidth (to 1 dB points) to help prevent out-of-band signals from saturating the preamplifier. The preselection filter can easily be changed to tailor the system to a specific application. In the Gapfiller Satellite application, for example, the bandwidth of the preselection filter was narrowed to 30 MHz.

Specifications for the image rejection filter are identical to those for the wideband preselection filter (225-400 MHz passband). This filter is used to eliminate image noise problems (i.e., a 3 dB loss in noise figure) caused by "folding" of the image frequency into the 70 MHz IF. Because of the wide (175 MHz) bandwidth at the image reject filter output, two LO ranges are required to down-convert to 70 MHz.

Antenna Interface Unit – For shipboard applications, the RF amplifier/filters are separately housed in the antenna interface unit (AIU). This enables the RF front ends to be positioned closer to the antenna array to reduce cable loss and pick-up. The AIU also contains four transmit/receive switches which are controlled from the modem (e.g., the WSC-3 receiver). The AIU is implemented by removing the RF amplifier from the adaptive array processor and mounting it inside the AIU. A functional block diagram of the AIU is shown in Figure B. The antenna inputs are fed directly into the transmit/receive (T/R) switch, which selects either the transmit signal or the RF front end path.

The RF front end is essentially the same as that described earlier, except that the preselection filter is narrower band, and the low noise RF amplifier is located in the AIU. The image reject filter remains within the adaptive array processor (not in the AIU). The preselection filter was selected to pass signals transmitted from Gapfiller Satellite for which signals of interest are located in the range from 248-255 MHz. The filter has a 30 MHz bandwidth contered at 260 MHz and approximately 1.5 dB loss at center frequency (see Figure B).

The narrower preselection filter was required to prevent potentially high-level UHF interference generated by on-board radar and communications equipment from saturating the RF amplifier.

The increase to a 5 dB noise figure was determined to be acceptable in view of this added protection and the signal-to-noise margins of the satellite signals.

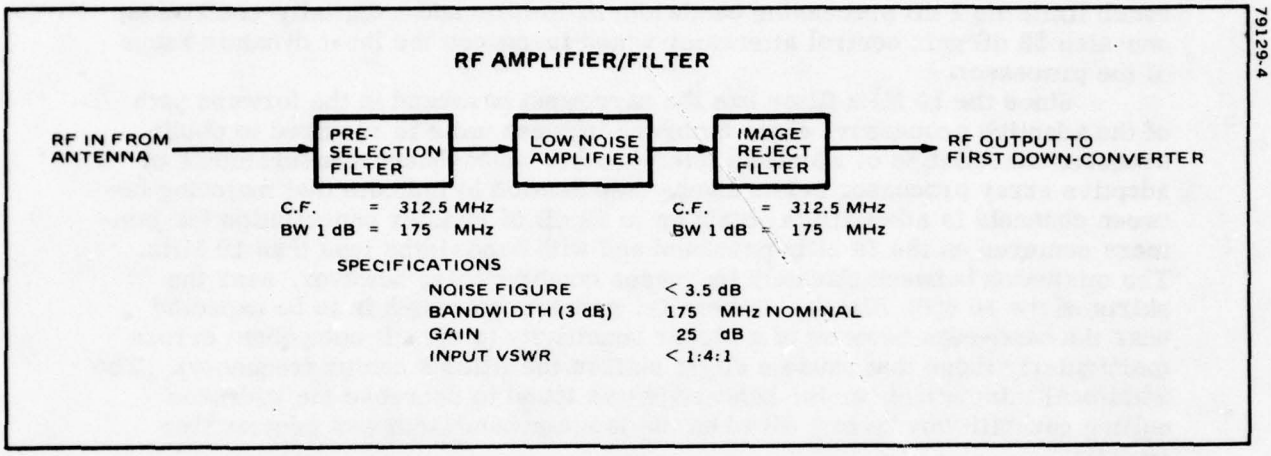

Figure A. RF Amplifier/Filter Stage. This stage has a low 3.5 dB noise figure and a preselection filter to reject interference outside the 225 to 400 MHz RF band.

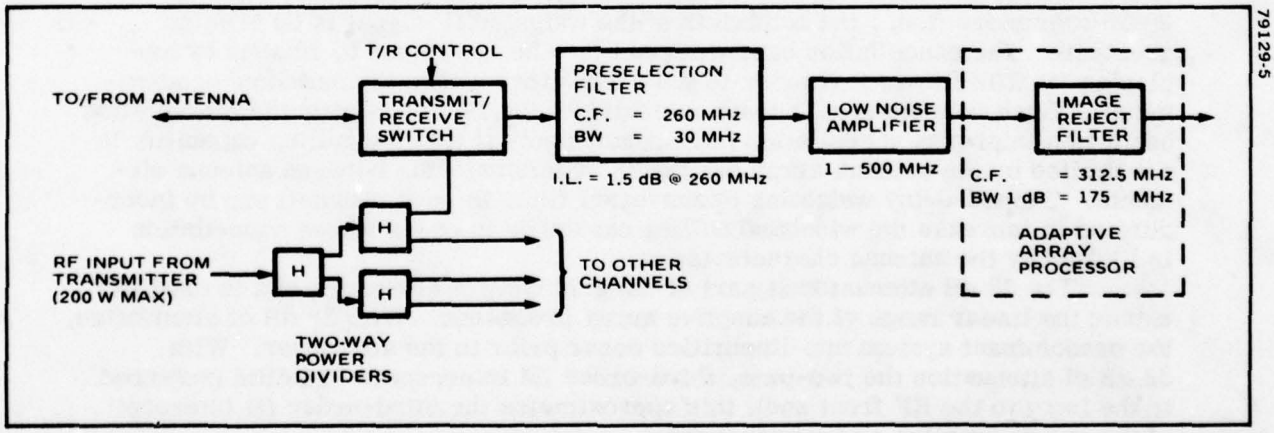

Figure B. Functional Diagram of the Antenna Interface Unit (AIU). In this shipboard application, the RF amplifier/filters are housed separately so they can be closer to the antenna. The AIU also includes a T/R switch to allow the antenna array to be used for transmitting.

2. DESIGN OF THE FIRST DOWN-CONVERTER AND 10 MHZ BANDPASS FILTER

The first down-converter stage converts the UHF input signals to a 70 MHz IF frequency. This stage is followed by a 10 MHz bandpass filter which establishes the cancellation bandwidth and increases processor dynamic range.

As shown opposite, the outputs of the RF amplifier/filter stage are applied to the first down-converter chain for down-converting the UHF signals to the 70 MHz IF of the adaptive processor. This stage also contains bandpass filters which limit the 1 dB processing bandwidth to 10 MHz and a digitally-controlled, one-step 32 dB gain control attenuator which increases the input dynamic range of the processor.

Since the 10 MHz filter has the narrowest passband in the forward path of the adaptive processor, close matching between units is required to obtain adequate cancellation of wideband interference. Subsequent measurements of adaptive array processor performance (see Section 5) indicate that matching between channels is adequate to obtain up to 28 dB of jammer cancellation for jammers centered on the 70 MHz passband and with bandwidths less than 10 MHz. The mismatch between channels increases considerably, however, near the skirts of the 10 MHz filters. Generally, greater mismatch is to be expected near the band-edge because of a higher sensitivity to circuit component errors (particularly those that cause a slight shift in the filter's center frequency). The additional mismatch near the band-edge was found to decrease the wideband nulling capability by up to 7 dB when the jammer bandwidth was greater than 10 MHz.

The capabilities for cancelling wideband jammers can be significantly improved by specifying matching requirements over a larger bandwidth (to the -20 dB points of the filters for example). Since filters are usually much easier to match near the center of the passband, the filters can also be widened to 30 MHz or more (i.e., the bandwidth of the weighted IF signal is 30 MHz or greatest). The cancellation bandwidth can then be restricted to 10 MHz by employing 10 MHz filters just prior to the correlators where the matching requirement is much less severe. Closer matching of the IF filters over the cancellation bandwidth improves cancellation performance only if that the nulling capability is not limited by the antenna array bandwidth or mismatching between antenna elements. Tapped-delay weighting (transversal filter in each channel) can be incorporated to increase the wideband nulling capability in cases where cancellation is limited by the antenna characteristics.

The 32 dB attenuator is part of the gain control attenuator and is used to extend the linear range of the adaptive array processor. With 32 dB of attenuation, the predominant system non-linearities occur prior to the attenuator. With 32 dB of attenuation the two-tone, third-order IM intercept is -14 dBm (referred to the input to the RF front end); this approximates the third-order IM intercept of the entire adaptive array processor.

The local oscillator (LO) frequencies used to downconvert to 70 MHz are divided into two bands to prevent a 3 dB noise figure loss due to folding of the image frequency. The LO is required to be below the signal frequency when the signal is in the upper half of the UHF band, and above the signal frequency when it occupies the lower half of the band. The local oscillator frequencies are thus defined to be 155 MHz to 242.5 MHz for signals in the band from 225 to 312.5 MHz, and 382.5 MHz to 470 MHz for signals in the 312.5 MHz to 400 MHz band. For signals at or near 312.5 MHz, either local oscillator frequency can be used since some overlap of the local oscillator frequencies may be allowed.

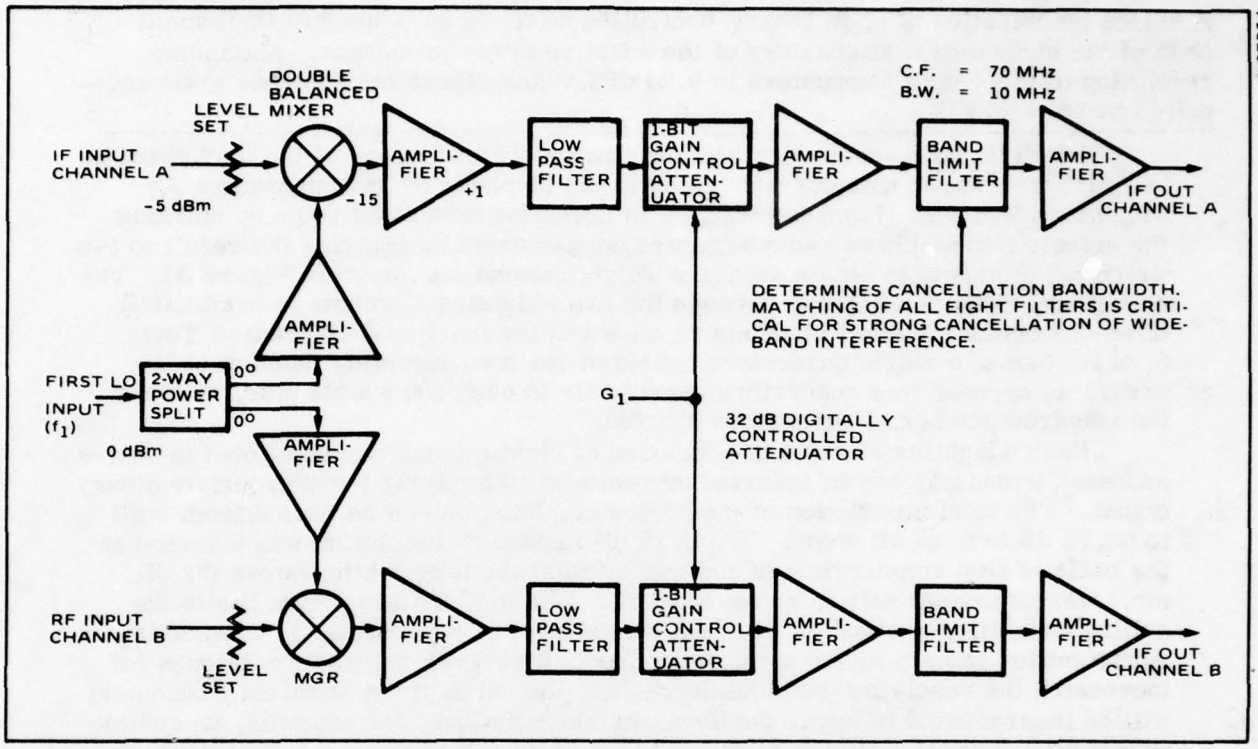

First Down Converter and Bandpass Filters. These devices are used to convert the UHF signals to the 70 MHz IF of the adaptive array processor and to establish the 10 MHz bandwidth.

3. DESIGN OF THE ADAPTIVE WEIGHTING ELEMENTS AND COMBINERS

A series combination of eight binary-controlled attenuators is used to implement each of the eight weight attenuators of the adaptive array processor. Maximum resolution of the weight attenuators is 0.25 dB, which allows interference to be cancelled by up to 36 dB.

The first down-converter/bandpass filter chains in each of the four channels is split three ways, with one path going to the in-phase (I) and quadrature (Q) weighting elements. I and Q weighting is implemented in this stage by splitting the signals into in-phase and quadrature components and applying the result to two weighting elements to obtain separate weight control (as shown in Figure A). The quadrature (I/Q) relationship between the two weighting elements is established after combining the other channels as shown in the functional diagram of Topic 3.A.1. Use of a single quadrature hybrid at the final summing junction of the array, as opposed to a quadrature hybrid pair to each I/Q weight pair, reduces the required number of quadrature hybrids.

Each weighting element is composed of eight attenuators connected in series and each attenuator can be inserted or removed by applying the appropriate binary signal. The total attenuation of the series combination can be varied from 0 dB to 63.75 dB in 0.25 dB steps. The 0.25 dB maximum resolution was selected on the basis of cost considerations and the fact that the larger attenuators (32 dB, etc.) were accurate only to within 0.25 dB. The 0.25 dB resolution limits the nulling capability to about 36 dB. Since this level of suppression is deemed insufficient for certain future applications, one of several different techniques for increasing the resolution (without decreasing the value of the smallest attenuator) will be incorporated in future designs. In one technique, for example, an analog weight attenuator is added to each I and Q channel. (See Figure B.) A much higher resolution, and thus improved interference cancellation, can be obtained in this manner. Methods for controlling the weights, and other methods for obtaining improved cancellation, are currently being examined.

One subject which has not been fully examined is the effect of pulses which can momentarily appear at the array output during the 5 μs interval required to switch the weights to a new value of attenuation. A pulse can occur when a high-level interference signal has been cancelled because the weights are at some point undefined during switching. The pulses had an unmeasureable effect on performance under the test conditions of Section 5, but feedback of these pulses to the $\underline{R}$ and $\underline{Q}$ cross-covariance measurements may degrade performance in future applications where greater interference cancellation is required. An additional circuit to gate out the feedback signal may therefore be required.

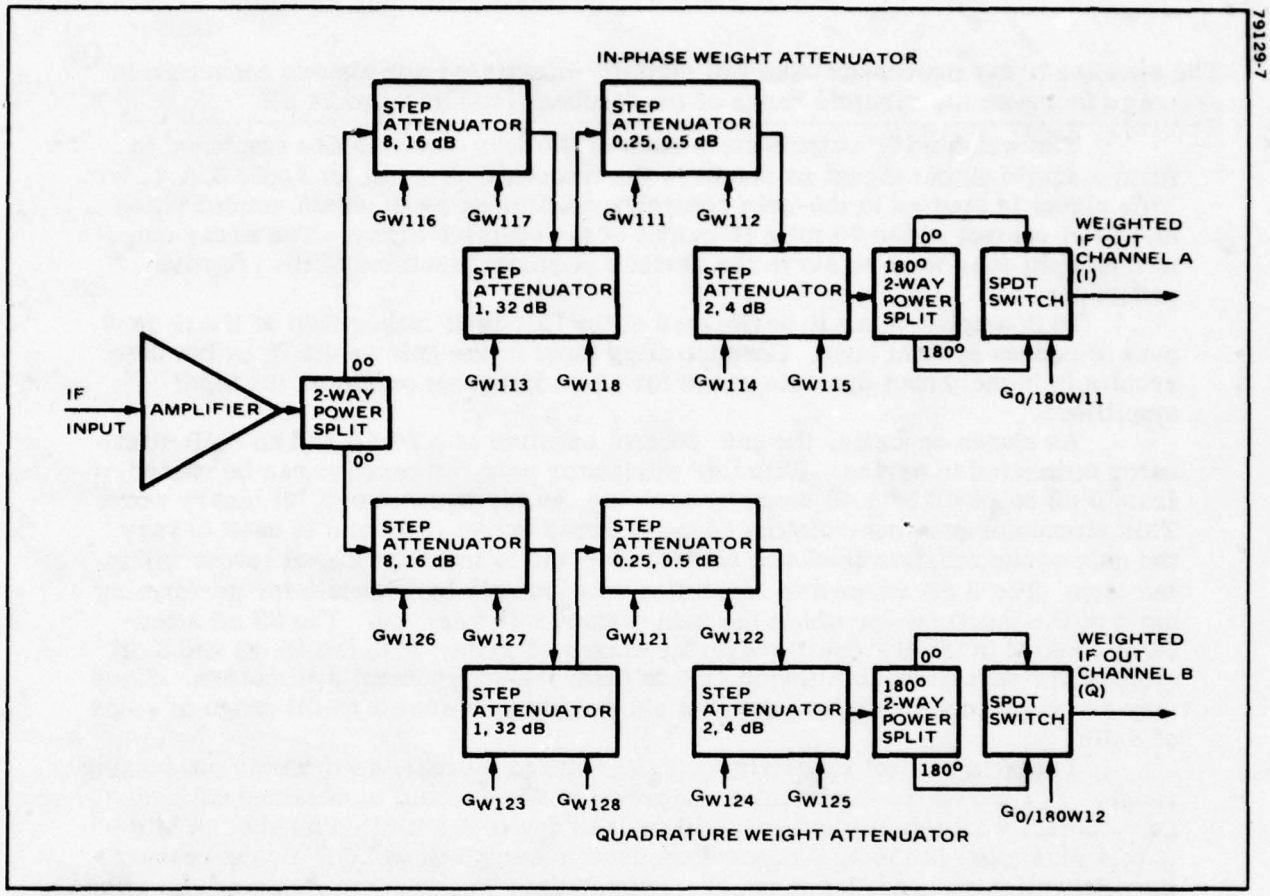

Figure A. Weight Attenuator Implementation. Each in-phase or quadrature attenuator can be adjusted from 0 dB to 63.75 dB in steps of 0.25 dB under digital control. The sign is controlled by means of a 180° hybrid and an SPDT switch.

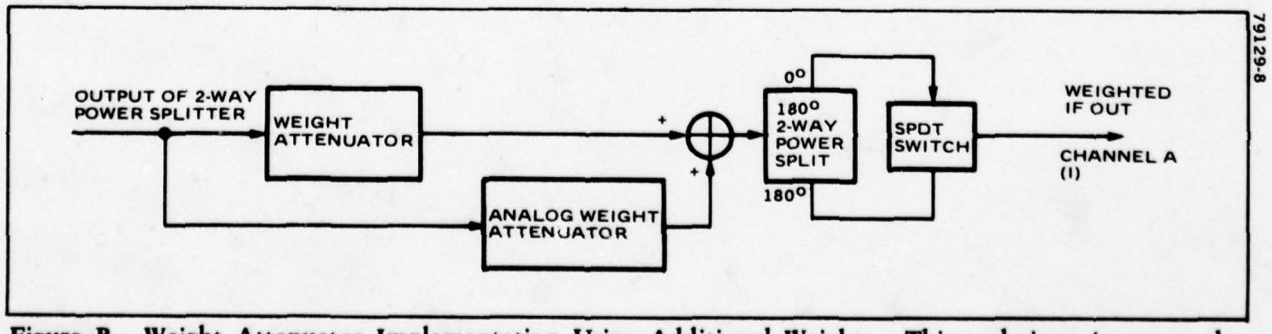

Figure B. Weight Attenuator Implementation Using Additional Weights. This technique increases the resolution of the digital weight attenuators and provides improved interference cancellation.

4. DESIGN OF THE GAIN CONTROL AMPLIFIER

The adaptive array processor uses two digitally-controlled attenuators connected in series to increase the dynamic range of the feedback loop by up to 24 dB.

The weighted IF outputs from each of the four channels are combined to form a single output signal as shown in the functional diagram in Topic 3.A.1. This signal is applied to the gain control/amplifier stage to obtain amplification and level control of the 70 mHz IF output of the adaptive array. The array output is then split four ways to serve the various required functions of the adaptive processor.

High amplification is performed at the IF output rather than at the IF inputs to reduce system cost. Concentrating most of the gain at the IF output also results in higher input dynamic range for given intercept points on the input amplifiers.

As shown opposite, the gain control consists of a 16 dB and an 8 dB attenuator connected in series. With this attenuator pair, attenuation can be varied from 0 dB to 24 dB in 8 dB steps by applying the appropriate two-bit binary word. This attenuator pair controls the adaptive array output level and is used to vary the gain of the adaptive feedback control loop and to maintain signal levels within the loop. The 8 dB attenuator resolution was found to be adequate for performing most of the functions for which the gain control was intended. The 32 dB attenuator located in the RF down-converter stages, together with the 16 dB and 8 dB attenuators described above, combine to form the gain control attenuators. Since they are connected in series, the gain can be adjusted over a 56 dB range in steps of 8 dB.

The gain control capability permits a large increase in dynamic processing range. For example, the jammer suppression which could be obtained without gain control would be limited to 24 dB or less due to the limited number of bits (8 bits plus sign) in the A/D connectors used to sample $\underline{R}$ and $\underline{Q}$. By decreasing the attenuation as large jammers are being nulled, the dynamic range can be effectively extended to permit jammer suppression well beyond the 36 dB limitation imposed by quantization in the weight attenuators.

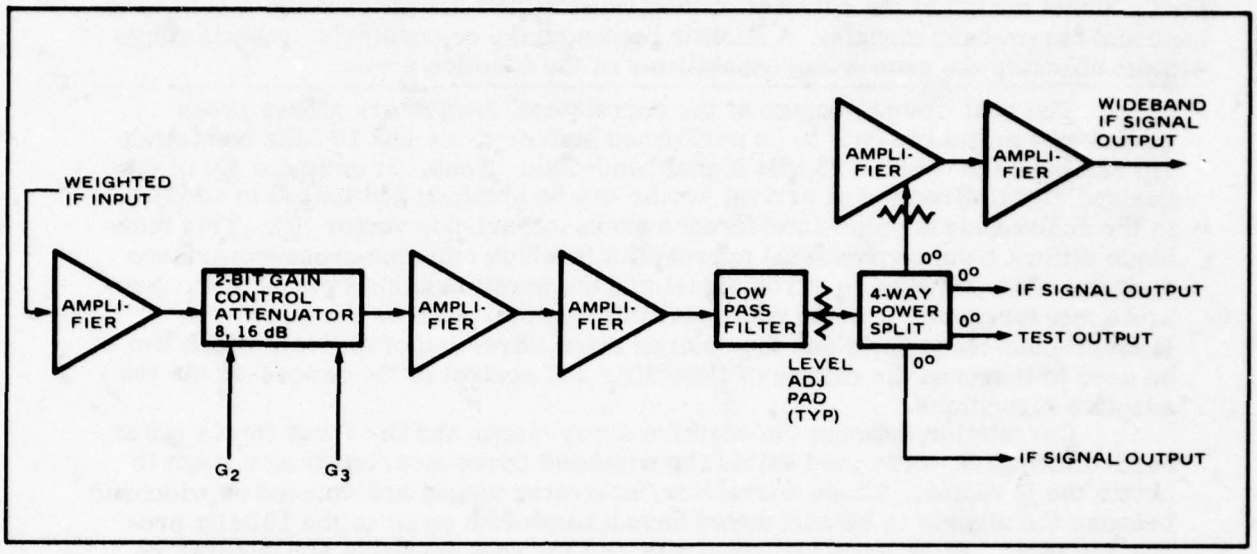

Gain Control Amplifier. The gain control capability permits an increase in dynamic processing range by up to 24 dB.

5. DESIGN OF THE CORRELATORS/INTEGRATORS

Dual channel design of the correlator/integrator allows for processing of both wideband and narrowband signals. A limiter improves the correlator's dynamic range without affecting the processing capabilities of the adaptive array.

The dual channel design of the correlators/integrators allows cross-covariance measurements to be performed both over the full 10 MHz bandwidth ($\underline{R}$) and over the desired 25 kHz signal bandwidth. Thus, an estimate ($\underline{Q}$) of the desired signal direction of arrival vector can be obtained and stored in addition to the desired signal-plus-interference cross-covariance vector ($\underline{R}$). This technique differs from conventional approaches in which only one cross-covariance measurement (between an error signal and the array inputs) is performed. Separate measurements provide additional information, such as the signal-to-jammer-plus-noise ratio and the desired signal direction of arrival, which can be used to increase the degree of flexibility and control of the processor via the adaptive algorithms.

Correlation between the adaptive array output and the array inputs (after hard-limiting) is performed within the wideband correlator/integrator stage to obtain the $\underline{R}$ vector. These correlator/integrator stages are denoted as wideband because the signals to be correlated have a bandwidth equal to the 10 MHz processing band. Eight units are required, one for each in-phase and quadrature component of the four-channel processor.

The array output is applied to a wideband 90° hybrid to establish the required I and Q feedback signals, as shown in the figure of Topic 3.A.1. Each I and Q signal is then split and applied to one side of each correlator/integrator. To obtain the reference input of the correlator, each antenna signal (bandlimited to 10 MHz) is first passed through a limiter (zero-crossing detector) and the reference signal is the limiter output. The limiter greatly improves the dynamic range of the correlator without affecting adaptive array capabilities and reduces the sensitivity of the adaptive loop response time to the input signal level.

Correlation between bandlimited versions of the adaptive array output and the array inputs (after hardlimiting) is performed within the narrowband correlator/integrator stage to obtain the $\underline{Q}$ vector. These correlators are denoted as narrowband because the signals to be correlated have a bandwidth equal to the 25 kHz desired signal bandwidth. The narrowband correlation implementation is similar to that of the wideband correlators except that correlation is performed at a 3 MHz second IF frequency rather than at 70 MHz (see next topic).

The correlator is a synchronous detector. Its output is applied to a video amplifier followed by a gated integrator. The video amplifier is equipped with a DC level adjustment to null any offsets accumulated in the series connection of the synchronous detector, video amplifier, gated integrator, sample and hold, and the video driver. The integration interval is approximately 200 μs. At the end of the interval, the integrator outputs are sampled and held, and the integrators are dumped. The dump and sample/hold commands are synchronous with the adaptive array processor but are asynchronous with respect to the PDP-11/05 computer.

Timing diagrams of the integrator dump and read control waveforms are shown at the bottom of the figure. G_{DUMP} and G_{READ} are applied to all of the integrators (and sample/holds), so that measurements are performed simultaneously in each channel.

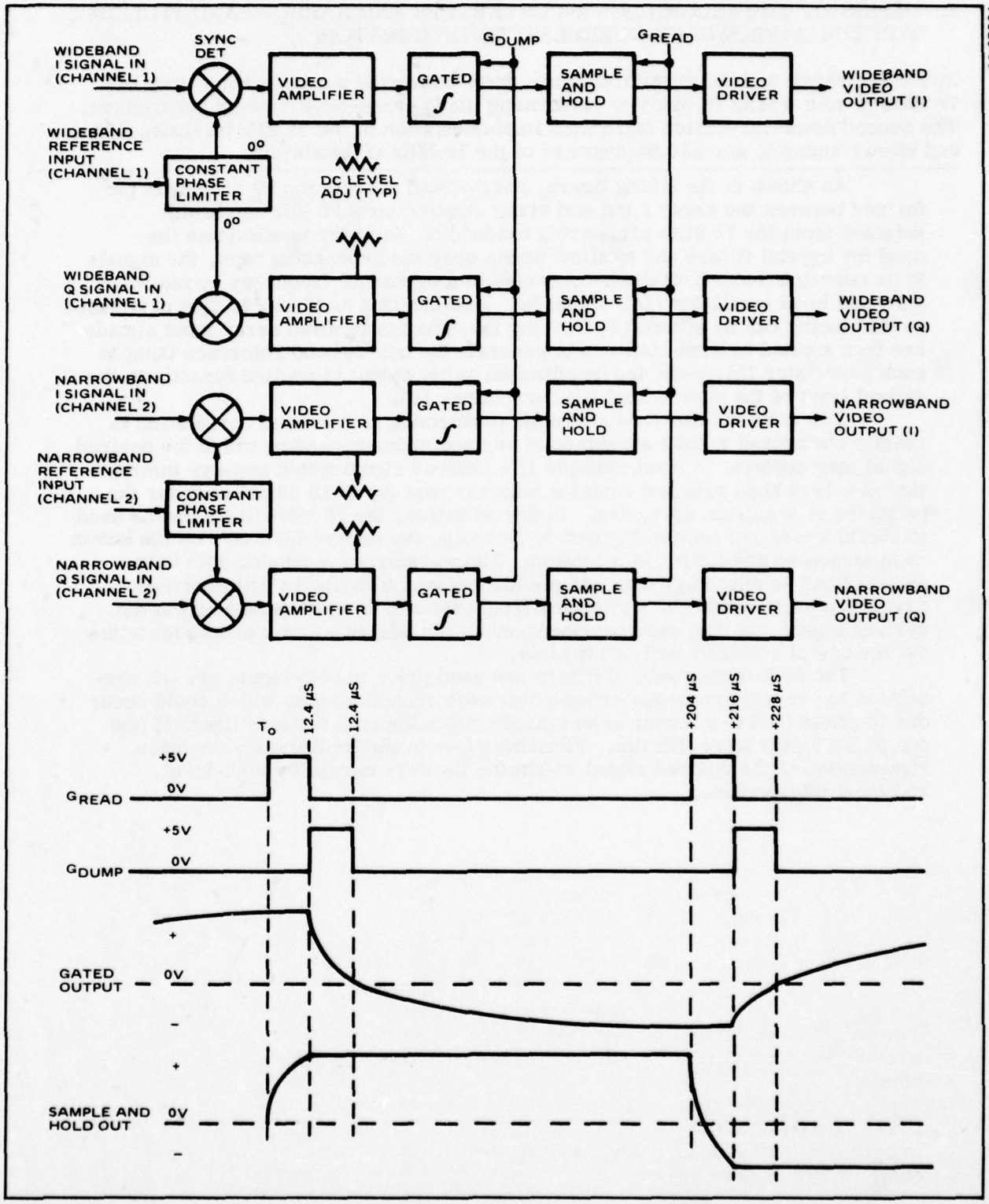

Dual Channel Correlation Detector. This design, which allows processing of both wideband and narrowband signals, incorporates a limiter to improve the correlator's dynamic range.

6. DESIGN OF THE SECOND DOWN-CONVERTERS AND NARROWBAND FILTERS FOR THE NARROWBAND CORRELATORS/INTEGRATORS

The array output and the array inputs are down-converted a second time from the 70 MHz IF to a 3 MHz IF prior to performing the Q cross-covariance measurement. The second down-conversion facilitates implementation of the 25 kHz bandpass filter and allows tuning to any 25 kHz segment of the 10 MHz IF bandwidth.

As shown in the facing figure, narrowband correlation (Q vector) is performed between the array input and array output over a 25 kHz bandwidth selected from the 10 MHz processing bandwidth. In order to eliminate the need for crystal filters and to allow tuning over the processing band, the signals to be correlated are first down-converted to a second IF frequency by means of a second local oscillator (LO) signal f_2. Bandlimiting to 25 kHz is then performed so that tuning can be effected by varying f_2. The bandlimited array input signals are then applied to hard-limiters to generate the narrowband reference input to each correlator (A), while the bandlimited array output is applied directly to the second input of the narrowband (Q) correlators (B).

The method described above for performing narrowband correlation is readily configured to take advantage of any spectrum-spreading which the desired signal may contain. A good example is a desired signal which conveys information at a 19.2 kbps rate and contains a higher rate (up to 10 Mbps) code for the purposes of spectrum spreading. In this situation, the 25 kHz filters can be used to obtain waveform processing gain by encoding the second LO based on the known code structure and timing information. The waveform processing gain thus obtained has an advantage over simple narrowband filtering in that jammers having the same bandwidth and center frequency can be distinguished from the desired signal and thus can be suppressed by the adaptive array processor without the use of selective null constraints.

The 25 kHz narrowband filters are used prior to both inputs of each correlator to prevent erroneous cross-covariance measurements which could occur due to phase (and to a lesser extent amplitude) mismatch between inputs if just one of the inputs were filtered. Filtering prior to the limiters also reduces suppression of the desired signal within the limiters caused by high-level, wideband interference.

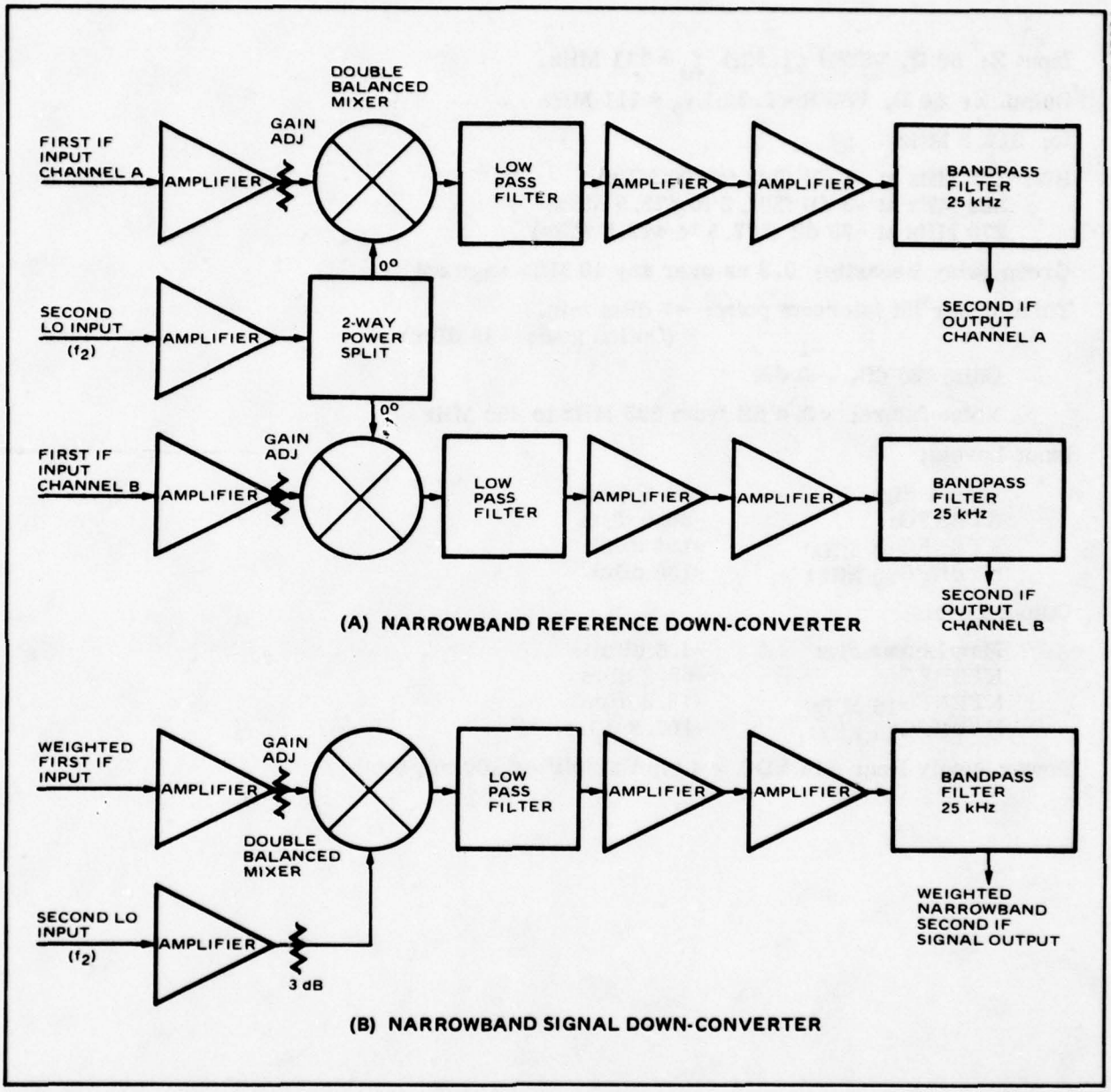

Second Down-Converters and Narrowband Filters. The second down-converters are used to convert to a second IF frequency of 3 MHz for tuning to any 25 kHz desired signal within the 10 MHz bandwidth.

7. PERFORMANCE REQUIREMENTS OF THE RF SUBSYSTEM HARDWARE – RF AMPLIFIER/FILTER

Input Z: 50 Ω, VSWR < 1.22:1 $f_o \pm 111$ MHz

Output Z: 50 Ω, VSWR < 1.22:1 $f_o \pm 111$ MHz

fo: 312.5 MHz

BW: 175 MHz at -1 dB (225 to 400 MHz)
222 MHz at -3 dB (201.5 to 423.5 MHz)
270 MHz at -20 dB (177.5 to 447.5 MHz)

Group delay linearity: 0.3 ns over any 10 MHz segment

Third order IM intercept point: +7 dBm min.
(Option goal: +43 dBm)

Gain: 25 dB, $^{+1}_{.-0}$ dB

Noise figure: < 3.0 dB from 225 MHz to 400 MHz

Input Levels:

Linear Sig:	-30.0 dBm
KTBNFG:	-90.0 dBm
$KTBNFG_{10\ MHz}$:	-104 dBm
$KTBNFG_{25\ kHz}$:	-130 dBm

Output Levels:

Max Linear Sig:	-4.8 dBm
KTBNFG:	-65.2 dBm
$KTBNFG_{10\ MHz}$:	-78.3 dBm
$KTBNFG_{25\ kHz}$:	-104.3 dBm

Power Supply Req: +15 VDC @ 40 mA amplifier 160 mA total

8. PERFORMANCE REQUIREMENTS OF THE RF SUBSYSTEM HARDWARE – FIRST DOWN CONVERTER AND BANDPASS FILTERS

Input Z: Chan. A, B: 50 Ω, VSWR < 2:1 fo ± 111 MHz
L. O. Input: 50 Ω, VSWR < 1.5:1 deom 115 MHz to 470 MHz

Output Z: Chan. A, B: 50 Ω, VSWR < 1.22:1 at 70 MHz ±5 MHz

f_O: 312.5 MHz

$f_{L.O.}$: 155 to 242.5 MHz
382.5 to 470 MHz

f_{IF}: 70 MHz ±5 MHz

BW: , RF: 175 MHz at -1 dB
LO: 455 MHz at -1 dB
IF: 10 MHz at -1 dB
16 MHz at -3 dB
60 MHz at -40 dB
≥ -60 dB @ 115 MHz

Gain: 19.5 with 0 dB $^{+1}_{-0}$ dB

Group Delay Linearity: 0.3 ns over the IF band at any point in the RF band

Noise Figure: < 11 dB

Low Pass Filter f_C: 90 MHz min

Gain Control Atten: 32 dB ± 0.25 dB
Logic 1 0 dB Gain Control

Gain Control Setting Time: < 5 μs

3rd Order IM Product Level: -60 dBm maximum for two input sig. at -4.8 dBm

Input Levels:

Max Linear Sig:	-4.8 dBm (ω/32 dB Gain Control)
KTBNFG:	-65.2 dBm
$KTBNFG_{10\ MHz}$:	-78.3 dBm
	-104.3 dBm
1st L.O.:	+2 dBm (with +14 dB gain driver)

Output Levels:

Max Linear Sig:	-17 dBm
KTBNFG:	-58 dBm
$KTBNFG_{10\ MHz}$:	-58 dBm
$KTBNFG_{25\ kHz}$:	-84.8 dBm

Power Supply Req: +24 VDC at 612 ma, +5 VDC at 3 ma

9. PERFORMANCE REQUIREMENTS OF THE RF SUBSYSTEM HARDWARE – WEIGHTING CIRCUITS

Input Z: 50 Ω, VSWR < 1.22:1 at f_{IF_1} ±5 MHz

Output Z: 50 Ω, VSWR < 1.22:1 at f_{IF_1} ±5 MHz

f_{IF}: 70.000 Mhz

BW: > 10 MHz at -1 dB points

Gain: -3 dB, ±1 dB

Group Delay Linearity: 0.3 nsec at f_{IF} ±5 MHz

Noise Figure: < 20 dB

3rd Order I.M. Level: < -106 dBm for two signals of -23.5 dBm at the input

Atten + Step Sizes:

Gate	Atten.	Tol.
W111 & W121	0.25 dB	±0.1 dB
W112 & W122	0.5 dB	±0.1 dB
W113 & W123	1.0 dB	±0.12 dB
W114 & W124	2.0 dB	±0.25 dB
W115 & W125	4.0 dB	±0.25 dB
W116 & W126	8.0 dB	±0.25 dB
W117 & W127	16.0 dB	±0.25 dB
W118 & W128	32.0 dB	±0.25 dB

When Gates are true, LOGIC 1, the atten. will be at min. loss.

Phase Shift Bit:

LOGIC 1 = 0°
LOGIC 0 = 180° ±2° RELATIVE TO LOGIC 1

All Gates shall be unbalanced 5V CMOS

Switch Settling Time: < 5 μs with all bits changing.

Input Levels:

Max Linear Sig: -24 dBm
KTBNFG: -65.8 dBm
$KTBNFG_{10\ MHz}$: -65.8 dBm
$KTBNFG_{25\ kHz}$: -91.8 dBm

Output Levels (A & B):

Max Linear Sig: -27.5 dBm
KTBMFG: -69.3 dBm
$KTBNFG_{10\ MHz}$: -69.3 dBm
$KTBNFG_{25\ kHz}$: -95.3 dBm

Power Supply Req: +24 VDC at 110 ma, +5 VDC at 12 ma

10. PERFORMANCE REQUIREMENTS OF THE RF SUBSYSTEM HARDWARE – GAIN CONTROL AMPLIFIER

Input Z: 50 Ω, VSWR < 1.22:1 f_{IF_1} ±5 MHz

Output Z: 50 Ω, VSWR < 1.22:1 f_{IF_1} ±5 MHz

f_{IF_1}: 70.00 MHz

BW:

f_{IF_2}: > 10 MHz @ -1 dB points

Gain:

WB IF, Output: 37 dB $^{+1}_{-0}$ dB

IF Output: 17 dB $^{+2}_{-0}$ dB w/o AGC

Group Delay Linearity: 0.3 ns for IF ± 5 MHz

Noise Figure: < 10 dB

3rd Order I.M. Product Level: FOR 2 sig. at -21 dBm at the input

WB IF_1 Output: -36 dBm
IF Output: -82 dBm

Gain Control Levels: 8 ± 0.25 dB, 16 2 0.25 dB (Attenuation minimum (Gain Control = 0) with LOGIC 1.)

Input Levels:

Max Linear Sig:	-31 dBm
KTBNFG:	-72.8 dBm
$KTBNFG_{10\ MHz}$:	-72.8 dBm
$KTBNFG_{25\ kHz}$:	-98.8 dBm

Output Levels:

	WB IF1	IF OUT
Max. Linear Sig:	-10 dBm	-30 dBm
KTBNFG:	-35.8 dBm	-55.8 dBm
$KTBNFG_{10\ MHz}$:	-35.8 dBm	-55.8 dBm
$KTBNFG_{25\ kHz}$:	-61.8 dBm	-81.8 dBm

Low Pass Filter f_c: 90 MHz min.

Logic to be CMOS Unbalanced +5 V

Relative gains are trimmed using fixed pads.

Power Supply Req: +24 VDC @ 440 mA, +15 VDC @ 9 mA, +5 VDC @ 1.5 mA.

11. PERFORMANCE REQUIREMENTS OF THE RF SUBSYSTEM HARDWARE – CORRELATOR/INTEGRATOR

Input Z: 50 Ω, (VSWR ≤ 1.2:1) @ f_c ±5 MHz

Output Load : 91 Ω ± 10%, ± jo

f_c Input: Chan. 1 - 70 MHz
Chan. 2 - 3 MHz

$BW_{IF\ CH1}$: 10 MHz @ -1 dB points $^{+2\ MHz}_{-0\ MHz}$

IF CH2: 25 kHz @ -1 dB points $^{+2\ kHz}_{-0\ kHz}$

BW_{Video}:	Prior to Correlation	After Correlation	Integration Interval
Chan 1	10 MHz	200 kHz	200 μs
Chan 2	25 kHz	200 kHz	200 μs

Phase Balance: ±2° all inputs

Group Delay Linearity: 0.3 ns. over BW_{IF}

3rd Order I. M. Level: > -50 dB for two -20 dBm input signals

Read & Dump Time: ≤ 5 microseconds

Input Levels:

Signal:	Chan 1 (WB)	Chan 2 (NB)
Max. Linear Sig:	-20 dBm	-19 dBm
$KTBNFG_{10\ MHz}$:	-45 dBm	-70.3 dBm
$KTBNFG_{25\ kHz}$:	-71 dBm	-70.3 dBm
System N. L. 10 MHz:	-34 dBm	-70.3 dBm
System N. L. 25 kHz:	-71 dBm	-70.3 dBm

Output Levels:

Signal:	Chan 1 (WB)	Chan 2 (NB)
Max. Linear Sig:	-24 dBm	-13.5 dBm
$KTBNFG_{10\ MHz}$:	-65.8 dBm	-81.8 dBm
$KTBNFG_{25\ kHz}$:	-91.8 dBm	-81.8 dBm

Output Levels: ±2V peak for a -19 dBm input. Spurious outputs are consistent with A/D LSB, < 8 mV peak. Self-noise is >10 dB below input KTBNF.

Notes:
1. All control signals are unbalanced CMOS (5) Volts
2. Chan 1 (WB) limit level is -45 dBm ref. to ref. input
   Chan 2 (NB) limit level is -70.3 dBm ref. to ref. input
3. Interchan isolation is greater than 70 dB
4. Power supply requirements: +15 VDC @ 270 mA, -15 VDC @ 35 mA
5. The sample & hold output droop is less than 8 mV in 192 μs

12. PERFORMANCE REQUIREMENTS OF THE RF SUBSYSTEM HARDWARE – REFERENCE DOWN-CONVERTER

Input Z: 50 Ω, VSWR < 1.22:1 fIF_1 ±5 MHz (Chan A & B)
50 Ω, VSWR < 2:1 f_{LO_Z} ±5 MHz (2nd L.O. INPUT)

Output Z: 50 Ω, VSWR < 1.22:1 fIF_2 ±20 kHz

fIF_1: 70.00 MHz

fIF_2: 3.00 MHz

fLO_2: 62 to 78 MHz

BW: fIF_1: > 10 MHz @ -1 dB points
fIF_2: > 25 kHz @ -1 dB points
≤ 40 kHz @ -3 dB points
< .5 MHz @ -60 dB points
fLO_2: > 30 MHz @ -1 dB points

Gain: 10 dB $^{+2}_{-0}$ dB

Group Delay Linearity: 0.3 ns over any 25 kHz segment of the IF_1 band

Noise Figure: < 20 dB

3rd Order I.M. Product Level: -81.5 dBm for two signals of -23.5 dBm at the inputs

Interchan. Isolation: L.O. Input to 1st IF Inputs: > 70 dB

Input Levels:

Max. Linear Sig:	-23.5 dBm
KTBNFG:	-65.8 dBm
$KTBNFG_{10\ MHz}$:	-65.8 dBm
$KTBNFG_{25\ kHz}$:	-91.8 dBm
2nd L.O.:	0 dBm (with +14 dB gain driver)

Output Levels:

Max. Linear Sig:	-13.5 dBm
KTBNFG:	-81.5 dBm
$KTBNFG_{10\ MHz}$:	-81.5 dBm
$KTBNFG_{25\ kHz}$:	-81.5 dBm

Power Supply Req: +24 VDC: 569 mA

13. PERFORMANCE REQUIREMENTS OF THE RF SUBSYSTEM HARDWARE – NARROWBAND SIGNAL DOWN-CONVERTER

IF Input Z: 50 Ω, VSWR < 1.22:1 @ 70 MHz ±5 MHz

2nd L.O. Input Z: 50 Ω, VSWR < 2:1 @ 70 MHz ±16 MHz

NB IF Output Z: 50 Ω, VSWR < 1.22:1 @ 3 MHz ±20 kHz

Frequencies: IF Input: 70 MHz
2nd L.O.: 62 MHz to 78 MHz
2nd IF Output: 3.00 MHz

Bandwidth: 1st IF: 10 MHz @ -1 dB POINTS
2nd IF: 25 kHz @ -1 dB POINTS
> 40 kHz @ - 3 dB POINTS
< 400 kHz @ -60 dB POINTS

Gain: 21 dB $^{+1}_{-0}$ dB

Group Delay Linearity: 0.3 ns @ 1st IF ± 5 MHz
0.3 ns @ 2nd IF ± 12.5 kHz

Noise Figure: < 15 dB

Isolation: 2nd L.O. to 1st IF Input: > 60 dB

Low Pass Filter f_c: 10 MHz @ -3 dB
< 62 MHz @ -30 dB

3rd Order I.M. Product Level: For 2 signals of -30 dBm at the input, the 2nd IF output shall be < -61 dBm

Input Levels:

Max. Linear Sig:	-30 dBm
KTBNFG:	-55.8 dBm
$KTBNFG_{10\ MHz}$:	-55.8 dBm
$KTBNFG_{25\ kHz}$:	-81.8 dBm

Output Levels:

Max. Linear Sig.	-9 dBm
KTBNFG:	-60.3 dBm
$KTBNFG_{10\ MHz}$:	-60.3 dBm
$KTBNFG_{25\ kHz}$:	-60.3 dBm

Power Supply Req: +24 VDC @ 306 mA

SECTION 4
DESCRIPTION OF THE DIGITAL CONTROL SUBSYSTEM

Section 4 – Description of the Digital Control Subsystem
Subsection A – Functional Description of the Processing Elements

1. OVERVIEW OF THE FUNCTIONAL DESIGN

The digital control subsystem consists of the PDP-11/05 computer, the ASR-33 teletype and the I/O interfaces between these devices, and is used to implement the different adaptive algorithms that determine the adaptive weights.

The digital control subsystem, shown in the figure, includes an 18-channel multiplexer, a 9-bit A/D converter with sample and hold, an input buffer, an output buffer, the PDP-11/05 minicomputer, and an ASR-33 teletype. Functions performed within the digital subsystem include analog-to-digital conversion of the cross-covariance measurements, I/O interfacing between the computer and the adaptive array processor, implementation of adaptive algorithms for controlling the weights, generation of timing signals, and interfacing between the user and the adaptive control software (via the teletype). Input data from the array processor consists of the $\underline{R}$ and $\underline{Q}$ vectors, and the output data consists of the weight vector $\underline{W}$ (K) and a 3-bit gain control word. Input data from the ASR-33 teletype consists of a software control program entered by punched paper tape and of program parameters entered on the keyboard. Data output to the printer gives information on the status of the adaptation process.

The 16 analog inputs representing components of the cross-covariance measurements $\underline{R}$ (1 x 8 vector) and $\underline{Q}$ (1 x 8 vector) are applied first to 16 inputs of the 18-channel multiplexer. The inputs are multiplexed and sampled sequentially and applied to the 9-bit A/D converter. With a 100 kHz sampling rate, each analog input can be sampled every 200 μs; hence, the 204 μs interval between integrator dumps. After conversion to digital form, each input is applied to an accumulator (an adder contained in the input buffer) which averages samples when required to obtain better estimates of $\underline{R}$ and $\underline{Q}$ or to allow the computer sufficient time to operate on the data. These accumulated values are reset each time new data is requested to be read into the computer. This feature allows variable-length integration of the correlator output data via the computer, with no change in the system external to the computer.

The DEC (Digital Equipment Corporation) PDP-11/05 computer was chosen over other possibilities primarily because of the asynchronous bus and the ease with which peripherals are integrated into the system. The PDP-11/05 has an architecture that enables all system elements – processor, memory, peripherals – to plug into a single asynchronous high-speed bus. Due to its asynchronous nature, the bus is compatible with devices that operate over a wide range of speeds. Faster devices can always replace slower ones, enabling hardware-implemented algorithms to replace software at minimal cost. Any pair of devices on the bus can send, receive, or exchange data without processor intervention. This allows for easy direct memory access (DMA) to interleave fetch of data from the outside world with algorithmic processing. A detailed description of the PDP-11/05 is given in a following topic.

The PDP-11/05 is interfaced with the buffer-synchronizer and the ASR-33 teletype. When data is to be transferred to or from the adaptive array, a software command is issued to relinquish control of the bus to the buffer-synchronizer. In one mode of operation, the buffer-synchronizer directs control of the I/O operation and then returns control to the computer's central processor. A complete input or output transfer within 200 μs is assured since the clock rate of the buffer synchronizer determines the rate at which input or output words are transferred.

The output buffer accepts sequential output words representing new weight and gain control attenuation values and assembles them into nine 9-bit registers. All the new values are then transferred to the attenuators at the same time.

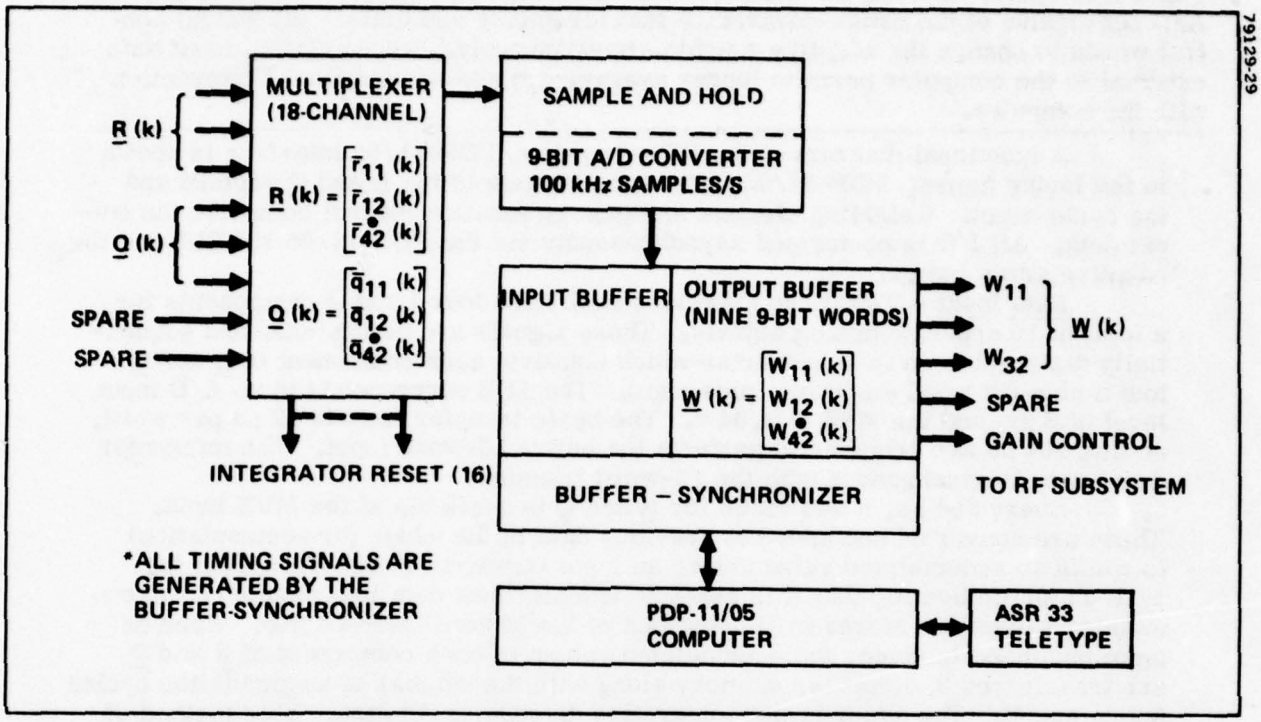

Control Subsystem. The PDP-11/05 computer uses a high-speed asynchronous bus so as to operate with other devices having a wide range of speeds.

2. DESIGN OF THE COMPUTER I/O DATA INTERFACE

The I/O interface between the computer and the RF subsystem performs the required A/D conversion of the cross-covariance measurements and buffers the weight control words to change the adaptive weights simultaneously. Accumulating input data external to the computer permits longer averaging times without direct interaction with the computer.

A functional diagram of the RF subsystem/PDP-11/05 interface is shown in the facing figure. PDP-11/05 input data consists of the R and Q vectors and the cycle count. Weighting element and gain attenuation control comprise the output data. All I/O is performed asynchronously via the PDP-11/05 UNIBUS and the adaptive array buffer.

Data Input – The R and Q vectors each have four I and Q components for a total of 16 separate analog signals. These signals are multiplexed and sequentially digitized in an A/D converter which converts each component of R and Q into a nine-bit word (eight bits plus sign). The LSB corresponds to an A/D input level of 8 mv and the MSB to 2.04 v. The basic transfer time is 12 μs per word, so that 204 μs are required to perform the entire 16-word input. The integrator dump gate is synchronous with the 16-word transfer.

Every 204 μs, a new value for R and Q is available at the MUX input. These are converted and added to previous data in the adder (or accumulation) to obtain an accumulated value unless an input command is received from the PDP-11/05 (indicating that it is ready to transfer new data into memory). Accumulated values are stored in 16 locations of the 32 word scratch pad. When an input command is given, the accumulated values of each component of R and Q are transferred to computer memory along with the number of accumulation cycles (cycle count). The adder is then cleared to dispose of old data. This method of accumulation prevents loss of data when the computer requires more than 204 μs to process the data, and permits a longer averaging time when required without direct interaction with the computer.

Prior to transfer of data to PDP-11/05 memory, each word is converted to a 16-bit 2's complement word using circuits external to the computer so that this conversion does not have to be performed in software. Accumulated values of the 16 words that comprise R and Q are also transferred to data memory (of the PDP-11/04) at a 12 μs per word rate.

Data Output – Control of each weighting element requires a 9-bit word (eight bits plus sign), and a single 3-bit word is required for gain control. These words are transferred sequentially from data memory to a set of 9 buffer registers (one register is a spare) upon software command. The buffer registers drive the weighting elements and the gain control directly, and enable all weight attenuators to be changed simultaneously. The nine word transfer from data memory to the registers requires 108 μs.

It is important to note that the value of the 9-bit word is linearly related to the value of attenuation expressed in decibels. The numeric value of attenuation and the control word are therefore nonlinearly related. Since a linear relationship is desirable to facilitate stabilization and control of the adaptive algorithms, the control word is converted to dB (using a subroutine in software) prior to its application to the weight attenuators.

Buffer-Synchronizer – The buffer-synchronizer unit interfaces with the computer and generates all of the timing signals for the analog conditioning and A/D conversion circuitry.

The buffer-synchronizer accepts and integrates the time control word from the computer. This word indicates how long each of the 20 channels is to be integrated and can be modified only after all 20 channels have been processed. Four bits, with a least significant bit weighting of 200 μs, allow computer selection of integration time from 200 μs to 3 ms. These data words are transferred to the computer's memory via a direct memory access (DMA) controller. The buffer-synchronizer also sorts and stores the output of the computer, routing the weighting information to the rest of the system.

I/O Overlap – Because of the I/O structure, an input cannot be performed simultaneously with an output. The R and Q vectors will thus represent an average measurement for two different weight vectors if the weights were changed during the interval between the last measurement and the current measurement. Since this generally leads to a degradation in performance, it is avoided in the current system by discarding the affected Q and R measurements.

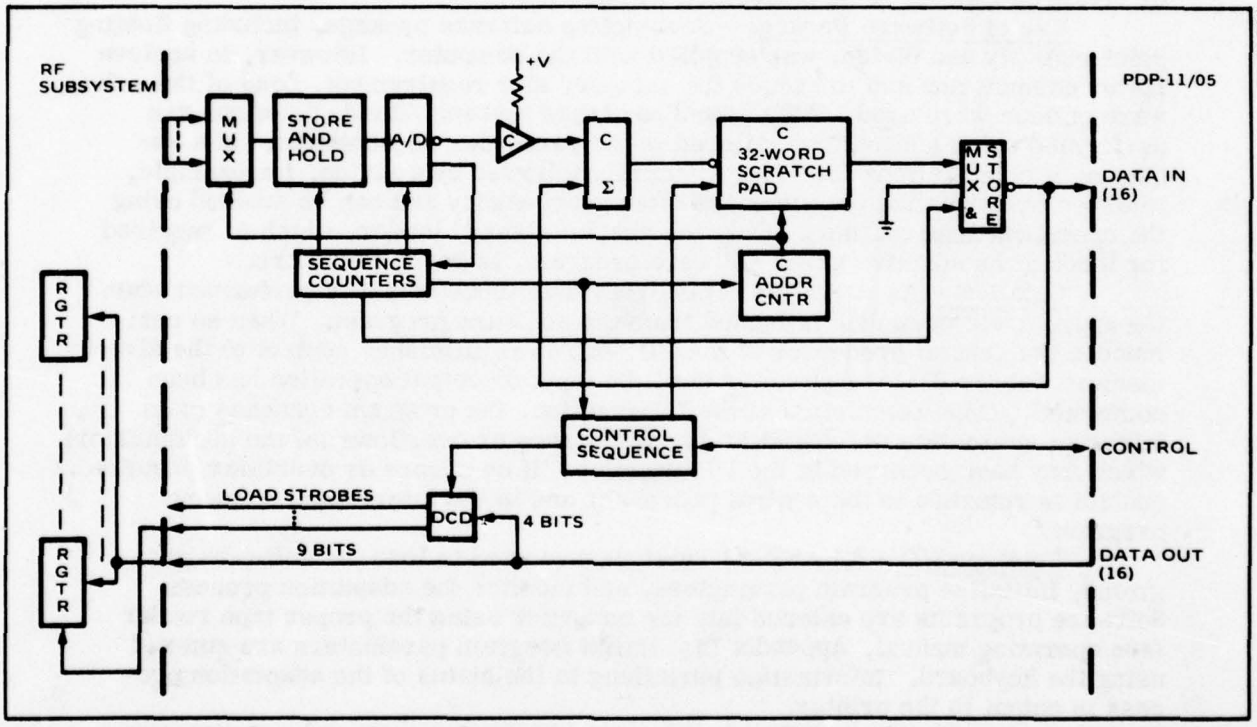

Computer I/O Interface. In this configuration, inaccurate R and Q vector measurements are discarded by the computer to avoid performance degradation.

3. DESCRIPTION OF THE PDP 11/05 COMPUTER

The PDP-11/05 is a 16-bit processor with a complete family of modules to characterize performance/cost tradeoffs, and full software support. It features a high speed asynchronous bus with direct memory access to permit rapid data transfer.

The Digital Equipment Corporation PDP-11/04 is a 16-bit processor, with eight general purpose registers, a hardware implemented stack, hardware interrupt handling, a powerful instruction set, a complete family of modules to characterize performance/cost tradeoffs, and full software support. General attributes of the PDP-11/05 computer are listed in the facing table. Selected features which pertain to use in the adaptive array processor circuit configuration are discussed in this topic.

8K Memory Option – The 8K memory option is sufficient for implementing most if not all of the envisioned algorithms. Less than 4K of memory is required by the current adaptive array software programs.

Hardware Multiply/Divide Option – The hardware multiply/divide option was selected to increase computation speed. This option allowed 16-bit multiply or divide operations to be performed within 6 μs.

Use of Software Package – A complete software package, including floating point multiply and divide, was supplied with the computer. However, to achieve faster computation and to reduce the memory size requirement, none of the software options were used. All I/O and hardware multiply/divide functions are performed using subroutines tailored to the particular requirement. In a sequence of computations involving a multiply followed by a divide, for example, intervening normalization steps are often unnecessary and can be avoided using the specialized subroutines. Only the absolute binary loader, which is required for loading the adaptive array software program, is resident in core.

Data I/O – As currently configured, data input/output is performed when the appropriate command is issued from the software program. When so commanded the central processor of the PDP-11/05 relinquishes control to the direct memory access (DMA) controller until the input or output operation has been completed. Upon completion of the I/O function, the program branches to an interrupt subroutine which checks for any errors or overflows (of the accumulator) which may have occurred in the I/O transfer. If no errors or overflows occurred, control is returned to the central processor and to the interrupted software program.

Teletype I/O – An ASR-33 Teletype was used to load the software programs, initialize program parameters, and monitor the adaptation process. Software programs are entered into the computer using the proper tape reader (see operating manual, Appendix D). Initial program parameters are entered using the keyboard. Information pertaining to the status of the adaptation process is output to the printer.

FEATURES OF THE SELECTED COMPUTER

- 16-bit processor
- Asynchronous operation – System components run at their highest possible speed; replacement with faster devices means faster operation without other hardware or software changes
- Modular component design
- Stack processing
- Direct memory access (DMA)
- Eight general purpose registers
- Automatic priority interrupt – assigns a master/slave device relationship on the asynchronous bus
- Vectored interrupts
- Powerful instruction set – includes single and double operand instructions
- Powerfail and automatic restart
- Complete software support
- Eight different addressing modes – for efficient manipulation of the data structures
- A collection of options which allow tailoring of the system to the application:
  - Hardware multiply and divide
  - Direct Memory Access Controller
  - Memory expansion from 5K words to 32K words. 8K memory option selected.

1. DESCRIPTION OF THE PROGRAM FLOW CHART

The processor software is designed to take the initial weights, gain control and modes of adaptation and, by use of either constant gain or variable gain adaptation, adjust the weights and adaptation modes to allow optimum processing of jammer signals.

The following flow graph summarizes the various functions and capabilities currently programmed in software on the PDP-11/05 computer. These functions include teletype I/O, adaptive array I/O, initialization of parameters, control of signal levels within the loop (using gain control), limiting the magnitude of internally computed weight values so as not to exceed the dynamic range of the weight attenuators, and implementing the computation for updating the weights. All but the latter function are described in this subsection. The computations for updating the weights, herein denoted as the adaptive algorithms, are discussed in Subsection C. Procedures for loading and operating the system software via the teletype or the PDP-11 switch registers are described in Appendix D, "Operating Manual".

Initialization (B) – At the beginning of the program, the initial weights, gain control and the mode(s) of adaptation are entered via the teletype. The mode of adaptation is selected on the basis of some information regarding the communication link such as desired signal level and interference levels. If the desired signal has a sufficiently high level and if the input-jammer-to-desired-signal-power is less than about 40–45 dB, for example, full adaptation (null-steering on jammers and beamforming on the desired signal) can be selected. Otherwise, the null-steering algorithm can be selected. When the input signal levels are changing or are unknown, a mode which automatically maintains signal levels within the dynamic range of the array processor can be selected. The weights can also be initialized so that the initial pattern is maximized on the desired signal (to obtain faster adaptation) if the desired signal location is known a priori.

Accumulated values of the $\underline{R}$ and $\underline{Q}$ are cleared in the final step of initialization. This prevents erroneous values of $\underline{R}$ and $\underline{Q}$ from being input in subsequent steps and is done by inputting $\underline{R}$ and $\underline{Q}$ under program control and then simply discarding the input values.

Constant Gain Adaptation – Software functions performed when adaptation is conducted with fixed values of the gain control attenuators and the internal loop gain constant (C2) are shown in the right-hand vertical column of the flowgraph (C). The loop for updating the weights begins with an input command and ends with the output of new values for the weight vectors. This process then repeats for continuous weight updates.

New values for $\underline{R}$ and $\underline{Q}$ are input six times per update at selected points within the loop. These inputs are successively stored in 12 1x8 vectors represented by $\underline{R}^{(1)} \ldots \underline{R}^{(6)}$, $\underline{Q}^{(1)} \ldots \underline{Q}^{(6)}$. By splitting the inputs into six different inputs, large values of $\underline{R}$ due to pulsed jammers can be separated from values obtained when the jammer was off. This permits pulsed jammers to be either separately processed or ignored, depending on whether the pulsed jammer affects the communication link. The intervals between successive inputs vary from 0.6 ms between the third and fourth inputs, to approximately 5 ms between the fifth and sixth inputs. Total time between weight updates, which is bounded below by the limited processing speed of the PDP-11 computer, is approximately 10 ms. It is thus possible to obtain an effective value for ΔT of 10 ms if all six input values are averaged. Note that this interval is much longer than required for obtaining accurate estimates of $\underline{R}$ and $\underline{Q}$ (see Appendix A).

Samples of $\underline{R}$ and $\underline{Q}$ are stored in $\underline{R}^{(1)}$ and $\underline{Q}^{(1)}$ in the first step of the software loop. These and the subsequent five input samples measure the cross-covariance data for the current weight vector. During the first iteration of the loop, the weight vector is equal to the initial weight vector.

Next, the square of the norm ($\| \underline{R}^{(i)} \|^2$) of each $\underline{R}^{(i)}$, i = 1, 2, ...6, is computed to give an indication of the average array output power between the (i-1)-th and i-th input* samples. The norms are then ordered by magnitude from smallest to largest.

The manner in which $\underline{R}^{(i)}$ and $\underline{Q}^{(i)}$ are averaged is determined in the next step. In the current program, the $\underline{R}^{(i)}$ and $\underline{Q}^{(i)}$ which correspond to the lowest n values of $\| \underline{R}^{(i)} \|^2$ ($1 \leq n \leq 6$) are averaged, where n has been loaded into location IFLAG via the teletype. The average values are stored in 16 locations represented by the 1x8 vectors $\underline{R}$ and $\underline{Q}$, which are subsequently used to compute the new weighting coefficients. The remaining (6-n) inputs are discarded. This procedure was implemented to prevent the adaptive array from nulling certain high-level pulsed interference sources when these interferers do not affect the communication channel because of short pulse duration and low repetition rates (up to about 600 Hz). This reserves available degrees of freedom for nulling jammers which do disrupt the communications channel. An example of a pulsed interferer is the shipborne AN/SPS-48 radar which generates harmonics in the UHF band. The adaptive array can be prevented from nulling this radar signal by setting n=2, although this has not yet been verified experimentally.

After $\underline{R}$ and $\underline{Q}$ have been determined by averaging, each of their components is shifted in phase to compensate for differential circuit delays between individual channels of the adaptive array. The phase shift is represented by the expression

$$\text{corrected value of } \underline{R} = \begin{bmatrix} e^{-j\phi_1} R_1 \\ e^{-j\phi_2} R_2 \\ e^{-j\phi_3} R_3 \\ e^{-j\phi_4} R_4 \end{bmatrix} \qquad (1)$$

where $\underline{R}_i$=i-th component of $\underline{R}$ = [in-phase R_i] +j [quadrature R_i] and similarly for $\underline{Q}$. ϕ_1 is equal to the differential phase shift between the two inputs of the i-th correlator when a CW signal centered on the 70 MHz IF passband is applied to the input of the i-th channel. Note that this procedure does not guarantee exact phase matching at the center frequency of the processor since the phase difference between the in-phase and quadrature components of R_i (or Q_i) is not exactly 90°. The effect of small errors in the quadrature relationship does not significantly affect adaptive array performance, however, because this error is removed by closed loop adaptation.

After correcting for insertion phase errors, the $\underline{R}$ and $\underline{Q}$ vectors are ready to be used in updating the weights. The updated weights are computed using one of the adaptive algorithms described in part C of this section, and are stored in a 1x8 block labeled W1. These new values are then tested to insure that their

* $\| \underline{R}^{(i)} \|^2$ is proportional to the square of the average output power.

1. DESCRIPTION OF THE PROGRAM FLOW CHART (Continued)

magnitudes do not exceed a value of one (which corresponds to the minimum zero dB attenuation). When one of the components of W1 exceeds one, it is set equal to one. This procedure prevents overflow of W1 which would result in erroneous weight attenuation.

Up to this point, the weight attenuators have remained unchanged from their previous values. The new weights have values from -1 to +1 (±0 dB) and are stored in eight storage locations (denoted by W1) with the decimal number 16320 (377 ØØ in octal) corresponding to a weight value of one (zero dB attenuation). Two methods for transferring these values to the weight attenuators are available in the program software. In the first method, the stored values are divided by 2^6 and applied directly to the weight attenuators. This method requires the least amount of time to perform, but has the disadvantage that the relation between W1 and the actual attenuation is highly non-linear. In the second method, which was the method used in the pattern range tests, the values of W1 are transformed so that W1 and the amount of attenuation is linearly related. For example, 16320 represents 0 dB attenuation and 1632 represents 20 dB attenuation.

Variable Gain Adaptation – With the variable gain option, the gain control attenuators and the loop gain constant (C2) are placed under program control. This option is selected by setting AFLAG = 1 during initialization. This option is implemented to maintain the output signal level within the dynamic range of the adaptive processor and to stabilize the adaptive algorithm, but is not intended to implement an accelerated gradient algorithm.

The procedure for adjusting gains, represented functionally in the left column of the flow graph (A), automatically adjusts the amount of gain control attenuation required to maintain $\| \underline{R} \|^2$ within the predetermined range given by

$$\text{DETMIN} < \| \underline{R} \|^2 < \text{DETMAX}. \qquad (2)$$

At the same time, C2 must be varied in order to maintain rapid but stable adaptation*.

The above objectives are not synonymous, since the rate of adaptation for a given value of C2 is proportional to the square root of the total input power. The output power, on the other hand, depends on the parameters of normalization (e.g., the preferred output signal level established by the method used to normalize the $\underline{Q}$ vector) and the signal environment, and is not directly related to the input jammer power because of cancellation.

For a constant (non time-varying) signal environment, this problem is easily solved by estimating the input signal power during the first weight update. This is achieved by initially setting one weight attenuator to zero dB and all others to maximum attenuation.** The method used is illustrated by the flow diagram. Before the first weight update, the amount of attenuation is increased until $\| \underline{R} \|^2$ falls within the bounds in Equation (2). For the purposes of adaptation, this gives a sufficiently accurate (±4 dB) estimate of the input signal power. Adaptation begins when the criterion on $\| \underline{R} \|^2$ is met.

In a system with infinite dynamic range, the amount of attenuation need not be changed once $\| \underline{R} \|^2$ is less than DETMAX. In the UHF adaptive array, however, the dynamic range of the $\underline{R}$ and $\underline{Q}$ measurements is limited to

*C2 is a program constant.

**The antenna elements are assumed to have nearly identical patterns.

48 dB (eight bits resolution), which translates to a 24 dB dynamic range at the array input. For this reason, the amount of gain control attenuation is decreased by 8 dB when jammer cancellation reduces $\| \underline{R} \|^2$ below DETMIN. At the same time, C2 is reduced by a factor of 2.5 (~4 dB) to maintain a constant rate of adaptation and to prevent loop instability. This procedure results in up to a 16 dB increase in dynamic range of $\underline{R}$ and $\underline{Q}$ when the gain control attenuation is reduced twice in the above fashion.

A difficulty with the above procedure occurs when the total received signal power changes (time-varying signal environment) since the amount of increase or decrease in power cannot be determined from $\underline{R}$ and $\underline{Q}$ without reinitializing the weights. * This leads to possible stability problems, to adaptation rates which are much slower than could otherwise be achieved or to insufficient gain. The present solution is only partially successful in alleviating the difficulty. A large increase in total input power (e.g., due to a new jammer) is either sensed immediately by causing $\| \underline{R} \|^2$ to increase, or is sensed later by causing $\| \underline{R} \|^2$ to increase due to loop instability. In either case, gain control attenuation is increased when $\| \underline{R} \|^2 >$ DETMAX so that proper adaptive array operation is soon reestablished (Note that C2 is not changed during this procedure). A large decrease of input signal power (e.g., due to a high-level jammer shutting off), on the other hand, may not significantly affect the values of $\underline{R}$ and $\underline{Q}$. The procedure programmed in software (see flow diagram) is successful in decreasing attenuation when a drop in input signal power occurs. However, it occasionally decreases attenuation when no change in the environment has occurred, thereby causing brief loop instability.

The dynamic range/adaptation time difficulties encountered can be eliminated in future implementations by improving the dynamic range, measuring the input power directly, or by implementing algorithms that are insensitive to input power levels.

*The alternative of reinitializing the weights to measure input power is to be avoided, since this can result in a large jammer signal appearing at the array output.

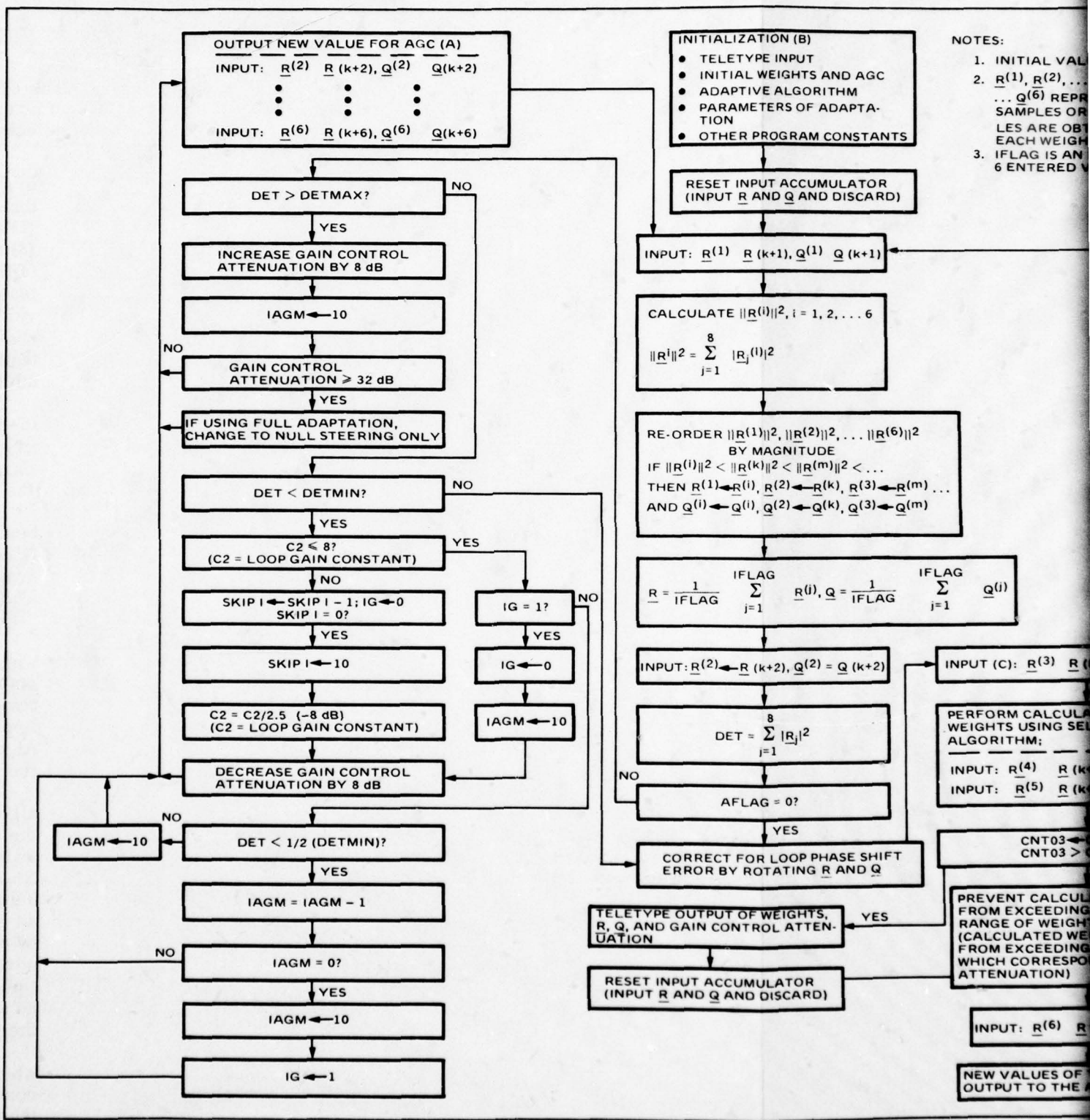

Flow Graph Showing Functions Performed by the PDP-11/105 Software. initialization, constant gain adaptation and variable gain adaptation.

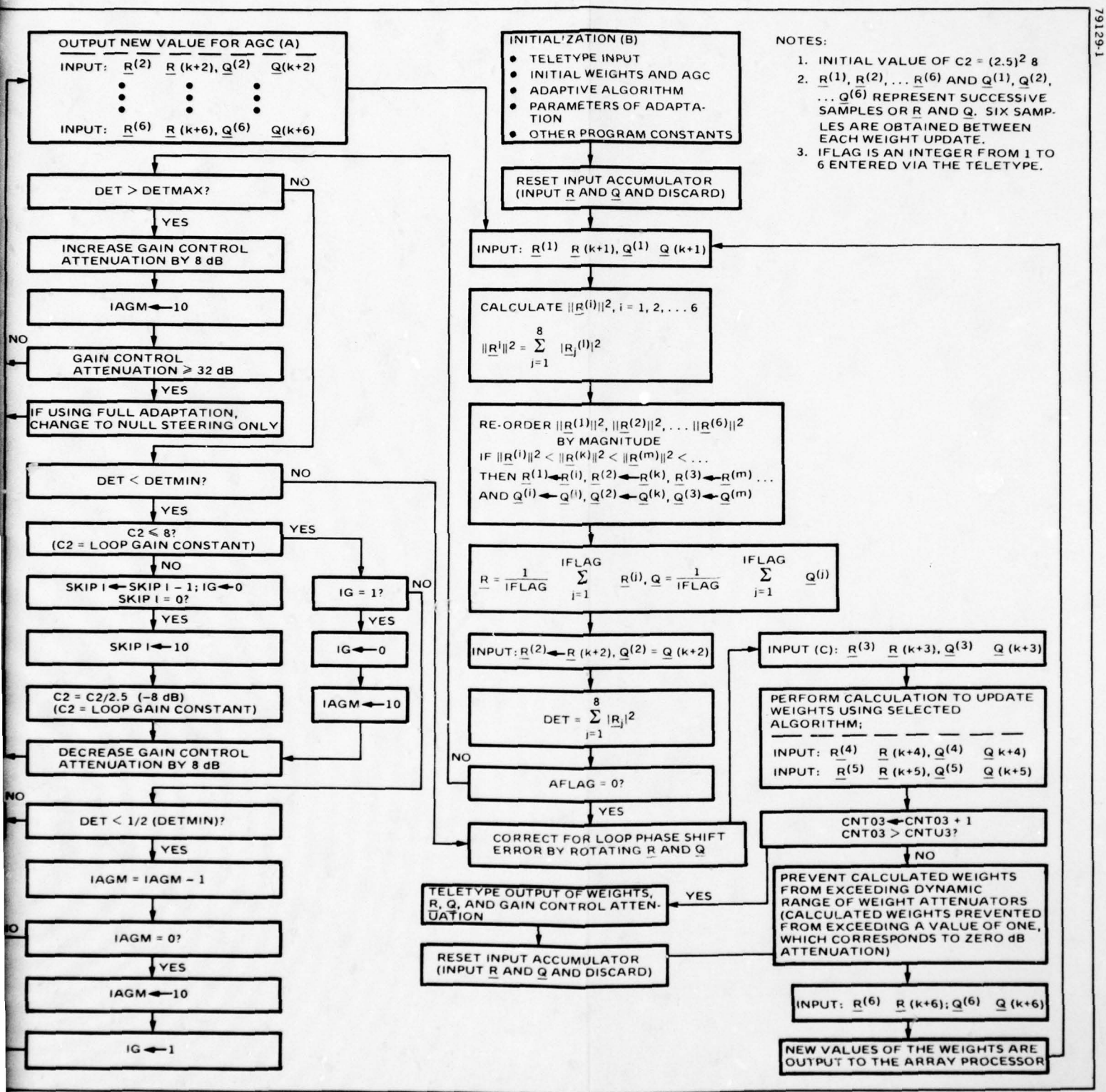

Flow Graph Showing Functions Performed by the PDP-11/105 Software. The major tasks are initialization, constant gain adaptation and variable gain adaptation.

1. OVERVIEW OF THE ADAPTIVE WEIGHT ALGORITHMS

The UHF adaptive array implementation provides the capability to evaluate a variety of adaptation algorithms. The steepest descent and null-steering algorithms were selected for implementation in order to demonstrate the hardware.

A large number of algorithms exist in the literature that can be utilized to adapt the antenna array to the required mean square error criteria. Those that show potential for this application can be grouped into the following classes: (1) steepest descent gradient, (2) sequential (Kalman) adaptation (recursive), (3) accelerated gradient, and (4) constrained main beam. The prime objective of these different techniques is to decrease the adaptation time. One important feature of the implementation is the capability of initializing the weights to provide a preformed beam if the general direction of the desired signal source is known a priori (open loop beam steering); This feature can allow a substantial decrease in acquisition time in addition to providing an initial S/I and S/N advantage.

One of the objectives of the current effort was to evaluate the flexibility of computer programming to incorporate a meaningful number of the repertoire of existing mean-square algorithms. This objective is discussed in the following paragraphs and a relative comparison of the algorithms is shown in the table on the facing page.

Steepest Gradient Descent – The classical approach to adaptive arrays has been the steepest descent algorithm proposed by Widrow (1967) and Applebaum (1966). The extension of the results for incorporation of the estimation of the desired signal is discussed by Riegler and Compton (1973), and Miller (1976). The general form of the algorithm is

$$\underline{W}(k) = \underline{W}(k-1) + K(k)\,[\underline{Q}(k) - \underline{R}(k)] \qquad (1)$$

where K(k) is selected as a compromise between adaptation time and final steady state solution. The value may be arbitrarily modified during the adaptation trajectory. Variants of this basic approach have been widely discussed by Applebaum, Widrow and others. Several variants of the Steepest Gradient Descent Algorithm were implemented to demonstrate the performance of the UHF adaptive array hardware. These are discussed in detail in the following topic.

Constrained Main Beam – The use of constrained main beam adaptation algorithms has been discussed by Frost (1972) and Applebaum (1974). In addition, the Coherent Sidelobe Canceller (CSLC), Null-steering algorithms, and algorithms utilizing open loop main beam steering can be viewed as variants of this approach. Null-steering algorithms and open-loop formation of the main beam are discussed below. Frost's lagrange multiplier approach to beam forming using the $\underline{Q}$ vector as a constraint leads to essentially the same optimum weight vector (they differ by a scalar constant) as other minimum mean-squared error algorithms discussed herein. Different results are obtained, however, when a null constraint or multiple constraints are imposed on the antenna patterns (via the weights). Although no attempt was made during the current effort to implement these constraints, the potential does exist for programming this type of optimization algorithm.

Null-Steering Algorithm – Null-steering denotes an adaptive technique wherein all interference signals and noise signals are minimized subject to a constraint which prevents the weights from shutting off. In the present context, these constraints are presumed to be imposed by setting the weights of one or more of the antenna channels to fixed values. The fixed weight values are entered open loop, and cancellation is obtained by adjusting the remaining "free" weights

to minimize the array output power. An algorithm of this type was implemented in the UHF adaptive processor using a modified steepest descent technique to obtain cancellation. This algorithm is discussed in detail in a following topic.

Open-Loop Beamforming – The UHF adaptive array system can be utilized as an open-loop beamformer. The accurate (9-bits plus sign) and stable programmable complex weights allow a mode of operation by computer programming wherein any antenna pattern, with its main beam pointed in a predetermined direction, may be formed subject to the constraints implied by the array geometry, the number of array elements, and their corresponding radiating properties. This main beam steering (or positioning) is accomplished by a direct (computer) calculation of the required weight settings based on an a-priori knowledge of the direction of arrival of the desired signal and the array factors enumerated above.

An open-loop main beam steering algorithm has been implemented in the UHF adaptive array. It can be used for rapid acquisition of signals with a-priori knowledge of elevation and azimuth position angles. Inasmuch as this approach can also provide an initial estimate for the element weights at the outset of adaptation which provide reduced sidelobes, accelerated jammer cancellation will

TRADEOFF OF ADAPTATION ALGORITHMS

Algorithm Class	Advantages	Disadvantages
Steepest Gradient Descent	• Well known classical approach – works • Simple to implement • Stable	• Slow convergence rate
Constrained Main Beam	• Quick acquisition with a prior signal location data • Can be made to maintain low sidelobes – less susceptable to transients of interference in sidelobes	• Computational requirement • CSLC variant is not fully adaptive
Null Steering	• Simple to implement • A priori signal location data not required	• Not fully adaptive
Sequential (Kalman) Adaptation	• Fast convergence rate • Processes measured data in optimum manner	• Substantial computational requirements
Accelerated Gradient	• Fast convergence	• Large number of measurements required • Large computational requirement • Potential for larger steady state errors and instability

1. OVERVIEW OF THE ADAPTIVE WEIGHT ALGORITHMS (Continued)

follow (Miller [1976]). Although the open loop main beam steering algorithm has been implemented, it will not be discussed here in detail since only very preliminary experimental tests were performed. Use of this algorithm is discussed further in the Operating Manual, Appendix D.

Sequential (Kalman) Adaptation – A sequential or recursive approach, drawing upon Kalman filter theory, has been applied to adaptive arrays by Baird [1974] and to a class of adaptive filters (transversal equalizers) by Godard [1974]. Although these approaches utilize an instantaneous measurement of X(t), they can be extended to utilize covariance measurement data only. This extension results in the following equation:

$$\underline{W}(k) = \underline{W}(k-1) + K(k)\,[\underline{Q}(k) - \underline{R}(k)] \quad (2)$$

$$K(k) = P(k-1)\,R_{xx}(k)\,[R_{xx}(k)P(k-1)R_{xx}(k) + \xi^2]^{-1} \quad (3)$$

$$P(k) = P(k-1) - K(k)\,R_{xx}(k)\,P_{k-1} \quad (4)$$

This approach requires that the system be programmed to measure $R_{xx}(k)$, the 4 x 4 covariance matrix of the array input signals, which requires at least 800 μs since a single column of the covariance matrix is measured during each ΔT, the integration time of the covariance measurement circuit. The measurement of $R_{xx}(k)$ need only be performed once for stationary environments. The value of ξ^2 is selected simply to preclude any computational difficulties arising from an ill-conditioned $R_{xx}(k)$ matrix.

A tradeoff will be required in future studies to evaluate the adaptation time improvement obtained by utilizing this approach. Although simulations have not been made by Hughes for this application, Godard [1974, p272] showed substantial improvement using this approach over the use of gradient algorithms for the transversal equalizer problem.

Accelerated Gradient – Techniques for increasing the speed of convergence of the gradient technique have been discussed by Reed [1974] and White. In addition, there exists substantial literature on accelerated gradient techniques for which a good discussion is given by Isaacs [1966]. One attractive approach is the use of Powell's [1962] gradient acceleration technique which, if the covariances are measured accurately, results in a three-step process to reach the optimum gain values. Unfortunately, the need to measure the equivalent of second partials adds to the time required. Also, the inherent inaccuracy due to the necessity of estimating the covariance terms with finite time measurements results in more than a three-step operation. It may, however, be desirable for the initial steps in adaptation. Although this approach was not implemented during the current phase of the contract, this class of algorithms could be implemented with software in the current system.

2. DESCRIPTION OF THE FULL ADAPTATION ALGORITHM USING STEEPEST GRADIENT DESCENT

An algorithm that adapts to maximize the array output signal-to-jammer-plus thermal-noise ratio, referred to as the full adaptation algorithm, has been programmed into the PDP-11 microprocessor. This algorithm uses the $\underline{Q}$ vector measurement to maximize the output desired signal and the $\underline{R}$ vector to simultaneously reduce the output-jammer-plus-thermal-noise power.

The full adaptation algorithm uses a steepest gradient descent technique which may be expressed mathematically in the form

$$\underline{W}(k+1) = \gamma_1 \underline{W}(k) + \gamma_2 \{q\underline{Q}(k) - \underline{R}(k)\} \tag{1}$$

where

$$q = \gamma_3 \left(\frac{1}{\| \underline{Q}(k) \|} - \gamma_4\right) \tag{2}$$

$\underline{W}(k)$ = weight vector at the k^{th} instant or iteration

γ_1 = exponential decay constant

γ_2 = loop gain constant

$\gamma_2\gamma_3$ = loop gain constant in the narrowband loops

γ_4 = constant to control output desired signal level

$\underline{Q}(k)$ and $\underline{R}(k)$ are defined in Appendix A.

The m-dimensional vectors $\underline{\tilde{X}}(t)$, $\Lambda(t)\underline{\tilde{X}}(t)$, $\underline{\tilde{Y}}(t)$, and $\Omega(t)\underline{\tilde{Z}}(t)$ are defined in Appendix A. The scalar q in Equation (2) is a function of the magnitude of $\underline{Q}$ and is used to normalize the output desired signal level.

For the purposes of comparison, the discrete LMS and modified Griffiths (1969) LMS algorithms can be written in the form

$$\underline{W}(k+1) = \underline{W}(k) + \alpha \underline{X}(t) [\tilde{r}^{\dagger}(t) - \underline{\tilde{X}}^{\dagger}(t) \underline{W}(k)] \tag{3}$$

$$\underline{W}(k+1) = \underline{W}(k) + \alpha [\underline{S} - \underline{\tilde{X}}(t)\tilde{X}^{\dagger}(t) \underline{W}(k)] \tag{4}$$

where $r(t) = \beta\tilde{S}(t)$, and β is an arbitrary constant (see Appendix A). If the loop gain constant α is suffieicntly small, Equations (3) and (4) may be approximated by

$$\underline{W}(k+1) = \underline{W}(k) + \alpha[\underline{S} - R_{xx}\underline{W}(k)] \tag{5}$$

where $\underline{s}$ represents the desired signal cross correlation vector and $\underline{R}_{xx}$ the covariance matrix of the input signals (see Appendix A). This weight equation converges to the desired solution

$$W_{opt}\Big|_{k\to\infty} = R_{xx}^{-1}\underline{S}$$

Equation (1) is similar to the LMS algorithms in that it utilizes the method of steepest descent to direct the weighting coefficients toward the optimum solution. The ensemble average of $\underline{R}(k)$ corresponds to the term $R_{xx}\underline{W}(k)$, and $\underline{Q}(k)$ corresponds to the vector $\underline{S}$ which directs the solution toward desired signal maximization under appropriate conditions.

The full adaptation algorithm differs from the LMS algorithm in some respects to take advantage of the unique UHF adaptive array implementation and to accommodate the applications for which it is designed. The most significant differences are manifested in the method used to obtain beam-pointing and in the separate treatment of the beam-pointing ($\underline{Q}$) and null-steering ($\underline{R}$) vectors. In the intended applications, only the spectral characteristics of the desired signal are known, i.e., s(t) and S are unknown. Desired signal information required for jammer separation is obtained using a modification of the ideal reference signal approach (Riegler and Compton (1974), Miller (1976)), wherein the reference signal $\tilde{r}(t)$ is estimated from the array output using filtering/waveform processing. Rather than generate an error signal $r(t) - \tilde{\underline{X}}^{\dagger}(t)\, W$, a separate vector $\underline{Q}$ is generated in the modified approach to permit monitoring of the output desired signal level and location and to allow flexibility for storing this vector for use as the estimate of desired signal direction-delay vector, $\underline{S}$.

Before discussing other aspects which distinguish Equation (1) from LMS algorithms consider the effect of the limiters on $\underline{Q}$ and $\underline{R}$. To simplify the discussion, assume that the effect of the limiters is to scale the magnitude of the ensemble average of the $\underline{R}$ and $\underline{Q}$ vectors as discussed in Appendix A. This assumption is valid for Gaussian input signals and holds approximately for certain other types of signals.

For sufficiently small values of γ_2 and γ_{2q}, and for $\gamma_1 = 1$, Equation (1) converges to satisfy the steady-state condition

$$q E\underline{Q}(k) = E\underline{R}(k) \qquad (k \text{ large}) \tag{6}$$

From Appendix B, this condition can be rewritten as (See Appendix A for definitions)

$$W(k) = \sqrt{\frac{P_{I_W}}{P_{I_N}}}\,\gamma_3 \left(\frac{2\sqrt{\frac{P_{I_N}}{\pi m}}}{\left\| R_{zz}\, W(k) \right\|} - \gamma_4 \right) R_{xx}^{-1}\, R_{zz}\, \underline{W}(k) \tag{7}$$

Under conditions where the signal-to-noise ratio of the array output signal is large within the 30 KHz desired signal band*, the matrix R_{zz} is approximated by

$$R_{zz} = E\left[\tilde{\underline{S}}(t)\, \tilde{\underline{S}}^{\dagger}(t) \right] = \underline{S}\, \underline{S}^{\dagger} \tag{8}$$

Under this assumption, it can be shown that the solution for $\underline{W}(k)$ in Equation (8) is given by

$$W(k) = \left[\frac{\sqrt{P_{I_N}}}{\left\| \underline{S} \right\|} \quad \frac{\sqrt{4/(\pi m)}}{\sqrt{P_{I_N}/P_{I_W}}\, \frac{1}{\gamma_3} + \frac{S_0}{1+S_0}\, \gamma_4} \right] R_{xx}^{-1} s = \beta_3 R_{xx}^{-1} S \tag{9}$$

---

* See Appendix B for a discussion of when this is a good assumption.

2. DESCRIPTION OF THE FULL ADAPTATION ALGORITHM USING STEEPEST GRADIENT DESCENT (Continued)

where

S_0 = the optimum output signal-to-jammer-plus-noise ratio in the 10 MHz processing band

The last equality indicates that the solution for $\underline{\bar{W}}$ optimizes the output-signal-to-jammer-plus-noise ratio. In addition, nearly optimum steady-state performance can be obtained under certain conditions even when the array output signal-to-noise ratio is not large (see Appendix B).

The steady-state output voltage (r.m.s.) of the desired signal is given by

$$V_s = \frac{1}{\sqrt{\pi}} \frac{\sqrt{P_{I_N}}}{\|\underline{S}\|} \frac{1}{\sqrt{P_{I_N}/P_{I_W}} \frac{1+S_0}{\gamma_3 S_0} + \gamma_4}$$

where the number of weighting coefficients (m) was set equal to four. The expression for V_s gives a clearer indication of how the normalizing constant q affects the output desired level. In the software, the constants γ_3 and γ_4 are selected so that

$$\sqrt{P_{I_N}/P_{I_W}} \frac{1+S_0}{\gamma_3 S_0} << \gamma_4 \tag{11}$$

under high-level interference conditions ($\sqrt{P_{I_N}/P_{I_W}}$ small) in order to desensitize the dependence of V_s on the input jammer level. The appropriate constants are determined a priori based on the maximum value of the left hand side which is expected in a particular application. Assuming (11) is satisfied, V_s is approximated by

$$V_s = \frac{1}{\sqrt{\pi}} \cdot \frac{\sqrt{P_{I_N}}}{\|\underline{S}\|} \frac{1}{\gamma_4} \tag{12}$$

This shows that V_s^2 increases in proportion to the input jammer to signal ratio within the 30 KHz desired signal band, but is insensitive to the input desired signal level when the signal to jammer plus noise ratio is greater than approximately 0 dB within the 30 KHz bandwidth. Normalizing the output signal level in this manner allows closer control of the magnitude of the steady-state weighting coefficients so that saturation of the weights can be prevented.

Equation (1) also differs from LMS algorithms when $\gamma_1 \neq 1$. Setting $\gamma_1 < 1$ de-emphasizes the effect of old data (past weight values) on the calculation of the current weight values and results in faster adaptation and thus better performance in rapidly changing signal situations. Unfortunately, it can also cause the output-signal-to-jammer-plus-thermal-noise ratio to decrease. The effect of γ_1 on the solution to the weight equation is exactly the same as if the thermal noise power in each channel were increased by the factor

$$\xi = 1 + \frac{2(1-\gamma_1)}{\gamma_2 \sigma^2} \sqrt{\frac{P_{I_W}}{\pi m}}$$

where σ^2 = the original thermal noise power in each channel. Equations (9) and (10) can be modified to account for $\gamma_1 \neq 1$ by replacing S_0 by the (lower) optimum output signal to jammer plus thermal noise ratios $S\gamma_1$ which would be obtained if the thermal noise in each channel were increased by the factor ξ. Note that the optimum signal to jammer plus noise ratio is greater than $S\gamma_1$ since the excess thermal noise is not actually added and thus does not appear at the array output.

In the current configuration, γ_1 is used to (1) place an upper bound on the longest time constant associated with convergence of $\underline{W}(k)$ and (2) insure thermal noise minimization when the contribution of thermal noise to the R vector measurement is too small to be resolved by the A/D converters. The latter condition occurs under high-level jammer conditions due to limiter suppression (in the wideband channel) or to the reduction in gain via the gain control attenuators. A rule of thumb suggests that if a particular jammer is to be suppressed, then $\xi\sigma^2$ should not exceed the input power of the jammer.

The following example, which was selected to be a typical test condition of the UHF adaptive array, will clarify some of the above concepts.

The following parameter values describe the approximate conditions of the test results for the case of the narrowband signal and wideband jammer (see Section 5). The desired signal is CW, and the jammer has an 8 MHz bandwidth centered on the desired signal frequency.

S = input desired signal power (one channel) = -93.3 dBm $< 0^o$

J = input jammer power (one channel) = -64.1 dBm $< 30^o$

T.N. = thermal noise power (one channel) = -98 dBm

S_0 = output-signal-to-jammer-plus-thermal-noise ratio = 8 dB

$\gamma_1 = 1 - 1.95 \times 10^{-3}$

$\gamma_2 \sqrt{\pi P_{I_W}} = 0.2$

$\gamma_4 = 0.35$

$\gamma_3 = 5.7$

$$\frac{2(1-\gamma_1)}{\gamma_2 \gamma_2} \sqrt{\frac{P_{I_W}}{\pi m}} = 24.0 \text{ (13.8 dB)}$$

$$\frac{\sqrt{P_{I_N}}}{\|s\|} = 2.0 \text{ (3.0 dB)}$$

$$\sqrt{\frac{P_{I_N}}{P_{I_W}}} = 224 \text{ (23.5 dB)}$$

2. DESCRIPTION OF THE FULL ADAPTATION ALGORITHM USING STEEPEST GRADIENT DESCENT (Continued)

Using these parameter values, one obtains

$$V_s \cong 3.2$$

This gives the equivalent signal voltage as determined from the measurement of Q. The true output signal level is determined by dividing V_s by the circuit gain from the array output to the output of the integrate dump circuits in the narrowband channel. After performing this normalization, one obtains

$$V_{s_{TRUE}} = 1.4 \times 10^{-5} \text{ volts rms}$$

or -66 dBm

This is in good agreement with the measured value of -68 dBm.

3. DESCRIPTION OF THE NULL-STEERING ALGORITHM

Null steering is used for adaptation when the desired signal input is low or when the output signal-to-jammer-plus-noise ratio does not allow accurate narrowband correlation. In the null steering technique, jammers are suppressed in a specific region of the external jammer environment.

Null-steering denotes an adaptive technique wherein all jammers and noise sources which originate from a specified region of the external environment are minimized. Null-steering can be used to provide jammer suppression whenever the beam steering vector cannot be accurately estimated. This situation occurs when the input desired signal power is low ($\tilde{<}$-120 dBm) or when the output signal-to-jammer-plus-noise ratio is insufficient for accurate narrowband correlation.

As currently programmed, null-steering is accomplished by minimizing the residue between signals received in a reference antenna and the signals received by one or more of the three remaining antennas (denoted the auxiliary antennas or elements). Specifically, $\| \underline{R} \|$ is minimized by adjusting the auxiliary weights using a steepest descent adaptation technique. The technique is illustrated in the facing figure and is represented mathematically by the iterative relation

$$\underline{W}'(k+1) = \gamma_1 \underline{W}'(k) - \gamma_2 \underline{R}' \qquad (1)$$

Here, $\underline{W}'$ and $\underline{R}'$ are ℓ-dimensional vectors ($\ell < m$), where ℓ equals the number of auxiliary antenna elements. In the hardware, the weighting coefficient in the reference channel (W_0) is held fixed at a preselected value during adaptation, so that the adaptive array output signal is given by

$$\tilde{Z}(t) = \tilde{X}_0(t)\, W_0 + \tilde{X}'^{\dagger}(t)\, \underline{W}'(k) \qquad (2)$$

where $\tilde{X}_0(t)$ and W_0 represent the reference antenna signal and weighting coefficient, respectively, and $\underline{\tilde{X}}'(t)$ represents the auxiliary antenna signals. Note that $\tilde{z}(t)$ and $\tilde{x}_0(t)$ are scalars, whereas $\underline{\tilde{X}}(t)$ and $\underline{W}'(k)$ are ℓ-dimensional vectors.

The null-steering algorithm is equivalent to the full adaptation algorithm with $\underline{Q}$ set equal to zero and with one constant weighting coefficient. Signals received by the reference antenna and one or more of the auxiliary channels are suppressed, the degree of suppression being related to the ratio J/ξ where (see Equ. 7 in Appendix B)

$$\xi = 1 - \gamma_1 + \frac{\gamma_2 \sqrt{\pi m}}{2\sqrt{P_{IW}}}\sigma^2$$

σ^2 = input thermal noise power in each channel of the adaptive array processor

J = input jammer power in each channel of the adaptive array processor

Because of the OE-82B antenna elements have approximately the same gain, it may be necessary to increase ξ to prevent active nulling of the desired signal if its level is high. Note, however, that this also prevents active nulling of jammers which have levels nearly equal to or smaller than the desired signal level.

79129

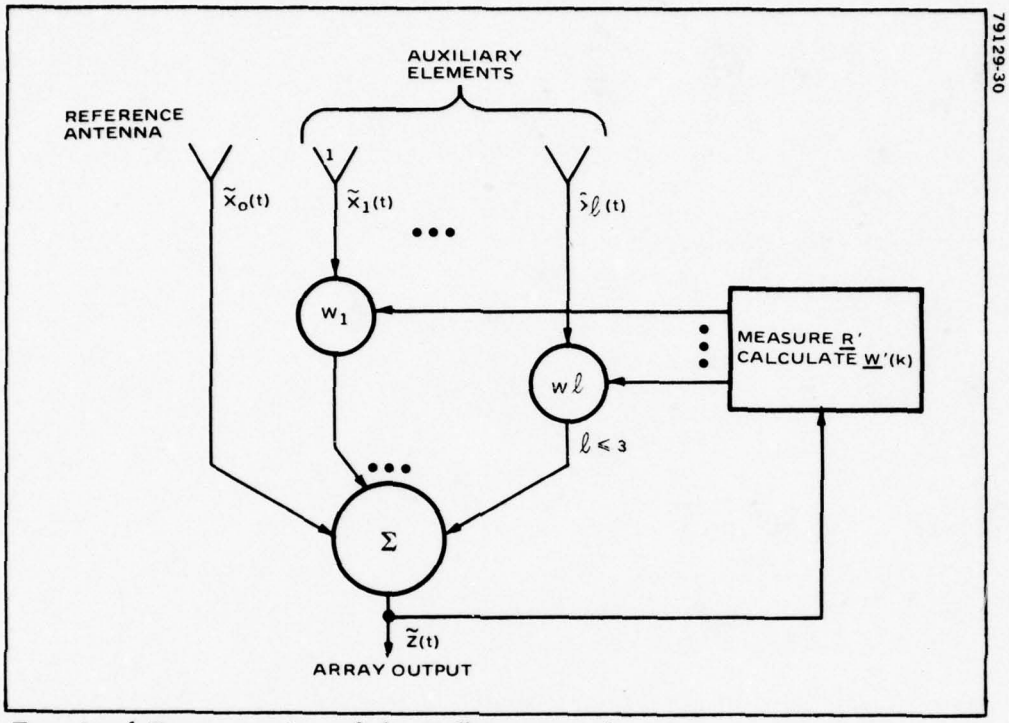

Functional Representation of the Null-Steering Algorithm. In this technique all jammers and noise sources from a specific area are minimized, thus allowing jammer suppression when the beam steering vector cannot be accurately estimated.

SECTION 5
TEST RESULTS

Section 5 – Results of Antenna Pattern Range Tests

1. DESCRIPTION OF THE PATTERN RANGE TEST CONFIGURATION

The adaptive array processor performance was evaluated on the pattern range using both an OE-82B antenna supplied by NRL and a Hughes four-element linear array comprised of four vertically polarized bow-tie elements. These test antennas were used to obtain antenna radiation patterns and to determine adaptive array processor performance under conditions similar to those encountered aboard ship.

The pattern range test configuration consisted of a desired signal source and two interference sources with separately located transmit antennas, a four-element receive array, the adaptive array processor and associated test and pattern recording equipment (See Figure A). System tests were conducted with the array mounted at the Hughes 100-ft antenna pattern range facility shown in Figure B.

The locations of antenna No. 1 and antenna No. 3 were fixed, while the angular separation between the desired and interfering sources was controlled by adjusting the azimuth and elevation of the four-element array and the azimuth of antenna No. 2. Antenna patterns were obtained by first allowing the adaptive array to stabilize in the signal and interference environment under test. The weighting networks were then locked by the computer program and the signal and jammer sources turned off. An antenna pattern was then measured by transmitting a CW signal from antenna No. 1 and recording the adaptive system output power as a function of the orientation of the four-element array relative to antenna No. 1. Antennas No. 1, 2, and 3 were all linearly polarized.

The receive antennas were either the four-element-square circularly polarized OE-82B array or the Hughes four-element linearly polarized array. These communications antennas are typical of those in shipboard installations. The OE-82B antenna, for example, is currently deployed for shipboard SATCOM applications and was used to test UHF adaptive array performance aboard the USS Richard E. Byrd (DDG-23).

The pattern range tests were conducted at a nominal 260 MHz RF frequency. Two types of desired signals and both narrowband and wideband interfering signals were used in the tests. The narrowband desired signal was obtained using a CW signal generator. This desired signal selection sufficed because adaptive array performance is insensitive to the type of modulation as long as most of the desired signal power is confined to the 25 kHz desired signal band. A spread-spectrum desired signal was generated using the NRL PTT spread-spectrum modem. Spreading was accomplished by modulating a 260 MHz carrier with a known P-N code. The code rate was 2.4 Mbps for most tests, corresponding to a spreading ratio of 21 dB when the information rate is 19.2 kbps.

The antenna interface unit (AIU) was used in the pattern range tests to perform RF preselection and amplification to match shipboard conditions as closely as possible. The RF preselection filter had a 260 MHz center frequency and a 30 MHz bandwidth. The measured system noise figure was approximately 5.5 dB with one weight attenuator set to zero dB and all others set to maximize attenuation (63.75 dB). Thus, the 6 dB noise figure requirement was satisfied.

The local oscillator frequencies shown in Figure B were selected so that a CW signal input at 260 MHz would fall in the center of the 70 MHz first IF and the 3 MHz second IF. The second LO (67 MHz) was modulated by the known P-N code when conducting tests with the spread-spectrum desired signal.

The pattern range test results are presented in the following topics. These results were selected as representative of the test performance of the UHF adaptive array.

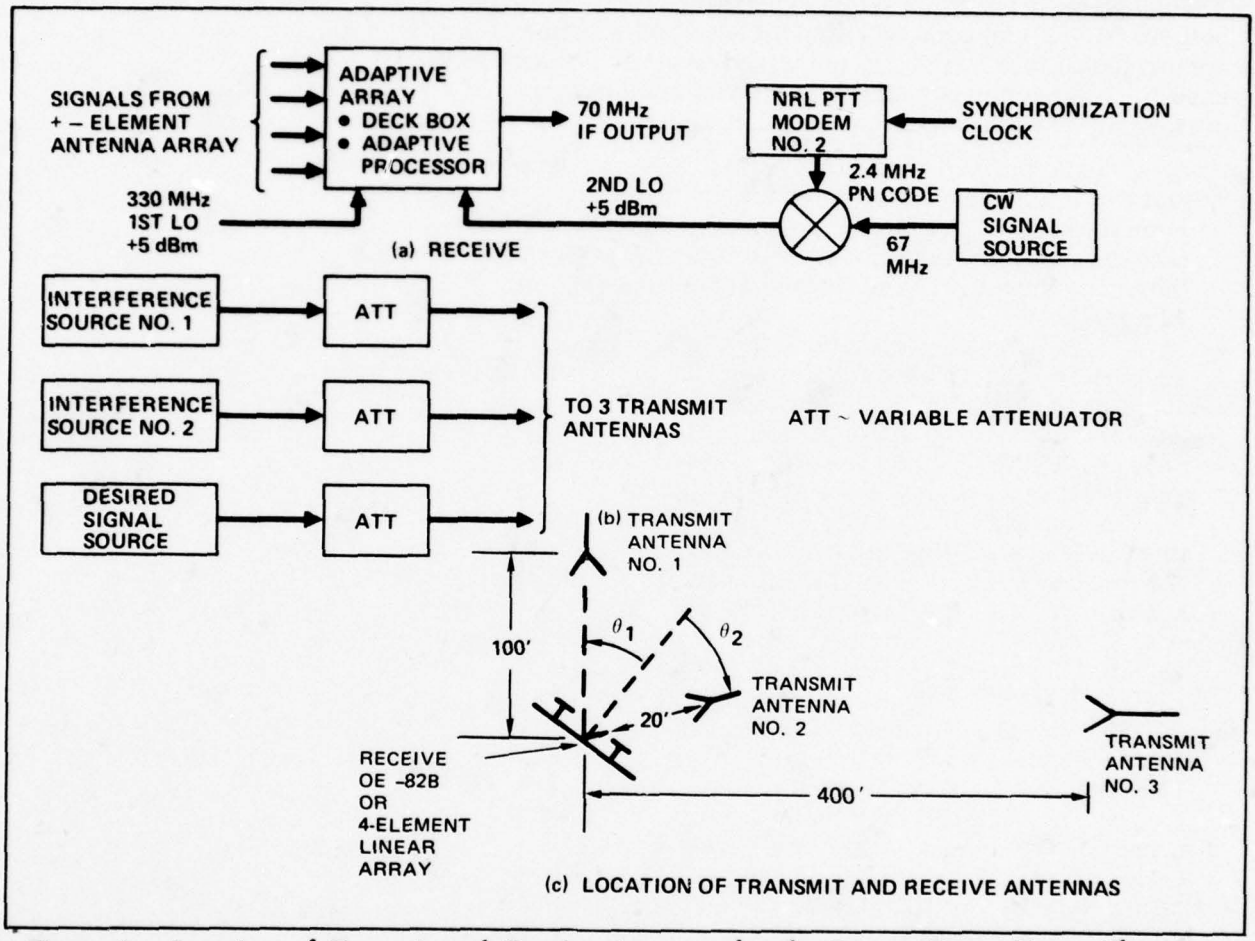

Figure A. Location of Transmit and Receive Antennas for the Pattern Range Test. The test configuration provides variable signal levels and locations for the three transmit antennas which are consistent with the intended shipboard environment and which are necessary for the proper evaluation of the adaptive processor.

77-01-224

Figure B. The Hughes 100-foot Antenna Test Range. The OE-82B antenna receive array and Antenna No. 2 are mounted on the receive site tower. Antenna No. 1 is mounted on the tower in the foreground.

2. ADAPTIVE ARRAY BEAMFORMING PERFORMANCE WITH NARROWBAND DESIRED SIGNAL

The adaptive array beamforming performance was evaluated using the OE-82B four-element array with a narrowband desired signal and either a narrowband or wideband jammer signal. Signal-to-jammer performance improved by 35 dB with the narrowband jammer when the adaptive array was used.

The array patterns were measured after adaptation for a narrowband desired signal and a narrowband jammer signal. Figure A shows steady-state adaptive array patterns for two different jammer locations with a broadside desired signal. The signal-to-jammer and signal-to-noise ratios before and after adaptation are indicated in the illustrations. These results were obtained using the full adaptation algorithm. Note that there is approximately 35 dB improvement in the signal-to-jammer ratio, while the signal-to-thermal-noise ratio has remained unchanged for angular separations of ±20 degrees between the desired signal and jammer signal locations. For smaller angular separations the signal-to-thermal-noise ratio decreases due to the limited spatial resolution of the OE-82B array elements, particularly when the angular separation is less than 10^{o}.

The array patterns were also measured using a wideband jammer signal with a 3 dB bandwidth of approximately 12 MHz. The adaptive processor has a 3 dB bandwidth of 15 MHz so that the level of jammer rejection is higher than would have been obtained with a wider band jammer due to the greater frequency dependent mismatch between channels near the passband edges. Figure B shows the beamforming performance both with and without the jammer and Figure C illustrates the spectrum analyzer display before and after adaptation. It is noted that after adaptation the signal-to-wideband-jammer ratio has been improved by approximately 25 dB and the signal-to-thermal-noise ratio has been improved by approximately 4 dB.

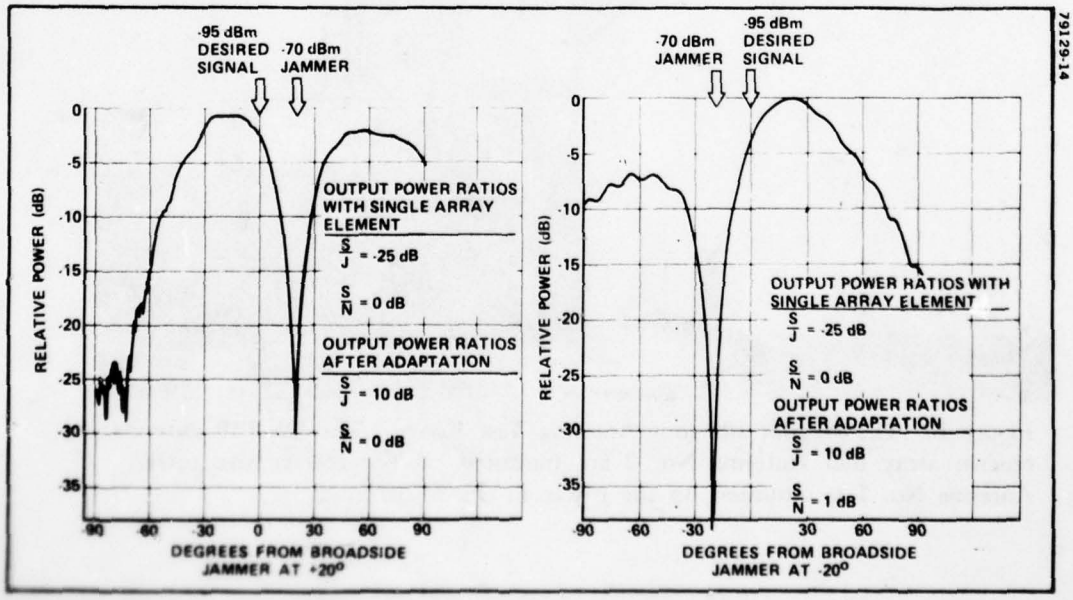

Figure A. UHF Adaptive Array Patterns After Adaptation Using OE-82B Antenna; CW Desired Signal and CW Jammer. For a CW jammer the improvement in signal-to-jammer ratio after adaptation is approximately 35 dB.

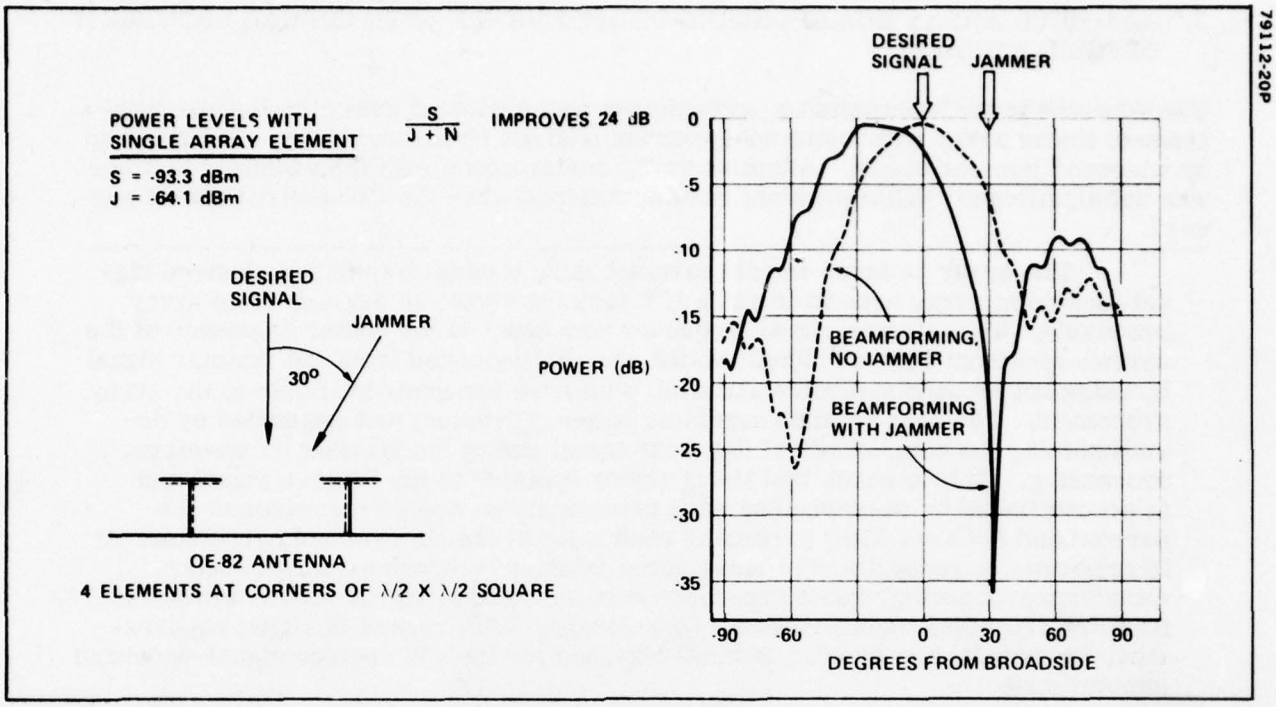

Figure B. UHF Adaptive Array Patterns After Adaptation, CW Signal, Wideband Jammer. For a wideband jammer (12 MHz), the improvement in signal-to-jammer ratio is approximately 24 dB.

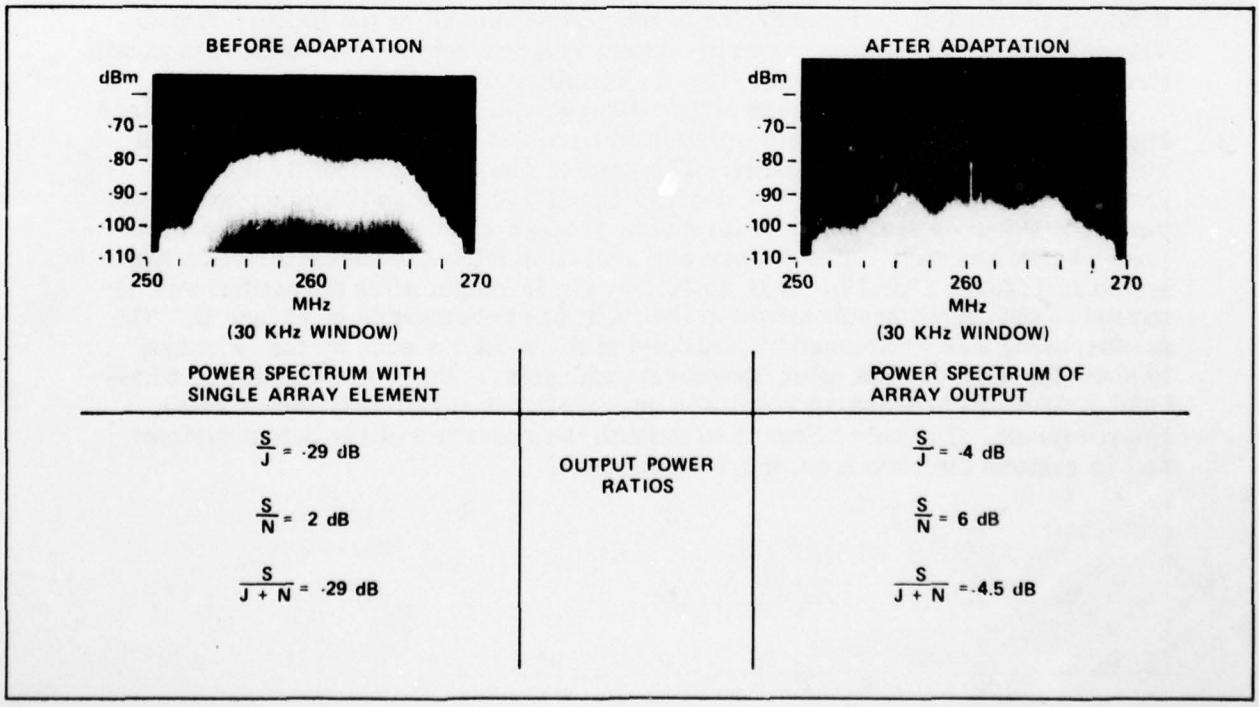

Figure C. UHF Adaptive Array Processor Provides 24 dB J + N Improvement; CW Signal, Wideband Jammer. The adaptive processor also improves the signal-to-thermal noise ratio by 4 dB.

3. ADAPTIVE ARRAY BEAMFORMING PERFORMANCE WITH SPREAD SPECTRUM DESIRED SIGNALS

The adaptive array beamforming performance was evaluated using the Hughes four-element linear array with a spread-spectrum desired signal and either a narrowband or wideband jammer signal. Adaptive array performance with the wideband jammer was not significantly different from results obtained when the CW desired signal was used.

The array patterns were measured using a spread-spectrum desired signal located at array broadside and a CW jammer signal 20 degrees from array broadside. The jammer signal frequency was equal to the center frequency of the spread-spectrum desired signal, which was distinguished from the jammer signal by using known code structure and timing information made available to the array processor. The narrowband correlator output ($\underline{Q}$ vector) was generated by de-emphasizing the components of the input signal due to the jammer by waveform processing. This ensures that the $\underline{Q}$ vector "points" to the desired signal and is accomplished by de-spreading each antenna signal before it arrives at the narrowband (25 kHz) filter preceding each input of the narrowband correlator. It is important to recognize that since some jammer components remain after waveform processing, some suppression of the desired signal occurs within the limiters preceding the narrowband correlators. With regard to signal suppression, the results are similar to those obtained for the CW desired signal-wideband jammer case.

Figures A and B show typical performance obtained with a spread spectrum desired signal and a CW jammer. Note that the IF output level is higher than that obtained under CW desired signal – CW jammer conditions. This is due to the negative signal-to-jammer ratio ($\approx$-6 dB) of the signal applied to the limiters and results in suppression of the desired signal at the limiter output. The desired signal level at the array output must therefore be increased to obtain the same value for $\underline{Q}$ as dictated by the adaptive algorithm.

The array patterns were also measured using a spread-spectrum desired signal located 40 degrees from array broadside and a wideband jammer signal 20 degrees from array broadside. The results are not significantly different from those obtained with the CW desired signal and wideband jammer conditions since the PN-code spreading/despreading process affords no appreciable waveform processing gain. The pattern and spectrum analyzer characteristics are shown in Figures C and D. It is noted that the IF output after adaptation was despread to obtain the result shown in the right hand photograph of Figure D. The de-spreading was performed by multiplying the local PN code by the IF output to show the array output after waveform processing. Since the jammer is wideband, waveform processing results in no significant signal-to-jammer ratio improvement. The only effect is to smooth the spectrum of the output jammer and to remove the code from the desired signal.

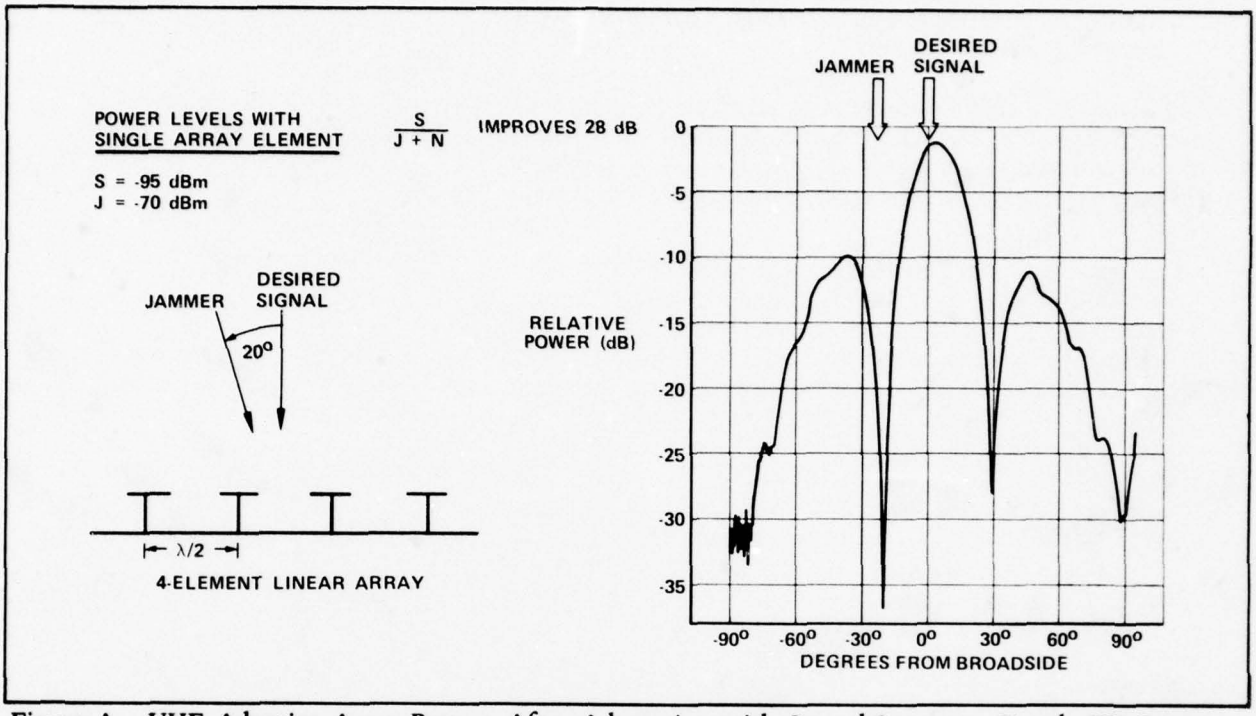

Figure A. UHF Adaptive Array Pattern After Adaptation with Spread-Spectrum Signal, CW Jammer on Center Frequency. The adaptive process forms a null in the antenna radiation pattern in the direction of the undesired jammer signal.

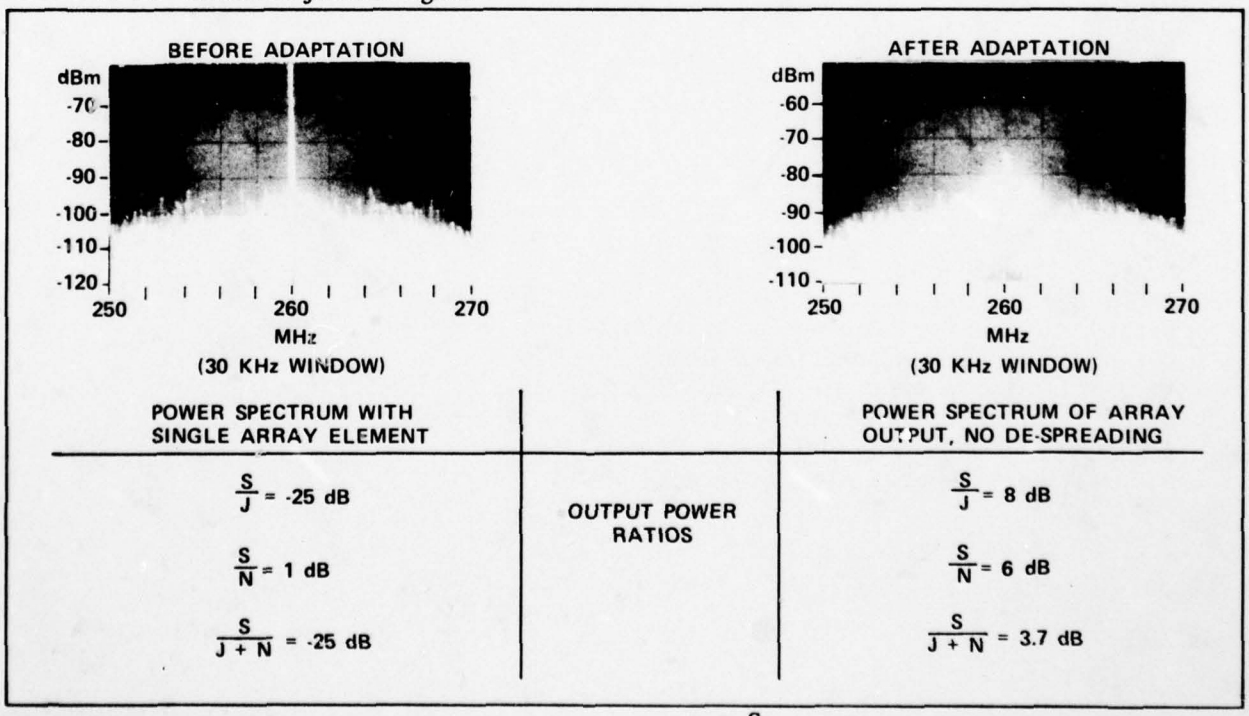

POWER SPECTRUM WITH SINGLE ARRAY ELEMENT		POWER SPECTRUM OF ARRAY OUTPUT, NO DE-SPREADING
$\frac{S}{J}$ = -25 dB	OUTPUT POWER RATIOS	$\frac{S}{J}$ = 8 dB
$\frac{S}{N}$ = 1 dB		$\frac{S}{N}$ = 6 dB
$\frac{S}{J+N}$ = -25 dB		$\frac{S}{J+N}$ = 3.7 dB

Figure B. UHF Adaptive Array Processor Provides 28 dB $\frac{S}{J+N}$ Improvement with Spread-Spectrum Signal, CW Jammer on Center Frequency. The spectrum analyzer is used to provide a calibrated display of signal, jammer, and noise power levels as a function of frequency content.

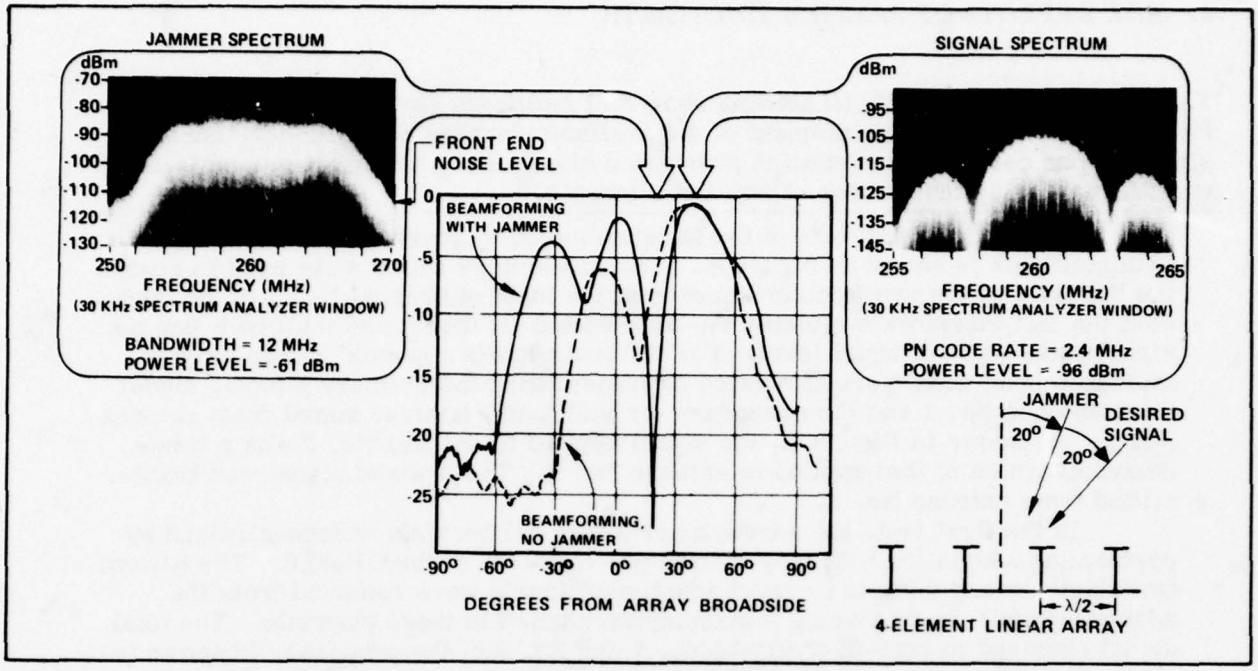

Figure C. UHF Adaptive Array Patterns After Adaptation; Spread-Spectrum Signal, Wideband Jammer. The pattern nulling capability of the adaptive process is excellent even with a wideband jammer signal.

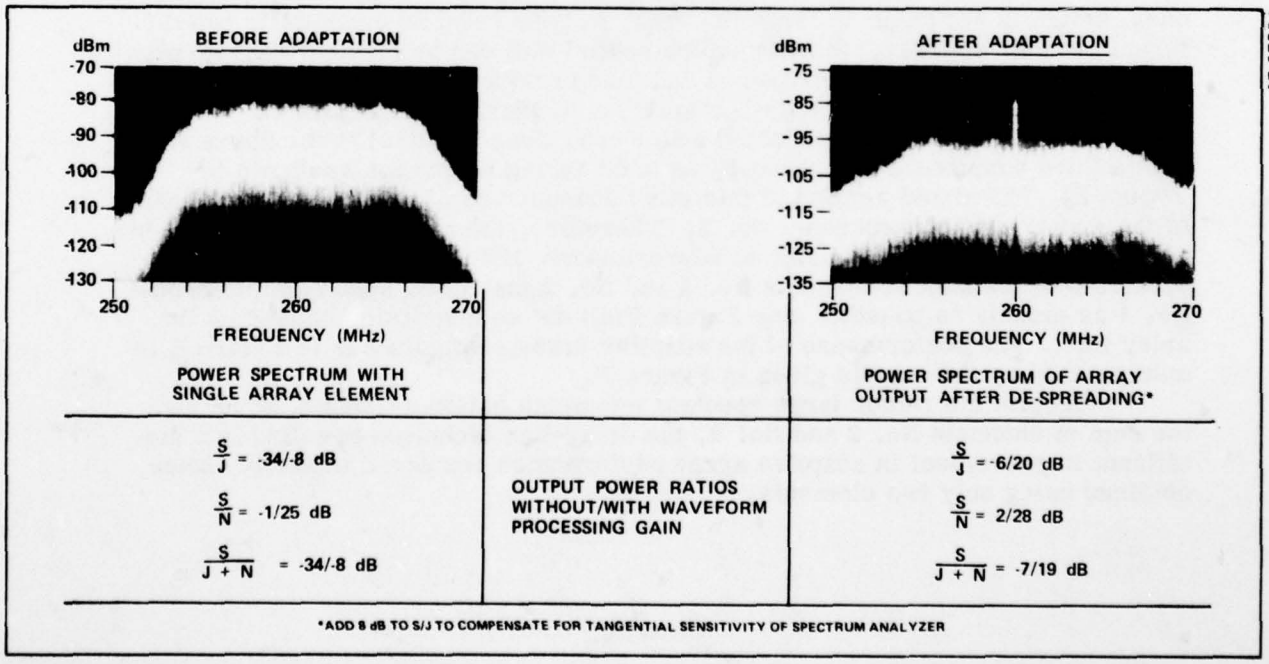

Figure D. Spectrum Analyzer Display Showing Signal and Noise Levels Before and After Adaptation. The UHF Adaptive Array Processor provides 27 dB $\frac{S}{J+N}$ Improvement with Spread-Spectrum Signal, wideband jammer. Spectrum analyzer window = 30 kHz; no video filtering used.

4. THE EFFECTS OF JAMMER MULTIPATH

Test results with the OE-82B antenna show that multipath seriously degrades performance due to overconstrainment of the available degrees of freedom. Use of a single tapped delay implementation provides a significant performance improvement without increasing the number of antenna elements.

A simplified diagram of the technique used to generate a jammer signal with multipath is shown in Figure A. The attenuators shown were used to equalize the level of the two jammer sources at the input of channel No. 1 of the deck box; the test therefore simulated the case where the direct and multipath jammer signal paths were of equal level. For the test results reported in this topic, multipath conditions were simulated by transmitting the primary jammer signal from antenna No. 1 and the secondary (or multipath) jammer signal from antenna No. 2. As shown in Figure B, the signal applied to antenna No. 2 was a time-delayed version of that applied to antenna No. 1. The desired signal was transmitted from antenna No. 3.

In the first test, the adaptive array was deliberately overconstrained by performing adaptation with only the top two elements of the OE-82B. The bottom two elements and their associated adaptive channels were removed from the adaptation process by placing maximum attenuation in these channels. The total signal received in each of channels No. 1 and No. 2 of the processor is shown in Figure C. Figure C(a) gives the best indication of the amount of delay between the jammer and its multipath signal because the jammer levels are most closely matched for this case. Since the spectral "nulls" occur 8.5 MHz apart, the delay between their arrival times at antenna No. 1 was approximately 120 nanoseconds, which is sufficient to force the array to treat them as essentially two different jammer sources. Since only one spatial null can be formed with two elements, the array is overconstrained and thus provides very poor performance in this case, as shown by the post-adaptation photographs in Figure D.

A second test was conducted under conditions identical to the above except a third adaptive array channel was used during adaptation as shown in Figure E. The signal applied to this third channel was a time delayed version of the signal applied to channel No. 2. Therefore, the number of array elements remained equal to two. A delay of approximately 120 ns was used so that the spectrum of the sum of channels No. 1 and No. 2 match the spectrum of channel No. 1 as closely as possible (see Figure F(a)) due to dispersion caused by the delay line. The performance of the adaptive array configured as in Figure E is summarized by the results given in Figure F.

Despite the rather large spectral mismatch between Channel No. 1 and the sum of channels No. 2 and No. 3, the delay-line technique resulted in a significant improvement in adaptive array performance compared to performance obtained using only two elements.

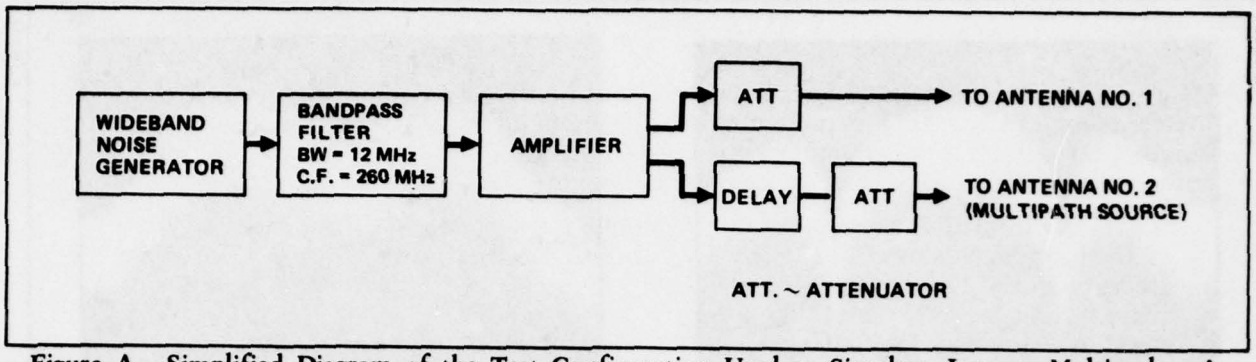

Figure A. Simplified Diagram of the Test Configuration Used to Simulate Jammer Multipath. A delay line and variable attenuators provide primary jammer and multipath signal control for evaluation of the adaptive processor.

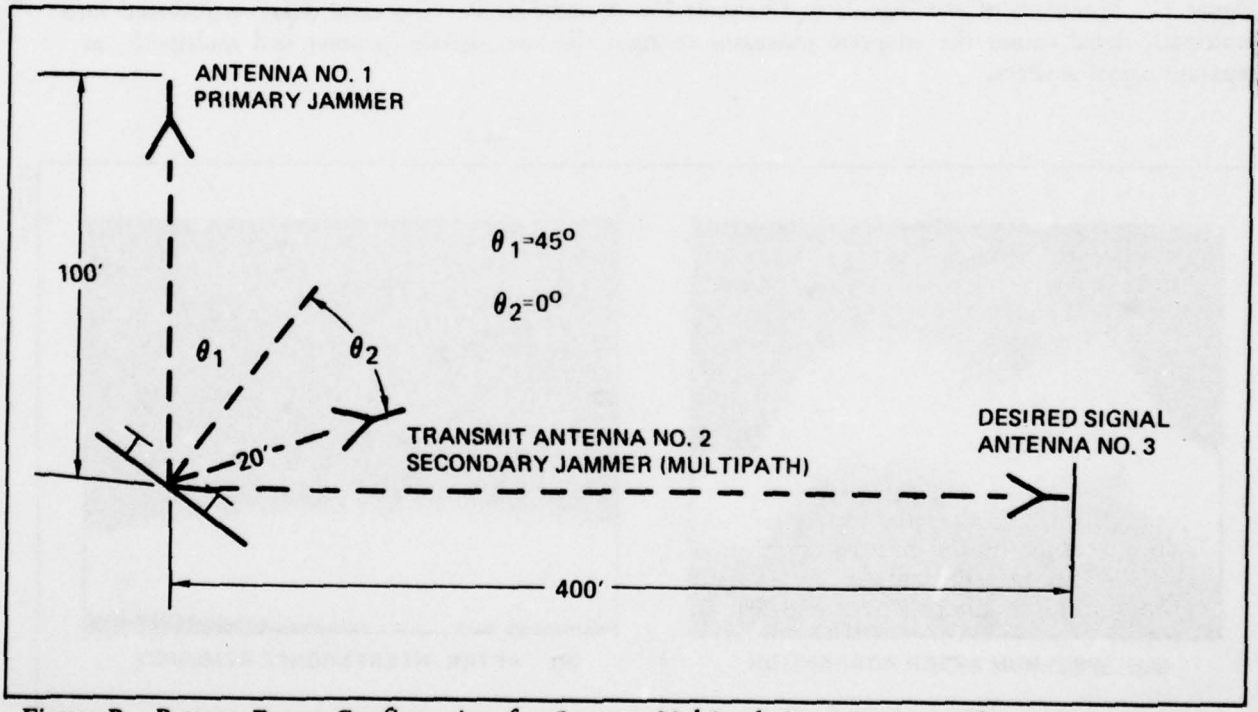

Figure B. Pattern Range Configuration for Jammer Multipath Investigation. The primary jammer signal is transmitted from Antenna No. 1 and the time delayed multipath signal is transmitted from Antenna No. 2.

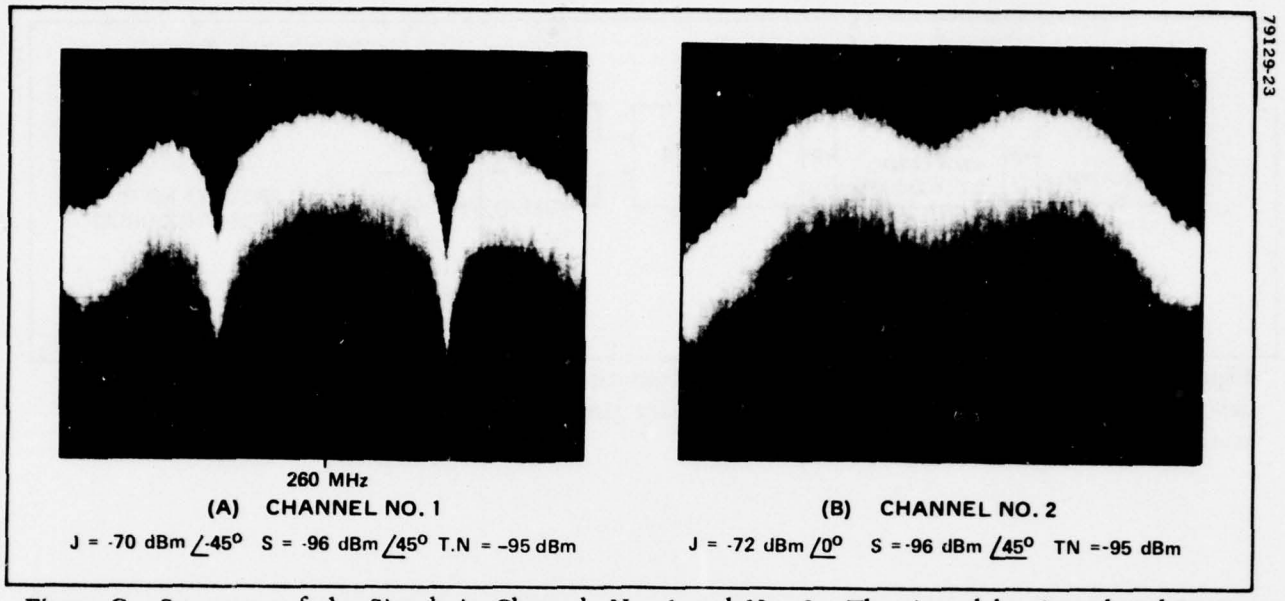

Figure C. Spectrum of the Signals in Channels No. 1 and No. 2. The time delay introduced into multipath signal causes the adaptive processor to treat the two signals (jammer and multipath) as separate signal sources.

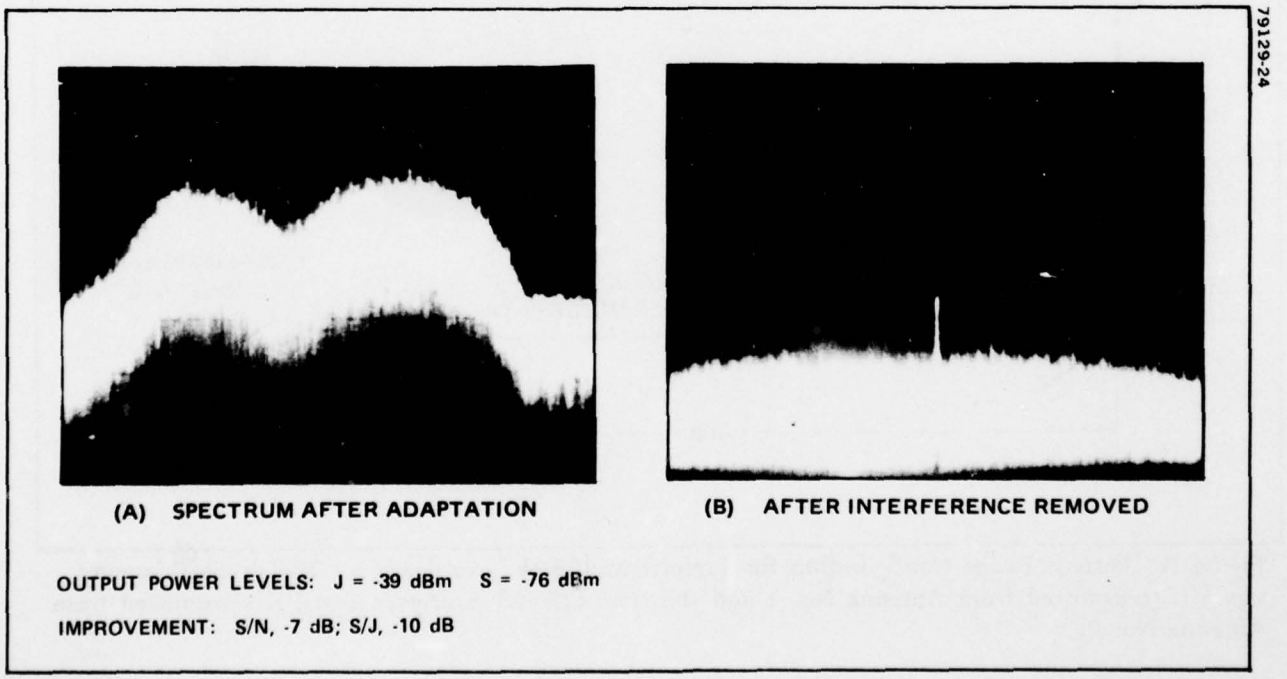

Figure D. Spectrum After Adaptation, Interference Removed. With only two elements of the OE-82 used in the adaptive process, only one spatial null can be formed. This overconstrained condition results in very poor performance.

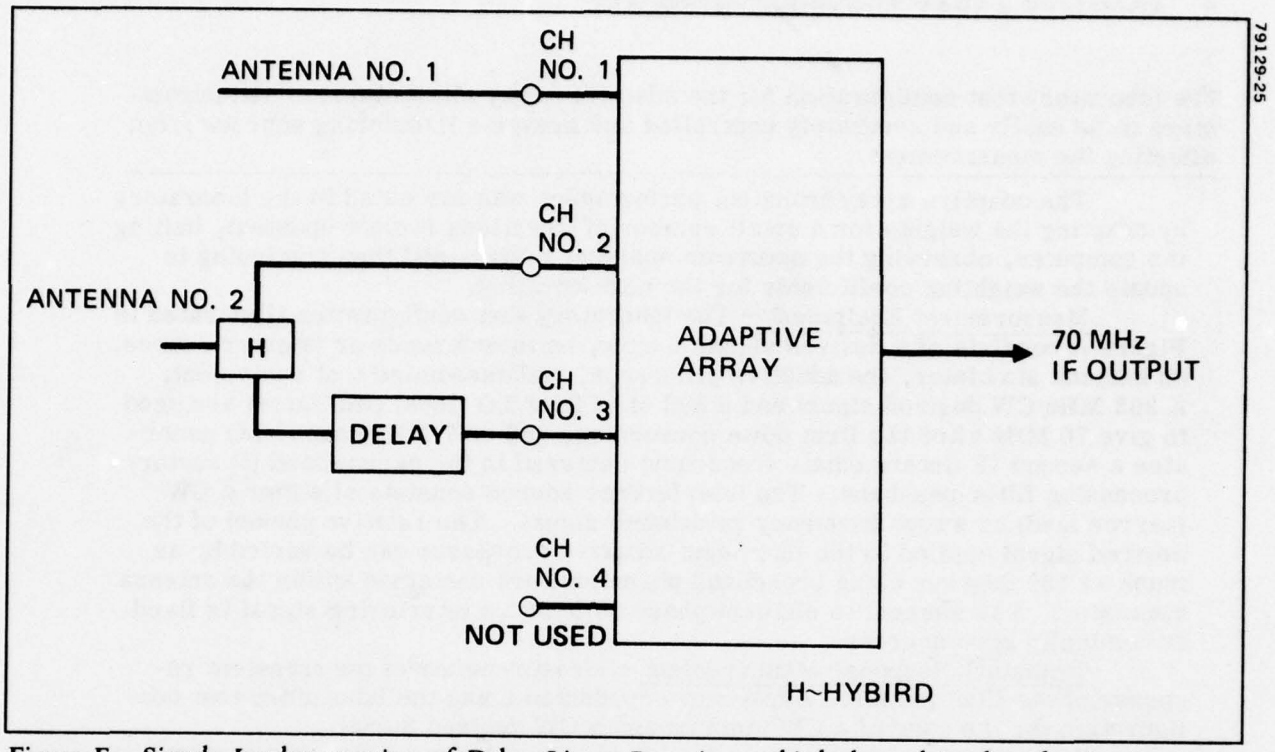

Figure E. Simple Implementation of Delay Line. By using a third channel in the adaptive processor, significant improvement in performance is possible.

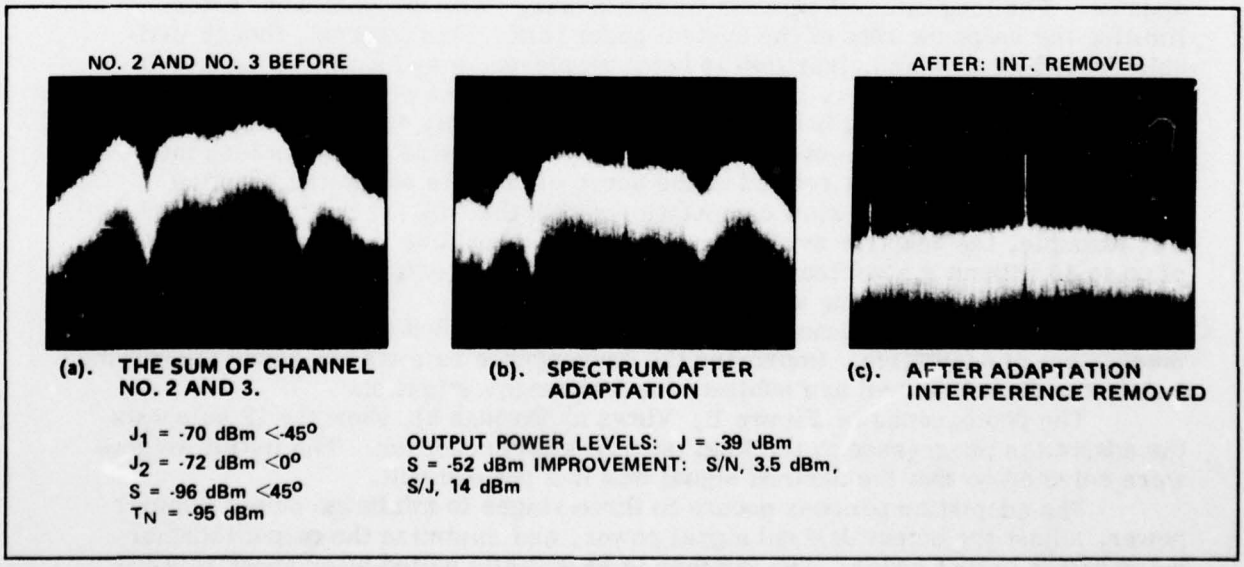

Figure F. Adaptive Array Performance with the Delay-Line Implementation of Figure E. Conditions are otherwise identical to those of Figure C. (a), shows the sum of signals received in channels No. 2 and No. 3 and (b), shows the IF output after adaptation. (c) shows the past-adaptation output when the input jammer is removed.

5. ADAPTIVE ARRAY TRANSIENT RESPONSE

The laboratory test configuration for the adaptive array allows input signal parameters to be easily and accurately controlled and prevents interfering sources from affecting the measurement.

The adaptive array transient performance was evaluated in the laboratory by adapting the weights for a small number of iterations (weight updates), halting the computer, observing the spectrum analyzer output, and then continuing to update the weighting coefficients for the next iteration.

Measurement Equipment – The laboratory test configuration illustrated in Figure A consists of a desired signal source, an interference or jammer source, an antenna simulator, the adaptive processor, and associated test equipment. A 262 MHz CW desired signal and a 332 MHz first LO (local oscillator) are used to give 70 MHz after the first down conversion, and a 67 MHz second LO generates a second IF (intermediate frequency) centered in the narrowband (Q vector) processing filter passband. The interference source consists of either a CW (narrowband) or swept frequency (wideband) signal. The relative phases of the desired signal applied to the four input adaptive processor can be varied by as much as 180 degrees using broadband phase shifters contained within the antenna simulator. The element to element phase shift of the interfering signal is fixed at nominally zero degrees.

Transient Response Measurement – Measurements of the transient response of the UHF Adaptive Array were conducted using the laboratory test configuration for the case of a CW jammer and a CW desired signal.

The rate at which the array is able to reject jammers and direct attention to the desired signal is a function of a number of parameters, including the type of adaptive algorithm employed, the input jammer-to-signal ratio, angular separation between the jammer and the desired signal, and the interval between weight updates. The long interval between weight updates is the predominant factor limiting the response rate of the system under test. This interval, though variable depending on which algorithm is being employed, may be as long as 8 to 10 milliseconds, which is very long compared to the inverse of the 10-15 MHz adaptive array processing bandwidth and is approximately 40 times longer than the correlator integration interval. It should be emphasized that this long interval between updates is not related to the speed of circuits within the adaptive electronics, but is due to slow computation within the PDP-11 digital computer. For example, the adaptive array convergence rate could be increased by a factor of up to 40 without a significant change in steady-state performance (under most conditions) by implementing a faster digital processor.

The transient response result presented is intended to illustrate the machanism of adaptation. Improving the convergence rate via improved algorithms and faster digital control are subjects for further investigation.

The photographs in **Figure B, Views a) through h),** show the IF output as the adaptation progresses to the final (steady-state) condition. The initial weights were selected so that the desired signal was in a pattern null.

The adaptation process occurs in three stages to minimize output jammer power, adjust the output desired signal power, and minimize the output thermal noise power in that order. The jammer is essentially nulled after about 30 iterations. The increased pattern gain in the desired signal direction at this point is simply a result of the pattern alteration required to null the jammer and does not indicate that the array has actively responded to the desired signal. The output desired signal level is adjusted to obtain the programmed value of Q

after about 200 iterations, which represents array response time to the desired signal. Minimization of the output thermal noise power begins at about the 300th iteration and the steady-state solution is attained after approximately 500 iterations.

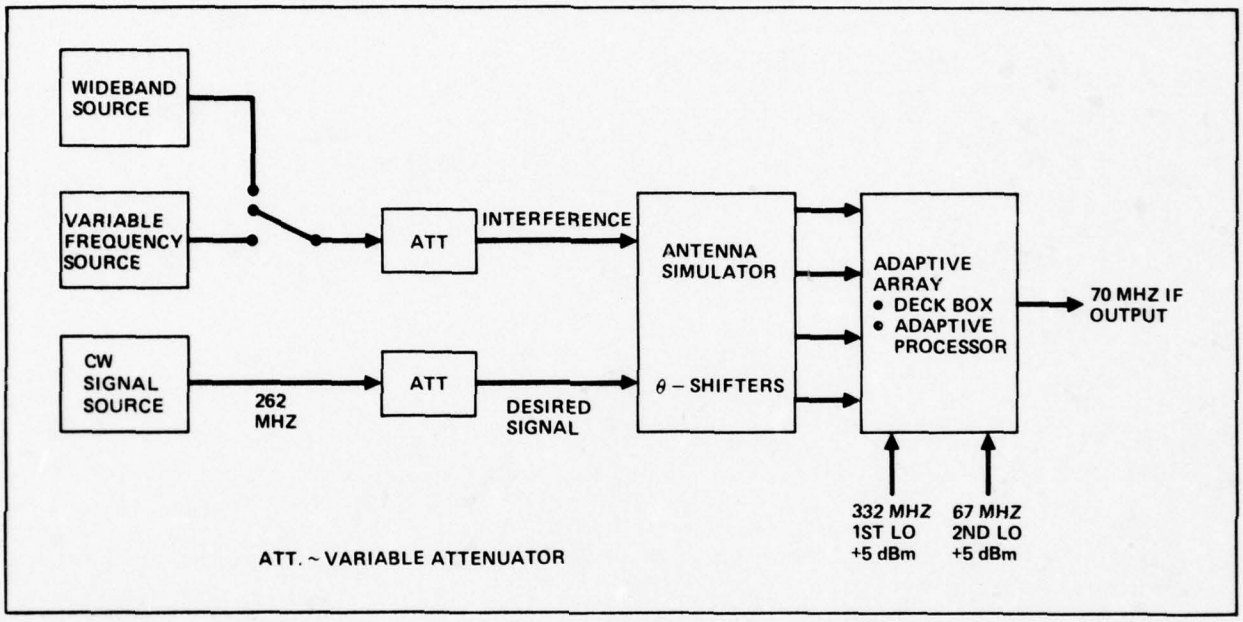

Figure A. Bench Test Configuration. Narrowband and wideband desired and jammer signal sources can be simulated in the laboratory. The relative phases of the signals applied to the four-channel adaptive processor can be varied by as much as 180 degrees to simulate different directions of signal arrival.

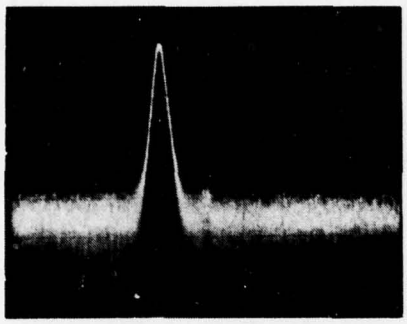

a. INITIAL

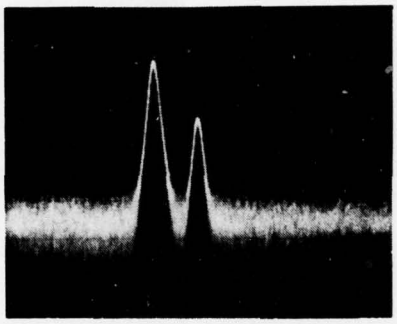

b. 10 ITERATIONS

c. 20 IT

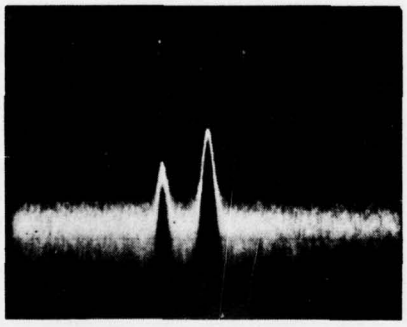

e. 60 ITERATIONS

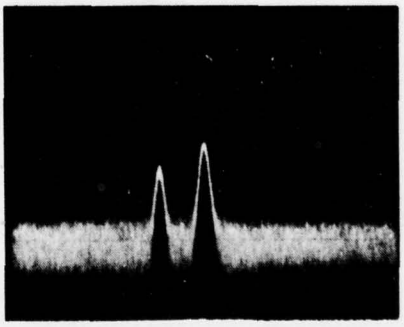

f. 200 ITERATIONS

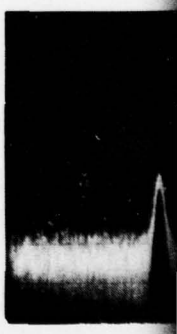

g. 300

Figure B. Adaptive
jammer signal is esse
ments in signal-to-no

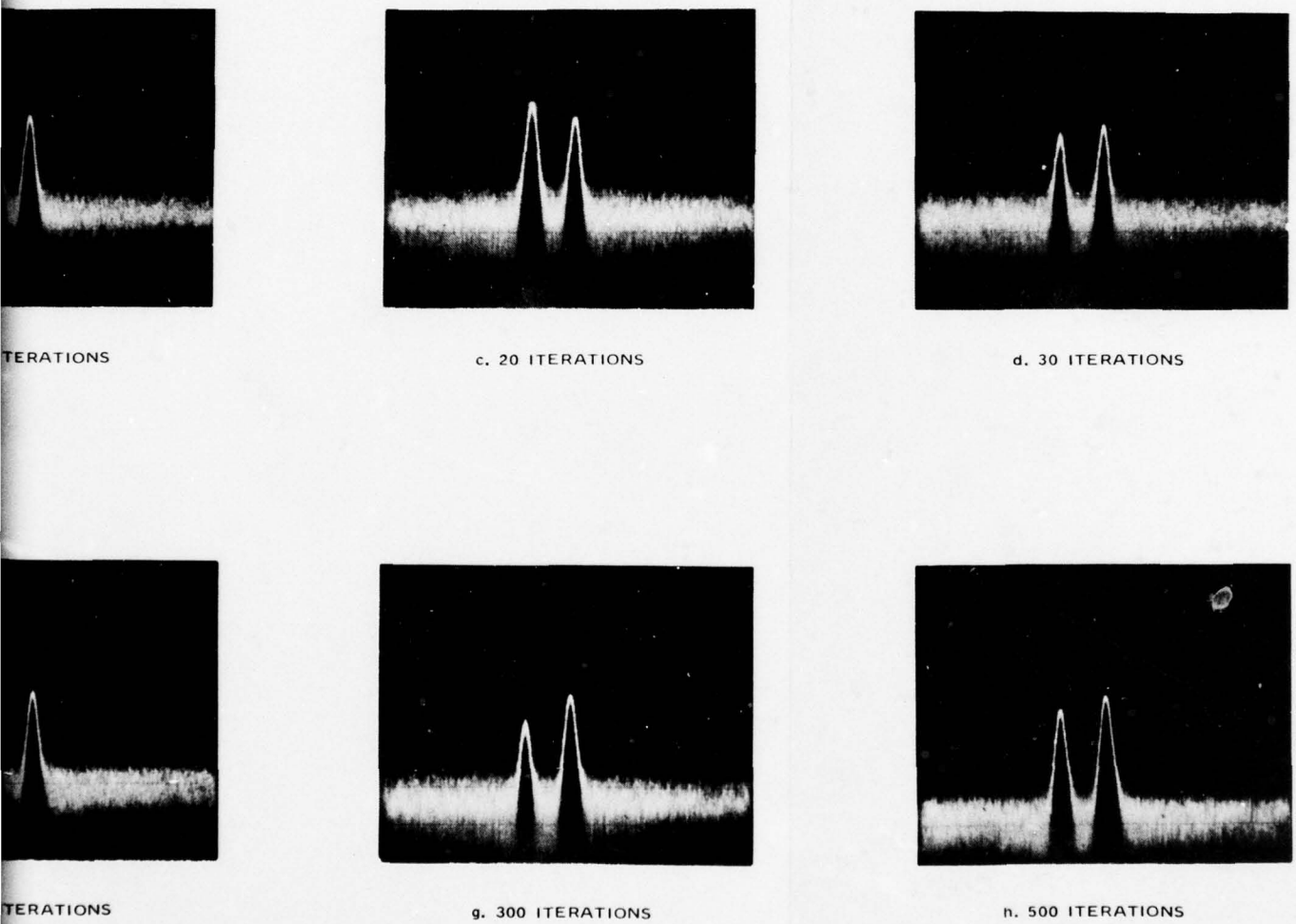

TERATIONS

c. 20 ITERATIONS

d. 30 ITERATIONS

TERATIONS

g. 300 ITERATIONS

h. 500 ITERATIONS

Figure B. Adaptive Array Output versus the Number of Weight Updates (Adaptive Iterations). The jammer signal is essentially nulled after approximately 30 iterations; however, to obtain further improvements in signal-to-noise ratio requires in excess of 300 iterations.

APPENDIX A
INFORMATION CONTAINED IN THE R AND Q VECTORS

AD-A055 942 HUGHES AIRCRAFT CO FULLERTON CALIF GROUND SYSTEMS GROUP F/G 17/4
UHF ADAPTIVE ARRAY DEVELOPMENT PROGRAM.(U)
JUL 77 D D EFFINGER, W R JONES, W R MASENTEN N00173-76-C-0353
UNCLASSIFIED FR77-14-763 NL

2 OF 2
ADA
065942

END
DATE
FILMED
8-78
DDC

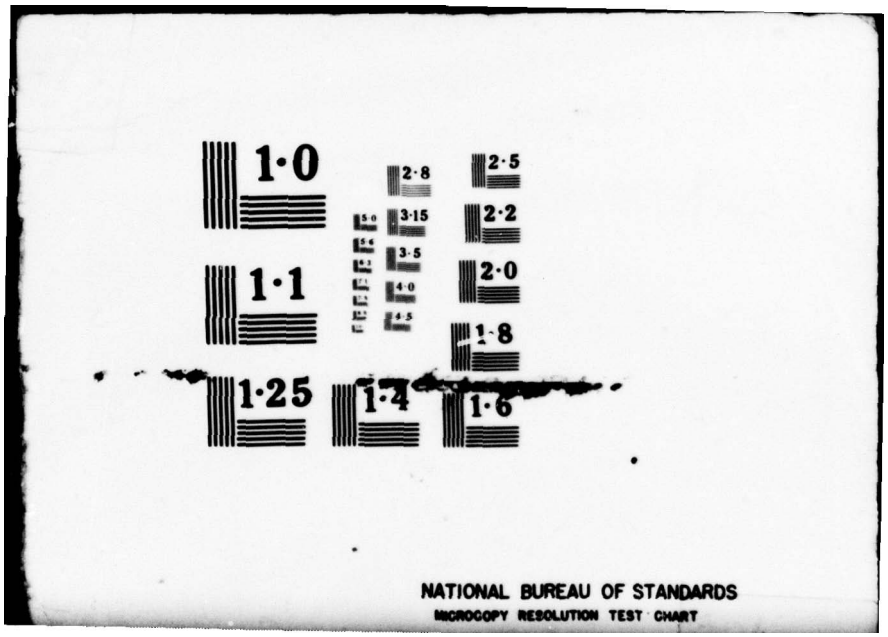
1·0
1·1
1·25
2·8
3·15
3·5
4·0
4·5
1·4
2·5
2·2
2·0
1·8
1·6
NATIONAL BUREAU OF STANDARDS
MICROCOPY RESOLUTION TEST CHART

Appendix A

INFORMATION CONTAINED IN THE R AND Q VECTORS

The vectors $\underline{R}$ and $\underline{Q}$ are known to provide sufficient information for iterative or recursive updating of the weighting coefficients to optimize the output signal-to-jammer-plus-noise ratio. Under full adaptation, $\underline{R}$ conveys null-steering information and $\underline{Q}$ conveys beam-pointing information.

At the $(k+1)^{th}$ sampling instant, the $\underline{R}$ and $\underline{Q}$ vectors are given by (see Figure A-1):

$$\underline{R} = \underline{R}(k) = \frac{1}{\Delta T}\int_{(k-1)\Delta T}^{k\Delta T} [\Lambda(\tau)\underline{\tilde{X}}(\tau)]\underline{\tilde{X}}^{\dagger}(\tau)\,\underline{W}(k)\,d\tau$$

$$\underline{Q} = \underline{Q}(k) = \frac{1}{\Delta T}\int_{(k-1)\Delta T}^{k\Delta T} [\Omega(\tau)\underline{\tilde{Z}}(\tau)]\underline{\tilde{Z}}^{\dagger}(\tau)\,\underline{W}(k)\,d\tau \qquad (1)$$

where

ΔT = interval of integration (an integer multiple of 204 μs)

$$\underline{\tilde{X}}(\tau) = \begin{bmatrix} \tilde{X}_1(\tau) \\ \tilde{X}_2(\tau) \\ \tilde{X}_3(\tau) \\ \tilde{X}_4(\tau) \end{bmatrix} = \text{complex envelope representation of the input signal vector at time } \tau.$$

$\underline{\tilde{Z}}(\tau)$ = complex envelope representation of the input signal vector bandlimited to 25 kHz.

† Denotes transpose

$$\underline{W}(k) = \begin{bmatrix} W_1(k) \\ W_2(k) \\ W_3(k) \\ W_4(k) \end{bmatrix} = \text{weight vector in the interval from } (k-1)\Delta T \text{ to } k\Delta T \text{ (assumed constant).}$$

$\Lambda(\tau)$ and $\Omega(\tau)$ represent 4x4 diagonal matrices which are introduced to account for the limiter (zero-crossing detectors) preceding the correlators. In complex envelope notation, a complex signal $\tilde{v}$ is modified by the limiter to $\tilde{v}/|\tilde{v}|$. The limiter outputs are therefore represented by the vectors:

$$\Lambda(\tau)\underline{\tilde{X}}(t) = \begin{bmatrix} \dfrac{\tilde{X}_1(\tau)}{|\tilde{X}_1(\tau)|} \\ \dfrac{\tilde{X}_2(\tau)}{|\tilde{X}_2(\tau)|} \\ \dfrac{\tilde{X}_3(\tau)}{|\tilde{X}_3(\tau)|} \\ \dfrac{\tilde{X}_4(\tau)}{|\tilde{X}_4(\tau)|} \end{bmatrix} \qquad \Omega(\tau)\underline{\tilde{Z}}(t) = \begin{bmatrix} \dfrac{\tilde{Z}_1(\tau)}{|\tilde{Z}_1(\tau)|} \\ \dfrac{\tilde{Z}_2(\tau)}{|\tilde{Z}_2(\tau)|} \\ \dfrac{\tilde{Z}_3(\tau)}{|\tilde{Z}_3(\tau)|} \\ \dfrac{\tilde{Z}_4(\tau)}{|\tilde{Z}_4(\tau)|} \end{bmatrix} \tag{2}$$

The i-th diagonal elements of $\Lambda(\tau)$ and $\Omega(\tau)$ are therefore $|\tilde{X}_i(\tau)|^{-1}$ and $|\tilde{Z}_i(\tau)|^{-1}$, respectively. Since $\Lambda(\tau)$ and $\Omega(\tau)$ are functions of $\underline{\tilde{X}}(\tau)$ and $\underline{\tilde{Z}}(\tau)$, the diagonal elements are random variables at a given instant of time τ.

The above relationships and definitions serve as a basis for determining the information contained in the $\underline{R}$ and $\underline{Q}$ vectors. For a fixed weight vector $\underline{W}$ and a stationary signal environment, the ensemble averages of $\underline{R}$ and $\underline{Q}$ are given by

$$E(\underline{R}) = E\{\Lambda(\tau)\,\underline{\tilde{X}}(\tau)\underline{\tilde{X}}^{\dagger}(\tau)\,\underline{W}(k)\} = A\,\underline{W}(k)$$

and

$$E(\underline{Q}) = E\{\Omega(\tau)\,\underline{\tilde{Z}}(\tau)\underline{\tilde{Z}}^{\dagger}(\tau)\,\underline{W}(k)\} = B\,\underline{W}(k)$$

where A and B are 4x4 matrices. The matrices A and B have been evaluated assuming each component of $\underline{\tilde{X}}(t)$ and $\underline{\tilde{Z}}(t)$ are zero-mean Gaussian random variables (Brennan [1971]); these matrices are given by

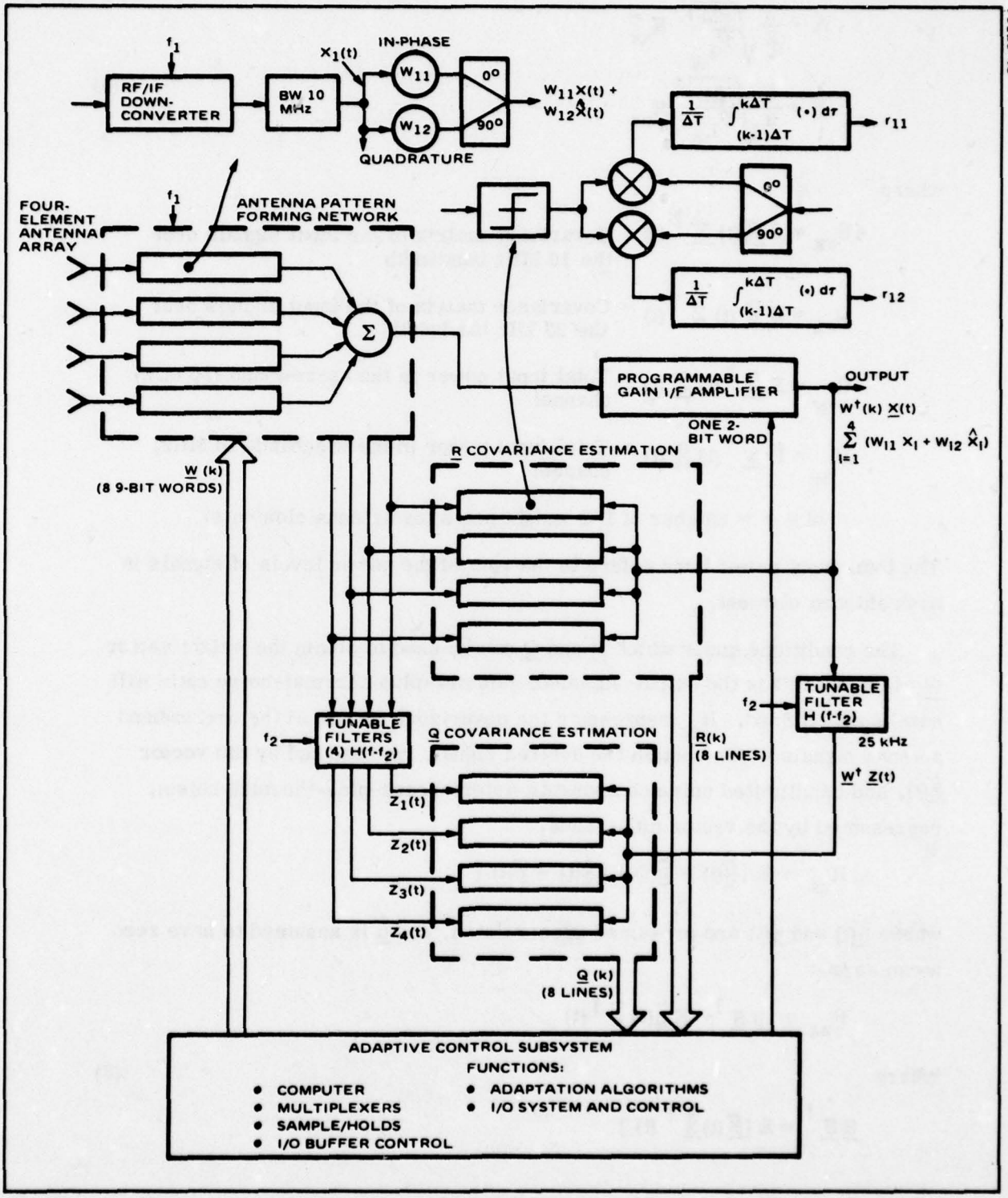

Figure A-1. Functional Implementation of UHF Adaptive Antenna Array. The versatility of the algorithms in the controller (computer), operating on the covariance estimates for vectors $\underline{R}(k)$ and $\underline{Q}(k)$, enable the antenna pattern forming network to simultaneously maximize the S/N and the S/I.

$$A = \frac{1}{2}\sqrt{\frac{\pi M}{P_{I_W}}}\ R_{xx}$$

$$B = \frac{1}{2}\sqrt{\frac{\pi M}{P_{I_N}}}\ R_{zz} \qquad (4)$$

where

$R_{xx} = E\,\underline{\tilde{X}}(t)\,\underline{\tilde{X}}^{\dagger}(t)$ = Covariance matrix of the input signals over the 10 MHz bandwidth

$R_{zz} = E\,\underline{\tilde{Z}}(t)\,\underline{\tilde{Z}}^{\dagger}(t)$ = Covariance matrix of the input signals over the 25 kHz bandwidth

$R_{I_N} = E\,\underline{\tilde{Z}}^{\dagger}(t)\,\underline{\tilde{Z}}(t)$ = Total input power in the narrowband (25 kHz) channel

$P_{I_W} = E\,\underline{X}^{\dagger}(t)\,\underline{\tilde{X}}(t)$ = Total input power in the wideband (10 MHz) channel

$M = 4$ = number of I/Q weight pairs (or antenna elements)

The total input power here refers to the sum of the power levels of signals in each antenna element.

The conditions under which $\underline{R}$ and $\underline{Q}$ can be used to obtain the weight vector $\underline{W}$ which optimizes the output-signal-to-jammer-plus-thermal-noise ratio will now be determined. R_{zz} represents the covariance matrix of the narrowband antenna signals which contain the desired signal, represented by the vector $\underline{\tilde{S}}(t)$, and bandlimited noise components (interference-plus-thermal-noise), represented by the vector $\underline{\tilde{n}}(t)$. Thus,

$$R_{zz} = E\,[\underline{\tilde{S}}(t) + \underline{\tilde{n}}(t)]\,[\underline{\tilde{S}}(t) + \underline{\tilde{n}}(t)]^{\dagger}$$

where $\underline{\tilde{S}}(t)$ and $\underline{\tilde{n}}(t)$ are presumed uncorrelated, and $\underline{\tilde{n}}$ is assumed to have zero mean so that

$$R_{zz} = \underline{S}\,\underline{S}^{\dagger} + E\,\underline{\tilde{n}}(t)\,\underline{\tilde{n}}^{\dagger}(t) \qquad (5)$$

where

$$\underline{S}\,\underline{S}^{\dagger} = E\,[\underline{\tilde{S}}(t)\,\underline{\tilde{S}}^{\dagger}(t)]$$

The product of R_{zz} and $\underline{W}$ during the interval $(k-1)\Delta T$ to $k\Delta T$ thus becomes

$$\begin{aligned} R_{zz}\underline{W}(k) &= [\underline{S}^{\dagger}\underline{W}(k)]\,\underline{S} + E\;\tilde{\underline{n}}(t)\,[\tilde{\underline{n}}^{\dagger}(t)\,\underline{W}(k)] \\ &= \beta\,\underline{S} + E\;\tilde{\underline{n}}(t)\,[\tilde{\underline{n}}^{\dagger}(t)\,\underline{W}(k)] \end{aligned} \tag{6}$$

where β is a complex-type scalar constant. To obtain a solution for $\underline{W}(k)$, impose the condition that $E(\underline{R})$ equals $E(\underline{Q})$. By (3) and (4), the solution for $\underline{W}(k)$ becomes

$$\begin{aligned} \underline{W}(k) &= \beta\sqrt{\frac{P_{I_W}}{P_{I_N}}}\;R_{xx}^{-1}\;[\underline{S} + \frac{1}{\beta}\,E\{\tilde{\underline{n}}(t)\,\tilde{\underline{n}}^{\dagger}(t)\,\underline{W}(k)\}] \\ &= \beta'\,[R_{xx}^{-1}\,\underline{S} + \frac{1}{\beta}\,R_{xx}^{-1}\,E\{\tilde{\underline{n}}(t)\,\tilde{\underline{n}}^{\dagger}(t)\,\underline{W}(k)\}] \\ &= \beta'\,[\underline{W}_{opt} + \text{noise term}] \end{aligned} \tag{7}$$

where $\underline{W}_{opt}$ is the weight vector which optimizes the output signal to jammer plus thermal noise ratio. By the above result, a necessary condition for optimizing the output-signal-to-jammer-plus-thermal-noise ratio (i.e. $\underline{W}(k) \to \beta'\underline{W}_{opt}$) is that the noise term becomes vanishingly small. It has been shown that this condition is satisfied if the 25 kHz filter reduces the output jammer power by at least 6 dB to 10 dB. This requirement is examined quantitatively in Appendix B.

In summary, the $\underline{R}$ and $\underline{Q}$ vectors can be used to maximize the output-signal-to-jammer-plus-thermal-noise ratio by determining the value of $\underline{W}$ such that

$$E\,\underline{R} = E\,\underline{Q} \tag{8}$$

A necessary condition that the resulting weight vector $\underline{W}$ gives S/N maximization is that the processing gain of the 25 kHz filter exceeds 6 to 10 dB.

The above procedure for maximizing S/N was based on the average values of $\underline{R}$ and $\underline{Q}$. The condition that $\underline{R}$ and $\underline{Q}$ closely approximate their ensemble averages $E(\underline{R})$ and $E(\underline{Q})$ is thus implicit to the derivation. However, since $\underline{R}$ and $\underline{Q}$ are time averages obtained over a finite interval ΔT, these measurements are noisy and deviate from their ensemble averages. This noise degrades the output-signal-to-noise ratio by introducing errors in the calculation of $\underline{W}$. The degree of degradation is a function of the signal environment and, in particular, the relationship between the averaging time (ΔT) and the bandwidth of the desired signal and interfering sources. An approximation for the degree of (S/N) degradation due to noise in $\underline{R}$ and $\underline{Q}$ is determined in Appendix C.

APPENDIX B
ALGORITHM CONVERGENCE USING AN ESTIMATE OF THE DESIRED SIGNAL

Appendix B

ALGORITHM CONVERGENCE USING AN ESTIMATE OF THE DESIRED SIGNAL

The beam-pointing vector $\underline{Q}$ is obtained by narrowband filtering the array output signal and obtaining its cross-covariance with the input signals band limited to the same bandwidth. The conditions under which signal-to-jammer-plus-noise maximization will occur are examined in this Appendix for the case where the jammer spectrum overlaps the desired signal spectrum.

The covariance matrices of signals in the narrowband and wideband processing bandwidths are given by

$$R_{zz} = E\underline{\tilde{Z}}\underline{\tilde{Z}}^{\dagger} = R'_{nn} + \underline{S}\underline{S}^{\dagger} \tag{1}$$

$$R_{xx} = E\underline{\tilde{X}}\underline{\tilde{X}}^{\dagger} = R'_{nn} + \underline{S}\underline{S}^{\dagger} \tag{2}$$

In other words, R_{zz} and R_{xx} differ by the difference between the noise covariance matrices R'_{nn} and R_{nn}. Using an approximation to account for the effects of the limiters, we have

$$R_{zz} = E\{\Lambda Z Z^{\dagger}\} = \frac{1}{2}\frac{\pi m}{P_{I_N}} R_{zz} = \frac{1}{2}\sqrt{\frac{\pi m}{P_{I_N}}}\,(R'_{nn} + \underline{S}\underline{S}^{\dagger}) \tag{3}$$

$$R_{xx} = E\{\Omega \underline{X}\underline{X}^{\dagger}\} = \frac{1}{2}\sqrt{\frac{\pi m}{P_{I_W}}} R_{xx} = \frac{1}{2}\sqrt{\frac{\pi m}{P_{I_W}}}\,(R_{nn} + \underline{S}\underline{S}^{\dagger}) \tag{4}$$

Now consider a signal environment composed of wideband jammers and a narrowband (30 kHz) desired signal. Assume further that the jammer spectra are rectangular with bandwidth B_J ($B_J > 30$ kHz) and centered on the desired spectrum. In this case,

$$R_{nn} = \frac{B_J}{30\ \text{kHz}} R'_{nn} + \sigma^2 \left(1 - \frac{B_J}{10\ \text{MHz}}\right) I = G_p R'_{nn} + \sigma'^2 I \tag{5}$$

where G_p represents the processing gain to jammers afforded by the 30 kHz filters and σ^2 represents the thermal noise power in each channel. Using the above relation, the average value of Equation (1) in Section 4.C.2, "Description of the Fully Adaptive Algorithm" becomes

$$\underline{W}(K+1) = \left(\gamma_1 - \frac{\gamma_2 q' \sqrt{\pi m}\,\sigma'^2}{2G_p\sqrt{P_{I_N}}}\right)\underline{W}(k) + \tag{6}$$

$$\frac{\gamma_2\sqrt{\pi m}}{2}\left\{\frac{q'}{\sqrt{P_{I_N}}}\,\frac{(G_p-1)}{G_p}\,\underline{S}\underline{S}^{\dagger}\,W(k) - \left[\frac{1}{\sqrt{P_{I_W}}} - \frac{q'}{G_p\sqrt{P_{I_N}}}\right]R_{xx}\underline{W}(k)\right\}$$

It is helpful to compare this result with the weight equation obtained when R_{zz} is assumed* equal to $\underline{s}\,\underline{s}^{\dagger}$. This "ideal reference"* equation is given by

$$\underline{W}(k+1) = \gamma_1\underline{W}(k) + \frac{\gamma_2\sqrt{\pi m}}{2}\left\{\frac{q}{\sqrt{P_{I_N}}}\,\underline{S}\underline{S}^{\dagger}\,W(k) - \frac{1}{\sqrt{P_{I_W}}}\,R_{xx}\underline{W}(k)\right\} \tag{7}$$

In order to obtain acceptable steady-state performance using an estimate of the desired signal, the coefficient of the $\underline{Q}$ vector (q) in equation (1) in Topic 4.C.2 must satisfy certain conditions. These conditions follow from the weight equation** (equation (6)) and apply for $\gamma_1 = 1$ and when the weights are near steady-state. In order to prevent the array from forming a beam in the direction of a jammer source (instead of toward the desired signal), q must not exceed the following bound:

$$q < G_p\sqrt{\frac{P_{I_N}}{P_{I_W}}} \tag{7}$$

In order to insure that the output-signal-to-jammer-plus-thermal-noise ratio is within $10\log_{10}(A+1)$ dB of the optimum value for an arbitrary signal environment q should not exceed the following bound:

$$q < \frac{A}{1 + A - 1 \times 10^{-3}G_p}\,G_p\sqrt{\frac{P_{I_N}}{P_{I_W}}} \quad (1 < G_p < 333) \tag{8}$$

Finally, in order to obtain a non-zero steady-state solution to equation (6), q must exceed the bound

---

* This was the assumption which led to the steady-state solution Equation (1) in Appendix A.

** Note that equation (1) in Topic 4.C.2 only applies when the variances of $\underline{R}$ and $\underline{Q}$ are negligibly small (large ΔT). See the section on the fully adaptive algorithm.

$$q > \sqrt{\frac{P_{I_N}}{P_{I_W}}} \tag{9}$$

An expression for q' and W is difficult to derive because of their dependence on the specific signal situation. The above bounds permit several observations to be made, however, since the bounds in equations (8) and (9) cannot both be satisfied for any value of q' unless

$$G_p > \frac{A+1}{A} \tag{10}$$

Therefore, the jammer bandwidth is required to be at least twice the 30 kHz desired signal bandwidth ($G_p > 2$) to obtain a signal-to-jammer-plus-thermal-noise ratio that is within 3 dB of optimum ($A = 1$), i.e., the 30 kHz narrowband correlator filters must provide at least 3 dB of processing gain.

The processing gain G_p is generally unknown because the bandwidth of individual jammers is unknown. Further, estimates of P_{I_N} and P_{I_W} are not available in the current UHF adaptive array implementation. In this case, q can be set equal to one so that it is greater than its lower bound under all conditions. The upper bound is then satisfied if

$$G_p > \frac{A+1}{A}\sqrt{\frac{P_{I_W}}{P_{I_N}}} \tag{11}$$

For the special case in which the signal environment contains a single interfering signal that is high level relative to the desired signal and thermal noise levels, or when all high-level interfering signals have equal bandwidths, G_p is approximated by

$$G_p \cong \frac{P_{I_W}}{P_{I_N}} \tag{12}$$

From (11) and (12), the condition on G_p which must be satisfied is given by

$$G_p \gtrsim \left(\frac{A+1}{A}\right)^2 \tag{13}$$

Therefore, when q is fixed at a value of one and when the signal environment contains a single high-level jammer or multiple high-level interferers of equal bandwidth, the interfering signal bandwidth B_j must exceed the desired signal bandwidth by a factor of at least $[(A+1)/A]^2$. For example, B_j must be greater than 120 kHz ($G_p = 4$ kHz with 30 kHz bandwidth filters) in order to obtain a steady-state output-signal-to-jammer-plus-thermal-noise ratio that is within 3 dB of the

optimum, i.e., the processing gain afforded by the narrowband (30 kHz) filters must exceed 6 dB.

In the UHF adaptive array processor, q is programmed in software as follows:

$$q = \gamma_3 \left(\| \frac{1}{\underline{Q}} \| - \gamma_4 \right) \tag{14}$$

and thus its value depends on the final value of $\| \underline{Q} \|$. When the signal-to-jammer-plus-noise ratio within the 30 kHz processing filter bandwidth is very large, then (follows from equation (1) in Appendix A)

$$q = \frac{1 + S_0}{S_0} \sqrt{\frac{P_{I_N}}{P_{I_W}}} > \sqrt{\frac{P_{I_N}}{P_{I_W}}} \tag{15}$$

where S_0 is the optimum output-signal-to-jammer-plus-noise ratio. Thus, the lower bound is always obtained when the output-signal-to-jammer-plus-noise ratio is large. In this case, the lower bound on G_p is given by

$$G_p \gtrsim \frac{1 + A}{A} \quad \frac{1 + S_0}{S_0} \tag{16}$$

A comparison of the above with equation (13) shows that q given by equation (16) results in an improved ability to process narrower-band jammers when $S_0 > A$. When $S_0 < A$, however, the reverse is true; better performance is obtained under wideband jammer conditions by setting q = 1 in this case.

APPENDIX C
SENSITIVITY OF STEADY-STATE PERFORMANCE TO NOISE IN THE R AND Q MEASUREMENTS

Appendix C

SENSITIVITY OF STEADY-STATE PERFORMANCE TO NOISE IN THE R AND Q MEASUREMENTS

The integration interval required to estimate the cross-correlation vectors $\underline{Q}$ and $\underline{R}$ is examined in this appendix. An approximation for ΔT is obtained based on certain simplifying assumptions required in order to apply previously derived analytical results.

Performance versus ΔT will be in the form of an approximation of the average output signal to noise ratio, first when the $\underline{Q}$ estimate is in error and then when the $\underline{R}$ estimate is en error. Additional averaging of data by the adaptive algorithm is not included; thus, the results to be presented reflect theoretical performance based on a single measurement of $\underline{Q}$ and $\underline{R}$ and will not depend on the particular algorithm used to perform full adaptation. $\underline{Q}$ and $\underline{R}$ are defined in Section 1. Two series of theoretical results will be presented: these results will then be related to the specifics of the UHF adaptive array.

The output signal-to-interference-plus-thermal-noise ratio (S_o) which can be achieved using $\underline{Q}$ as the beam-steering vector is first examined. In a previous analysis [Miller, 1976], the statistical properties of S_o normalized to the optimum output-signal-to-interference-plus-thermal-noise ratio ($S_{o\ opt}$) were determined under the following assumptions:

- The array output signal, bandlimited to the 25 kHz desired signal band, gives a good approximation to the desired signal except for a constant phase and amplitude error
- The envelope of the desired signal has a constant amplitude (e.g., biphase modulation, FM).
- The jammers approximate zero mean Gaussian processes
- $S_{o\ opt} \lesssim 0$ dB
- The signal environment is stationary

The statistics of $S_o/S_{o\ opt}$ were determined for the situation where the average signal (cross-covariance) vector $\underline{S}$ is replaced by its estimate or determined from ℓ independent samples of the cross-covariance as follows:

$$\underline{\hat{S}} = \beta \sum_{i=1}^{\ell} \underline{X}(i\Delta\tau)\,\tilde{S}^*(i\Delta\tau) \tag{1}$$

where $\Delta\tau$ is the interval between independent samples of the product $\underline{\tilde{X}}(t)\,\tilde{S}^*(t)$, $\tilde{S}(t)$ represents the desired signal (or a good approximation to the desired signal), $\underline{\tilde{X}}(t)$ represents the array input vector, and β is an arbitrary constant. It is important to note that $\underline{\tilde{X}}(t)$ represents the signal and jammers in the full bandwidth of the processor (10 MHz in the UHF adaptive array). The weight vector $\underline{W}$ which caused the relation

$$\lim_{T_1 \to \infty} \frac{1}{T_1} \int^{T_1} \underline{\tilde{X}}(t)\,\underline{\tilde{X}}^{\dagger}(t)\,\underline{W}\,dt = \underline{\hat{S}} \tag{2}$$

to be satisfied was then determined. This criterion leads to optimization of the output-signal-to-interference-plus-noise ratio when $\ell \to \infty$ ($\underline{\hat{S}} \to \underline{S}$).

The actual value of S_o is less than $S_{o\ opt}$ due to the difference between the estimate and the average value of $\underline{\hat{S}}$. This is illustrated by the graph in Figure A. Here, the average value of the output-signal-to-interference-plus-noise ratio is plotted as a function of the number of independent samples (k) used to estimate $\underline{S}$. The vertical scale is normalized to $S_{o\ opt}$, while the horizontal scale is normalized to $1/S_{o\ opt}$. The parameter m represents the number of weight controls (antenna elements) in the adaptive antenna array (m = 4 in the UHF adaptive array). Briefly, the results indicate that approximately $m \cdot S_{o\ opt}$ independent samples must be averaged to obtain an output signal-to-interference-plus-thermal-noise ratio that is within 3 dB of the optimum value.

The relationship between $\underline{R}$ vector averaging and steady-state performance may also be evaluated using the results of a previous analysis [Miller, 1976]. Results from this analysis were obtained under the assumptions that the jammers and the thermal noise approximated stationary, zero-mean, Gaussian processes. Similar to the procedure for evaluating the estimate $\underline{\hat{S}}$, the statistics of $S_o/S_{o\ opt}$ were determined when the average value of $\underline{R}$ is replaced by its estimate $\underline{\hat{R}}$ as follows:

$$\underline{\hat{R}} = \frac{1}{\ell\,\Delta T} \sum_{i=1}^{\ell} \underline{\tilde{X}}(i\Delta\tau)\,\underline{\tilde{X}}^{\dagger}(i\Delta\tau)\,\underline{W} \tag{3}$$

Here, $\Delta\tau$ represents the interval between independent samples of the intput signals $\underline{\tilde{X}}(t)$. The weight vector $\underline{W}$ which caused the relation

$$\underline{\hat{R}} = \frac{1}{\ell\,\Delta T} \sum_{i=1}^{\ell} \underline{\tilde{X}}(i\Delta t)\,\underline{\tilde{X}}^{\dagger}(i\Delta t)\,\underline{W} = \underline{S} \tag{4}$$

to be satisfied was then determined. This criterion leads to optimization of the output signal-to-interference-plus-thermal-noise-ratio when $\ell \to \infty (R \to R)$. The number of samples which need to be averaged to achieve a given level of performance is illustrated in Figure B. These results apply to a four-element adaptive array (m = 4) and show that the required number of independent samples increases as the optimum output signal-to-interference-plus-noise ratio increases.

In order to relate the results shown in Figures A and B to the integration time T_1 required for the $\underline{Q}$ and $\underline{R}$ vector measurements, an equivalent interval between independent samples must be determined so that the discrete sums in (1) and (3) can be related to the integrals in $\underline{Q}$ and $\underline{R}$. To do this, it is assumed that the jammers and thermal noise approximate white noise processes band-limited to 10 MHz. By the Nyquist theorem, the smallest interval between independent samples is 1/B, where B = 10 MHz. Neglecting the effects of the limiters, $\underline{Q}$ and $\underline{R}$ can then be approximated by

$$\underline{Q} = \frac{1}{T_1}\int_0^{T} \underline{y}(t)\,\underline{y}^t(t)\,\underline{W}\,dt \doteq \frac{1}{\ell_1 \Delta_1 \tau} \sum_{i=1}^{\ell_1 \Delta \tau_1} \underline{\tilde{X}}(i\Delta\tau_1)\,\tilde{S}^*(i\Delta\tau_1)$$

$$\underline{R} = \frac{1}{T_2}\int_0^{T_2} \underline{\tilde{X}}(t)\,\underline{\tilde{X}}^t(t)\,\underline{W}\,dt \doteq \frac{1}{\ell_2 \Delta\tau_2} \sum_{i=1}^{\ell_2 \Delta 2\tau} \underline{\tilde{X}}(i\Delta\tau_2)\,\underline{\tilde{X}}^t(i\Delta\tau_2)\,\underline{W}$$

where

$$\Delta\tau_1 = \Delta\tau_2 = 1/B = 100 \text{ ns.}$$

Consider, for example, a situation in which $S_{o\ opt}$ = 4 dB; i.e., consider a set of conditions on the desired signal and jammer locations and power levels and on the antenna array such that the maximum achievable output-signal-to-interference-plus-jammer ratio is 4 dB (an example of such a situation is given in the test results). Then, in order to obtain and output signal-to-interference-plus-noise ratio that is within 1 dB of optimum, T_1 must be greater than approximately 1 μs and T_2 must be greater than approximately 8 μs. These are very short intervals of time in relation to the minimum 200 μs integration interval available in the UHF adaptive array processor. However, several important factors have not been accounted for in the above derivation. First, the jammers need not be wideband. For example, the presence of narrowband jammers and the use of narrowband filters prior to the antenna input leg of the $\underline{Q}$ correlators can increase the required measurement time for $\underline{Q}$ by as much as a factor of 400 (10 MHz/25 kHz, where the desired signal bandwidth is 25 kHz). A similar scaling may also be required in the case of estimating $\underline{R}$. The 200 μs integration intervals are thus more in line with the requirements for nulling narrowband jammers. This required integration time for narrowband jammers is an area for future study.

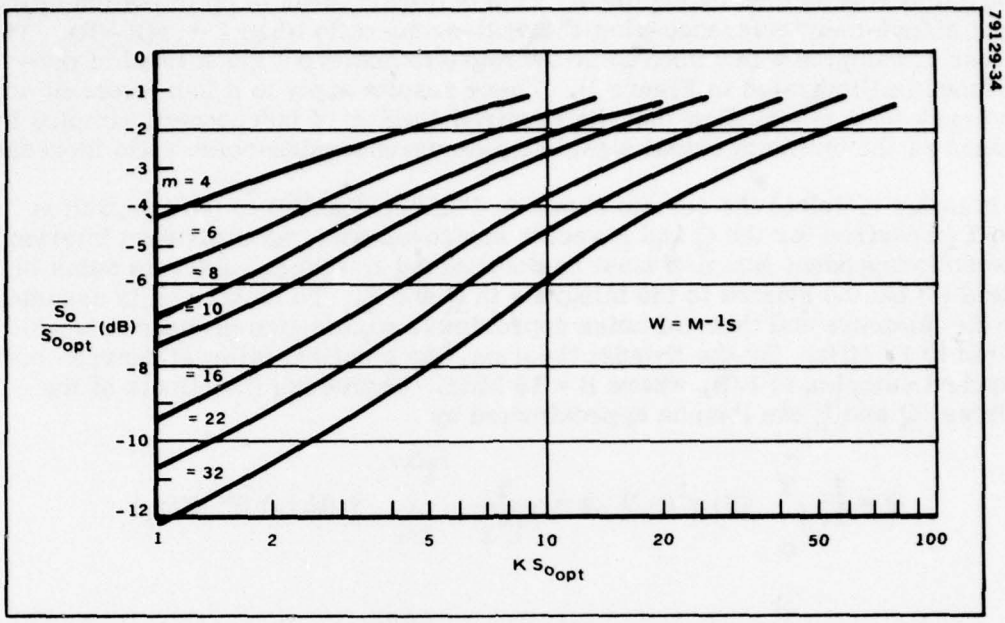

Figure A. Adaptive Array Performance for K Independent Measurements. Shown is the average normalized output signal-to-noise ratio versus K $S_{o\ opt}$ when the desired signal cross-covariance vector (corresponding to Q) is estimated. For the UHF adaptive array, m = 4.

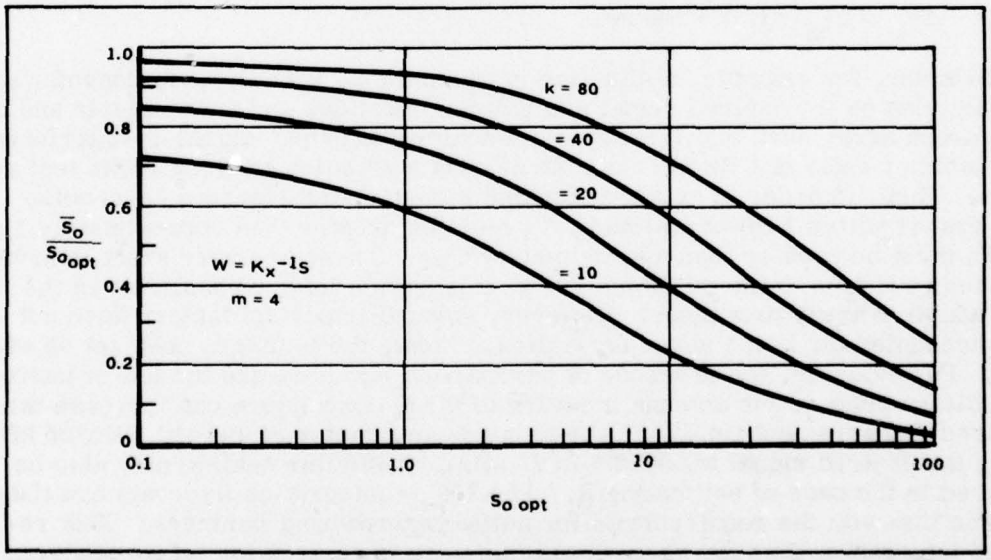

Figure B. Adaptive Array Performance for K Independent Measurements. Shown is the average normalized output signal-to-noise ratio versus the optimum output signal-to-noise ratio for several different sample sizes (K).

APPENDIX D
OPERATING MANUAL

OPERATING PROCEDURES FOR COMPUTER PROGRAM CONTROL

A. Start Up Procedure

1. Turn on Adaptive Processor
2. Turn on Computer
3. Turn on Teletype (to LINE)-

B. Starting the Computer Program (Also use to restart the program at any time).

1. Set the ENABLE/HALT switch to HALT.
2. Set the switch register (SR) to the starting address of the program to be run. The starting address (SA) is given on the paper tape used to load the program.
3. Press LOAD ADDR.
4. Set ENABLE/HALT to ENABLE
5. Press START.
6. The teletype should be printing out. If not, then see "Loading a New Control Program".

C. Running the Computer Program

1. After printing an initial statement, the teletype will print "K=". To this, respond with the number "1" and press the carriage return key (CR).
2. The teletype next prints out "W_{11}=". To this respond with three digits XYZ, where X = 1 to 3, Y = 1 to 7, and Z = 1 to 7. The value entered here determines the initial amount of attenuation to be placed in the in-phase attenuator of weight #1.

   The number XYZ is to be interpreted as an octal representation of the binary state of the 8 bit weight attenuator as follows:

   Convention: Binary "1" => No attenuation
   Binary "0" => attenuation

   Bit Position and Attenuator Value:

9	8	7	6	5	4	3	2	1	0	
--	sign	32	16	8	4	2	1	.5	.25	dB

Examples:

Desired Sign	Desired Attenuation	Binary Representation	Teletype Entry (XYZ)
+	0 dB	1 1 1 1 1 1 1 1 1	377
-	0 dB	0 1 1 1 1 1 1 1 1	-377
+	0.25 dB	1 1 1 1 1 1 1 1 0	376
-	0.5 dB	0 1 1 1 1 1 1 0 1	-375
+	3 dB	1 1 1 1 1 0 0 1 1	363
+	Maximum Att.	1 0 0 0 0 0 0 0 0	000 or (CR)

3. After entering the desired value for XYZ, press carriage return (CR). The teletype will then print "W_{12}=". W_{12} is the quadrature attenuator associated with Channel 1. The value for this attenuator is entered as in Step 2.

4. The next weight corresponds to the in-phase attenuator associated with Channel #2 and typed as "W_{21}= ". Again, its value is entered as in Step 2.

5. This process continues until a value has been entered for each of the eight weight attenuators W_{11} to W_{42}.

6. The teletype next prints "AGC =". To this, respond with a single digit number from 0 to 7 and hit (CF). The value entered determines the amount of attenuation placed in the gain control.

Number Entered		Relative RF to IF Gain *
AGC =	0	56 dB
	1	48 dB
	2	40 dB
	3	32 dB
	4	24 dB
	5	16 dB
	6	8 dB
	7	0 dB

(*) The absolute RF to IF gain is about 40 dB when AGC = 7

7. The teletype next prints "MODE =". The value entered here selects the desired adaptive algorithm as follows:

Value Entered		Algorithm
Mode =	02	Open loop beamforming
	03	Full adaptation
	13	Null - Steering

The adaptation algorithm for nulling only (Mode = 01) is called by the null-steering algorithm (Mode = 13) and should not be called via the teletype.

8. After entering the mode and pressing (CR), the teletype prints "M(K)=". This parameter is for future use and should be ignored. Simply press (CR).

9. The teletype next prints "J =". Unless MODE = 13, ignore this by pressing (CR). If MODE = 13, use this parameter to select the weight element to be held fixed during the nulling algorithm. The value entered for J thus ranges from 1 to 4.

10. The teletype next prints "IFLG =". This also is a parameter to be used in future algorithm modifications. Ignore it by pressing (CR).

11. The teletype next prints "AFLG =". As presently implemented, this parameter can be ignored by pressing (CR) unless it is desired to have an automatically adjusted loop gain when operating with full adaptation (MODE = 3). If this latter option is desired enter "1" then (CR).

12. The teletype next prints "NO. OF FREE ELEMENTS = ". Ignore this parameter unless the null-steering algorithm (MODE =13) is used. Enter 0, 1, 2, or 3, depending on how many elements are to be used to null signals received by the $J^{\underline{th}}$ element (see Step 9).

13. As soon as (CR) is pressed in Step 12, the computer executes the adaptation routine selected in Step 7 subject to the control parameters entered in Steps 8 to 12. Unless the open-loop beamforming routine was selected, go to Step 15.

14. If the open-loop beamforming routine is being used (MODE = 02), the teletype will print "THETA =". After entering the value of "THETA" and then (CR), the teletype prints "PHI =". THETA and PHI are the beam-pointing parameters Θ and Ø which are entered in degrees using octal notation. The angles are represented by three numbers XYZ. For example;

Θ (Degrees)	Ø (Degrees)	THETA (XYZ)	PHI (XYZ)
0	- 5	000	-005
-30	10	-036	012
30	60	036	074
30	90	036	132
120	-20	264	-024

Convention:

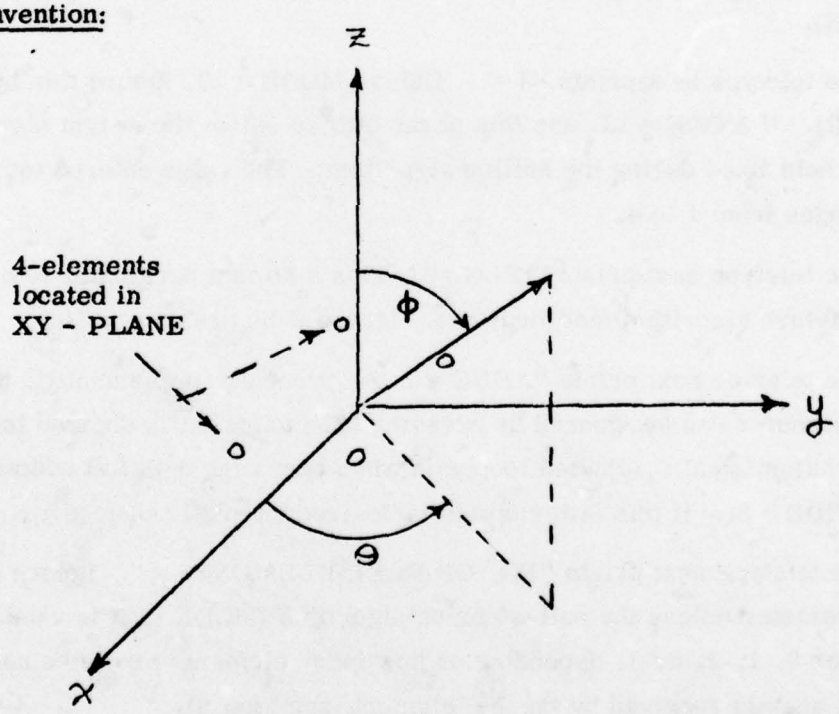

NOTE: The relative position of the four elements must be entered into the computer via the switch register for proper operation of the beamforming routine. See the section on open-loop beamforming.

15. The controller begins to perform the adaptation routines after pressing carriage return in the previous step, (#13 or #14). Adaptation continues until a predetermined point in the routine is reached. At this point, the teletype prints out the current values of the W, R, and Q vectors. When the printout occurs depends on which adaptation algorithm is being used.

In the open-loop beamforming routine, the weight values which properly point the beam are sent to the array processor. The resulting values for W, R, and Q are then printed out, and the computer halts. The weight values remain fixed until the program is restarted or until the CONT switch (be sure ENABLE/HALT switch is in ENABLE position) is pressed. When CONT is pressed, the teletype responds with "THETA =" so that new values of Θ and $\emptyset$ can be entered.

In the full adaptation and null-steering (MODE = 03 and MODE = 13, respectively) routines, the values of W, R, and Q are printed out periodically so that the state of the machine can be determined as adaptation progresses. Note that this periodic printout is for the purpose of testing and is not intended for use during standard operation. The period between printouts can be varied or the printouts can be eliminated entirely by following a procedure outlined in the main body of the Final Report.

An example teletype input/output is shown on the next page. User inputs are underlined, while teletype output is not (carriage returns are not shown). In the particular example shown, the in-phase weight attenuator of Channel #1 is set to zero attenuation and all other weight attenuators are set to full attenuation (63.75 dB). Zero attenuation is also set into the gain control attenuators. The full adaptation algorithm (MODE = 03) was selected. The printout following "NO. FREE ELEMENTS = " gives the weight vector and R and Q vector component values after a predetermined adaptation interval.

```
ENTER K,AGC WORD,AND INITAL WEIGHTS

  K=1
W11=377
W12=
U21=
W22=
W31=
W32=
U41=
U42=
AGC=7

MODE=03
M(K)=
  J=
IFLG=
AFLG=
NO. FREE ELEMENTS=
  W=-10553   37613  -33037   14677  -07264   37614   12152   37702
  R=-00001   00022  -00015   00016  -00003   00021   00010   00017
  Q=-00011   00030  -00023   00013  -00006   00027   00005   00031
DET= 00022
  K= 00001
AGC= 00007
```

D - Entering a Fixed Set of Weight Values

To enter fixed values for W_{11}, W_{12}, W_{21}, W_{22}, W_{31}, W_{32}, W_{41}, W_{42}, and AGC, simply follow steps 1 to 6 in "Running the Computer Program". The values will be transmitted to the processor after entering a value for "AGC" and pressing (CR) on the teletype. These values will remain fixed regardless of whether the computer is subsequently in the RUN or HALT state.

E - Reading the W, R, and Q Vectors from the Teletype Output

The state of the adaptive array just prior to printout is typed in the following format:

```
     1I      1Q      2I      2Q      3I      3Q      4I      4Q
W=-01300   13024  -07315   05227   12601   14634   13261  -15374
R=-00035  -00064   00056  -00045   00071  -00003   00046  -00050
Q=-00002   00000   00002   00000   00006   00000   00011  -00002
DET= 00072
K= 00001
AGC= 00007
```

where 1I and 1Q represent the in-phase and quadrature components of channel #1 and so on, and where

W = the weight vector
R = the wideband correlator output
Q = the narrowband correlator output

1. The Weight Vector

The printout of the weight vector is the octal representation of the "value" of the weight attenuators. The attenuation is calculated by converting the output value to decimal and dividing by 16,320. For example, the attenuation in weight W_{12} (= 13024_8) is calculated as

$$20 \log_{10} \left\{ \frac{4 \times (8)^0 + 2 \times (8)^1 + 0 \times (8)^2 + 3 \times (8)^3 + 1 \times (8)^4}{16,320} \right\} = -9.21 \text{ dB}$$

The actual value is determined by rounding the above result to the nearest 0.25 dB i.e., 9.25 dB. Note that the quantity in brackets is a voltage ratio and that its maximum value is one. The value of one occurs when 37700 is printed and corresponds to zero dB attenuation.

2. The R and Q Vectors

The values for R and Q are octal representations of the correlator output voltages after being corrected for the non-zero loop insertion phase. If no correction were performed, then the value printed is directly related by the factor (2/255) to the appropriate correlator output voltage. For example, the voltage at the output of the quadrature component of the channel #1 wideband correlator (R_{12} = -00064) would be given by

$$\left[\frac{2}{255}\right] \times R_{11} = -\left[\frac{2}{255}\right]\left[4 \times (8)^{0} + 6 \times (8)^{1}\right] = -0.408 \text{ Volts}$$

if no phase correction were being used. With phase correction (which is employed in all adaptive algorithms), the corrected I and Q components of the i^{th} correlator are given by

$$(R_{iI}) \text{ corrected} = \text{REAL}\left\{(R_{iI} + jR_{iQ})\, e^{j\theta_{c_i}}\right\}$$

$$(R_{iQ}) \text{ corrected} = \text{IMAG}\left\{(R_{iI} + jR_{iQ})\, e^{j\theta_{c_i}}\right\}$$

where θ_{c_i} = the correction angle of the i^{th} channel.

F - Loading a New Control Program

The following steps describe a procedure for loading an adaptive array control program into the PDP-11 computer. The absolute loader is assumed resident in core (see PDP-11 manual entitled "Pager Tape Software Programming Handbook" p. 6 - 8 for instructions on loading the absolute loader if it is not resident in core).

Loading the Paper Tape Program

1. Turn ON PDP-11 and the teletype.
2. Set the paper tape reader switch to STOP.
3. Place the paper tape containing the adaptive array control program into the paper tape reader. The starting point should be somewhere before the first non-zero character on the tape.
4. Set the ENABLE/HALT switch to HALT.
5. Set the switch register (SR) to 37500 and press LOAD ADDR.
6. Set ENABLE/HALT to ENABLE.
7. Press START switch on PDP-11.
8. Move paper tape reader switch to START. The paper tape will begin passing through the reader station as data is being loaded into core.
9. If this procedure is followed and if no mechanical errors in the reader have occurred, then the entire tape will be read and the teletype will print out the message.

   ENTER K, AGC WORD, AND INITIAL WEIGHTS
   K =

   During this printout, move the paper tape reader switch to STOP to prevent it from obtaining a value for K by reading the next character on the paper tape. Go to part C "Running the Computer Program".

NOTE: If the reader stops in the middle of the tape, see p 6 - 10 of "Paper Tape Software Programming Handbook".

SYSTEM ALIGNMENT PROCEDURE

The following procedure should be used for adjusting Correlator DC Offsets and System IF Gain.

A. DC CORRELATOR OFFSET

The DC offset of each of the 16 correlator outputs can be adjusted to zero using the following procedure:

1. Set all eight weight attenuators to maximum attenuation (enter ØØØ on the teletype for each weight) - (See: Operating Procedures for Computer Program Control).
2. Set the gain control attenuators to 24 dB (enter AGC = 4).
3. Apply a -95 dBm C.W. signal to each of the four deck box inputs. Its frequency should be centered on the adaptive array passband.
4. Use a sensitive oscilloscope to view the multiplexed correlator outputs. (correlator and sync output jacks are located on the rear of the Receiver/Processor). Settings: 10 mV/cm 0.5 ms/cm. The correlator outputs appear in the following

$$R_{1I},\ R_{1Q},\ Q_{1I},\ Q_{1Q},\ R_{2I},\ R_{2Q},\ Q_{2I},\ Q_{2Q},$$
$$R_{3I},\ R_{3Q},\ Q_{3I},\ Q_{3Q},\ R_{4I},\ R_{4Q},\ Q_{4I},\ Q_{4Q},\ \text{N.C.}^{*},\ \text{(REPEAT)}$$

5. Remove the top cover and adjust each correlator output to 0 volts $\pm$ 4 mV in any order. The adjustment points are shown in Figures D-1 and D-2.

B. IF GAIN ADJUSTMENT

The gain from the deck box input to the IF output monitor point is set equal to 40 dB in each of the four channels by using the following procedure:

1. Set the in-phase weight attenuator of the channel to be adjusted to zero attenuation. Set all other weight attenuators to maximum attenuation. Set the gain control attenuator to zero attenuation.

* Not connected

2. Apply a CW signal to the deck box input corresponding to the channel being adjusted. The frequency should be centered on the array passband. Any level up to -70 dBm may be used.

3. Adjust the gain (see Figure D-3) to obtain a signal level at the IF output 40 dB higher than the level at the deck box input.

4. REPEAT this process for the other three channels.

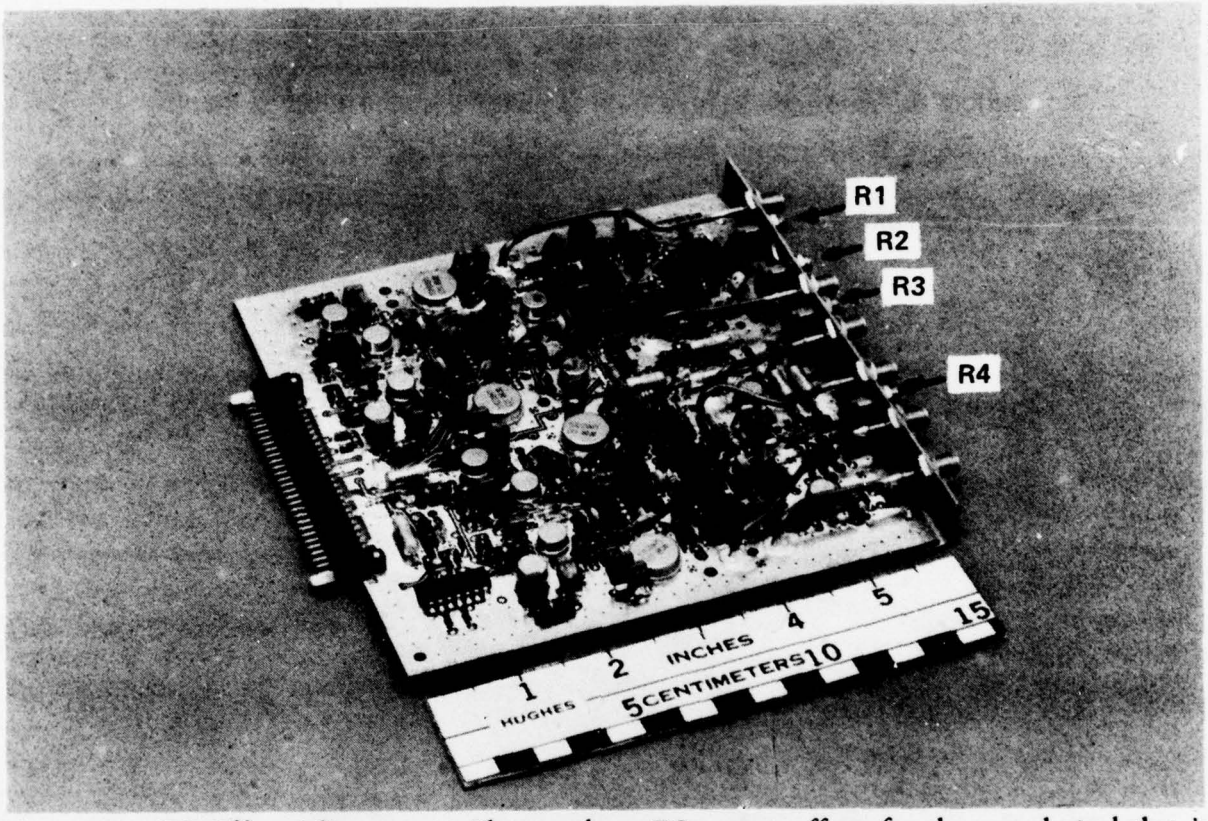

Figure D-1. DC Offset Adjustments. The correlator DC output offsets for the one channel that is shown are adjusted by means of R1, R2, R3 and R4. There are a total of 16 offset adjustments for the four channels of the processor.

CORRELATOR OUTPUT																
CORR ASSY	A1				A2				A3				A4			
DC OFFSET ADJ	R2	R1	R3	R4	R2	R1	R3	R4	R2	R1	R3	R4	R2	R1	R3	R4
CORR CARD PIN NO.	21	17	39	35	21	17	39	35	21	17	39	35	21	17	39	35
MULTIPLEXER CARD PIN NO.	58	44	46	48	50	32	34	36	56	54	52	70	68	66	64	72
CORRELATOR OUTPUT	R_{1I}	R_{1Q}	Q_{1I}	Q_{1Q}	R_{2I}	R_{2Q}	Q_{2I}	Q_{2Q}	R_{3I}	R_{3Q}	Q_{3I}	Q_{3Q}	R_{4I}	R_{4Q}	Q_{4I}	Q_{4Q}
BIT NO.	1	2	3	4	5	6	7	8	9	10	11	12	13	14	15	16

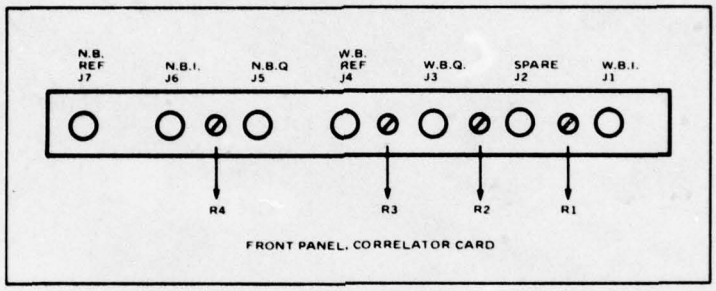

79129-36

Figure D-2. Pin Numbers for Monitoring Correlator Outputs. After multiplexing, the correlator outputs appear in time sequence as indicated by "bit number". The multiplexer output monitor is located on the rear panel of the adaptive array processor.

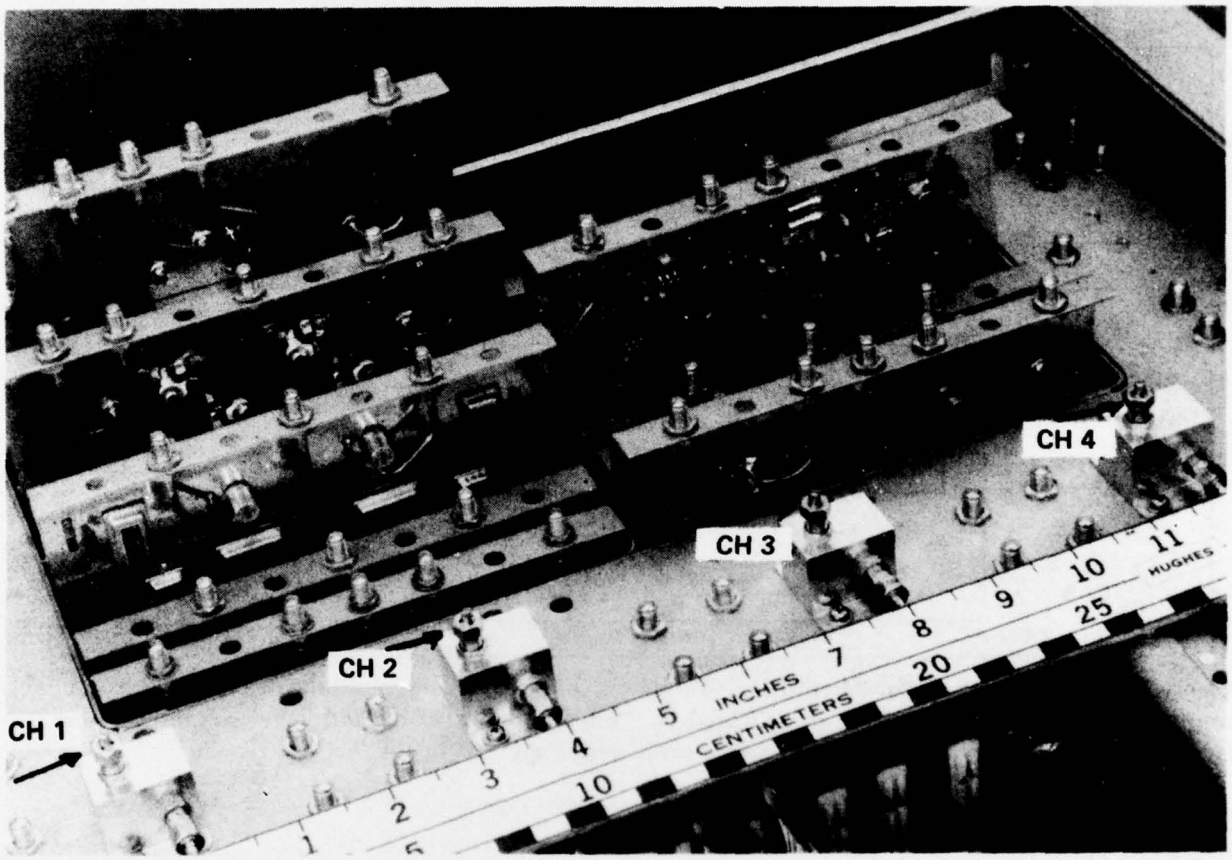

Figure D-3. Top View of the Adaptive Processor. The gain adjustments for each channel are used to set the IF signal level prior to the weight attenuators.

REFERENCES

Applebaum, S.P., "Adaptive Arrays," Special Projects Laboratory SPL-TR-66-1, August 1966, Syracuse University Research Corporation, Syracuse, N.Y.

Applebaum, S.P., and Chapman, D.J., "Adaptive Arrays With Main Beam Constraints," Proc. Adaptive Antennas Workshop, March 11-13, 1974. Vol. I, NRL Report 7803, pp 29-48

Baird, C.A., :Recursive Processing for Adaptive Arrays," Proc. Adaptive Antenna Workshop, Vol. 1, 11-13 March 1974

Brennan, L.E., and Reed, I.S., "Effect of Envelope Limiting in Adaptive Array Control Loops," IEEE Trans. on Aerospace and Electronic Systems, Vol. AES. 7, No. 4, July 1971, pp 698-700.

Compton, R.T., Jr., "Adaptive Antennas for Spread Spectrum Communications Systems," The Ohio State University Electroscience Laboratory, Department of Electrical Engineering; Prepared Under Contract N00014-67-A-0232-0009 for Office of Naval Research, Arlington, Va.

Frost, O.L., "An Algorithm for Linearly Constrained Adaptive Array Processing," Proc. of the IEEE, Vol. 60, No. 8, August 1972

Godard, D., "Channel Equalization Using a Kalman Filter for Fast Data Transmission" IBM Journal, Research and Development, May 1974.

Isaacs, D., "Algorithms for Sequential Optimization of Control Systems," Advances in Control Systems, Vol. 4 (1966) Academic Press, Inc., New York

Miller, T.W., "The Transient Response of Adaptive Arrays in TDMA Systems", PhD Dissertation, The Ohio State University, University Microfilms, 1976

Powell, M.J.D., "An Iterative Method for Finding Stationary Values of a Function of Several Variables." The Computer Journal, pp. 147-151, July 1962

Reed, I.S., Mallet, J.D., and Brennan, L.E., "Rapid Convergence Rate in Adaptive Arrays", IEEE Trans. Aerospace and Electronic Systems, Vol ASE-10, pp. 853-863. November 1974

Reinhard, K.L., "Adaptive Antenna Arrays for Coded Communications," PhD Dissertation, The Ohio State University, 1973

Riegler, R.L., and Compton, R.T., Jr., "An Adaptive Array for Interference Rejection," Report 2552-4, 16 February 1970, The Ohio State University Electroscience Laboratory, Department of Electrical Engineering; Prepared Under Grant NGR-004-013 for National Aeronautics and Space Administration

White, W.D., "Accelerated Convergence Technique", Proc. Adaptive Antennas Workshop, March 11-13, 1974. Vol. I, NRL Report 7803, pp. 191-215

Widrow, B., Mantey, P.E., Griffiths, L.J., and Goude, B.B., "Adaptive Antenna Systems", Proc. IEEE, Vol. 55, No. 12 (December 1967), pp. 2143-2159